Selective Sorting and Purification of Semiconducting-Single-Walled Carbon Nanotubes Based on Supramolecular Approach

利光, 史行

https://doi.org/10.15017/1932007

出版情報：九州大学, 2017, 博士（工学）, 論文博士
バージョン：
権利関係：

学位論文

Selective Sorting and Purification of Semiconducting-Single-Walled Carbon Nanotubes Based on Supramolecular Approach

平成 29 年 1 月　博士（工学）申請

九州大学カーボンニュートラル・エネルギー国際研究所

利光　史行

Contents

Chapter 3

Recognition and separation of semiconducting-SWCNTs using fullerene carrying copolymers

Chapter 4

Chirality separation of semiconducting- and metallic-SWCNTs using coordination polymers

Chapter 1

Preface

1-1. Introduction

Single-walled carbon nanotubes (SWCNTs) possess a unique one-dimensional structure[1] with remarkable electronic, mechanical, thermal and photophysical properties.[2-5] Not only their structural characteristics, but also opto-electronic properties derived from their diameters and chiral indices, denoted as (n,m)SWNTs, are important for a deep understanding of their fundamental intrinsic properties.[6-10] Due to the difficulty in the synthesis of SWNTs with a specific chiral index, SWNT chirality-sorting has been an anticipated technique for realizing practical applications of SWNTs, especially in the field of nano-electronic devices. Highly purified semiconducting-SWNTs (sem-SWCNTs) not containing metallic-SWNTs (met-SWNTs) are specifically required for electronic devices, such as field-effect transistors and photovoltaic applications[11, 12] because the met-SWNTs decrease and reduce the efficiency of their associated devices[13, 14]. Hence, the separation/purification of SWNTs according to their chirality is one of the most important issues in the science of carbon nanotubes. Such approaches can be simply classified into two ways containing the covalent- and non-covalent functionalization of the SWNT sidewalls[15]. To preserve the intrinsic SWNT properties, the latter method has an advantage over the former one. This paper describes the efficient and precise sorting of the chirality of SWCNTs using several supramolecular approaches using optical isomer recognition (Chapter 2), bulky π system (Chapter 3), metal complex (Chapter 4) and hydrogen bond polymer (Chapter 5), all of which ingeniously utilized weak interactions.

1-2. **Chirality of the SWCNT**

As referred in the previous section, SWCNT have various isomers with different chirality indexes. The structures can be totally symmetric that produces optical isomers with their rolling vectors with right-handed and left-handed (Fig. 1-1).

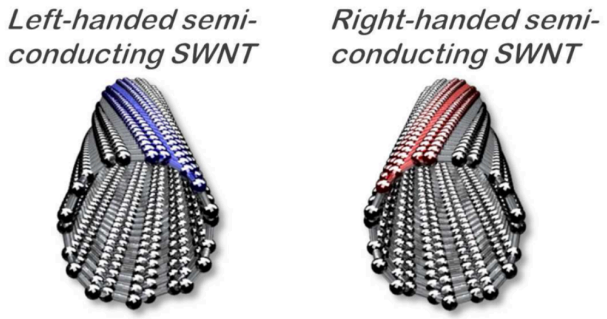

Figure 1-1. Schematic drawing of semiconducting SWNT enantiomers and chemical structures. Adapted from ref. 67 with kind permission. Copyright 2012 Journal of the American Chemical Society.

Not only their optical properties but also its electronic characters can be described according to the structure, which is metallic, semi-metallic and semiconducting (Fig. 1-2). Hirana et al. previously reported experimental observation of SWCNT electronic structures and prediction of the electronic states for the semiconducting chirality of SWCNTs using the equation (1) (Fig. 1-3),[16] where E is E_{red}, E_{ox}, or E_F, θ is chiral angle of the SWCNT and A, B, B', C and C' are constants determined by the fitting procedures.

$$E = A + B/d + B'/d^2 + (C/d)\cos 3\theta + (C'/d^2)\cos 3\theta \qquad (1)$$

For the applications using SWCNTs in opt-electronic devices, separation of the metallicity and chirality is important issue. In general, as seen in Fig. 1-3, the electronic property of semiconducting SWCNTs are related its diameter, although, there is definite differences in their electronic properties are exist. Note that SWCNTs are usually produced

with a small range of diameter distribution according to the used methods and catalyst, in which always two to one production possibility for semiconducting and metallic SWCNTs. The limited range of diameters in the production of SWCNT means the small difference get more important for the applications of SWCNT. Hence, it is very important to sort the chirality of SWCNTs in the given materials.

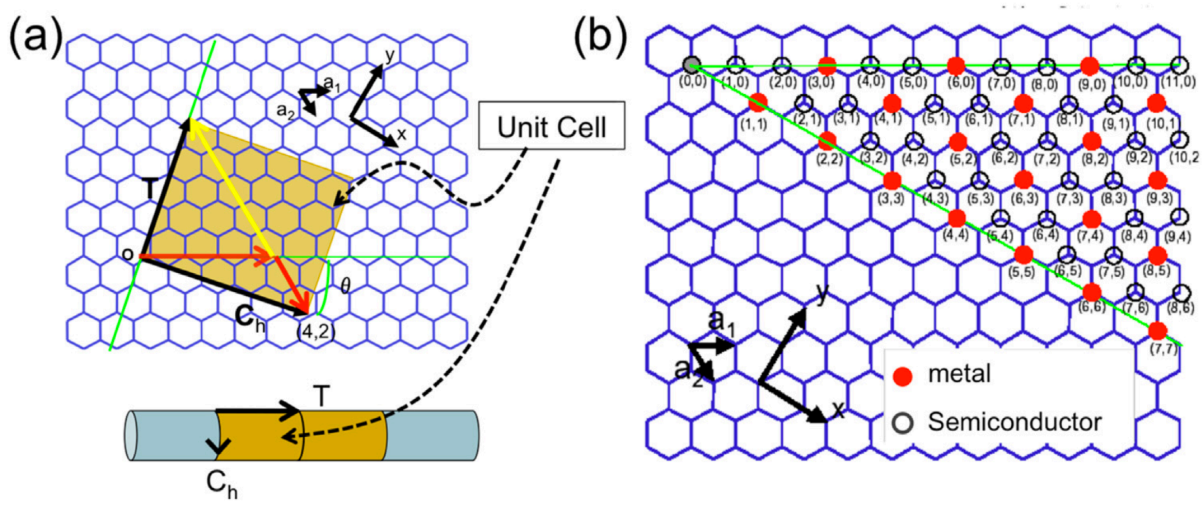

Figure 1-2. Graphic representation showing the structure of SWNTs. (a) Schematic illustration of the structures of a (4,2) SWNT with lattice chiral vector Ch and tube axis T. (b) Graphene sheet map showing the chirality of various metallic and semiconducting SWNTs with Ch from (0,0) to the shown SWNT chirality. Adapted from ref. 14 with kind permission. Copyright 2015 Elsevier Ltd. All rights reserved.

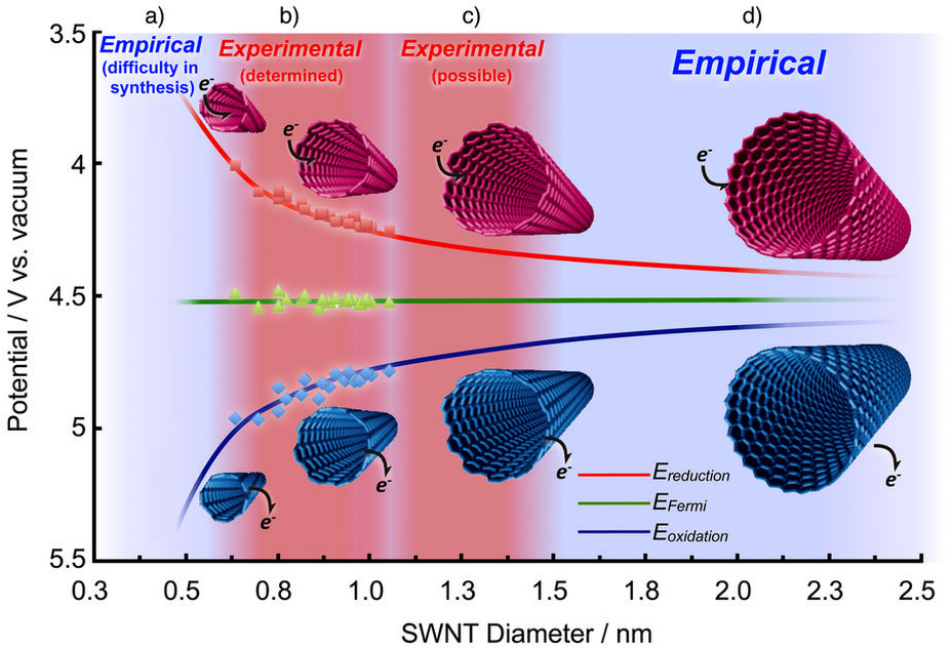

Figure 1-3. Experimental determination of the redox potentials of the SWNTs based on in situ PL electrochemical analysis is limited to the narrow diameter range (regions b and c) of the SWNTs; an empirical equation is needed in the ranges a and d due to i) the difficulty in synthesis of the SWNTs (region a), and ii) the very low sensitivity of an IR-enhanced InGaAs detector together with the difficulty in individual dissolution of the SWNTs (region d) that make in situ PL electrochemical analysis impossible. Adapted from ref. 16 with kind permission. Copyright 2013 Springer Nature.

1-3. Sorting the semiconducting-SWCNTs

Due to the difficulty in the synthesis of SWNTs with a specific chiral index, SWNT chirality-sorting has been an anticipated technique for realizing practical applications of SWNTs, especially in the field of nano-electronic devices. Chirality of SWCNTs represents the arrangement of carbon atoms and electronic properties as semiconducting- or metallic-SWCNTs with using chiral index (n,m). To date, various methods have been presented for such separation including density gradient ultracentrifugation (DGU)[17,18] and gel chromatography techniques[19,20], aqueous two-phase extraction method[21] use of polyfluorenes[22,23] and oligo DNAs[24,25]. While, DGU and chromatography techniques are

rather complex, the methods using polymers such as DNAs and synthetic polymers are preferred by their facile, non-destructive and one-pot separation of the sc-SWCNTs; however, removal of the wrapped polymers on the SWCNTs is difficult in principle.

1-3-1. Using mechanical forces for separating chirality of SWCNTs

SWCNTs are tubular and hollow structured materials and, furthermore, completely consist of π conjugated surfaces, which make the separation and even solubilization to any solvent difficult. The first report that efficiently solubilize SWCNTs in the solvent is performed using aqueous micelles. From the stacked bundles of SWCNT to the isolated form (Fig 1-4), the aid of ultra-sonication is inevitable. The stronger the ultra-sonication is, the critical their damage becomes more serious, that means the balance of reservation of SWCNT character is depending on the performance of the solubilizing surfactants. Fig. 1-5 shows several representatives of useful surfactants with alkyl chains and natural backbones (bile salts and nonionic bio-surfactants)[26]. DGU (Fig. 1-6) and agarose gel-column chromatography (Fig. 1-7) are based on the solubilization and the interaction between the SWCNTs and these surfactants.

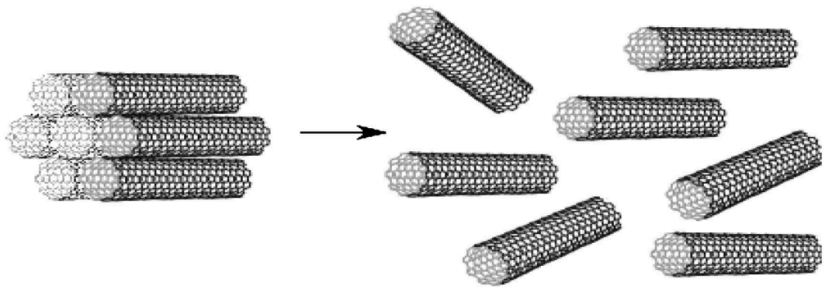

Figure 1-4. From bundled nanotubes to individually solubilized nanotubes.

Although the separation is very clear, these methods with physical external forces are based on strong ultra-sonication, which potentially harms the structures of π conjugated structures of SWCNTs.

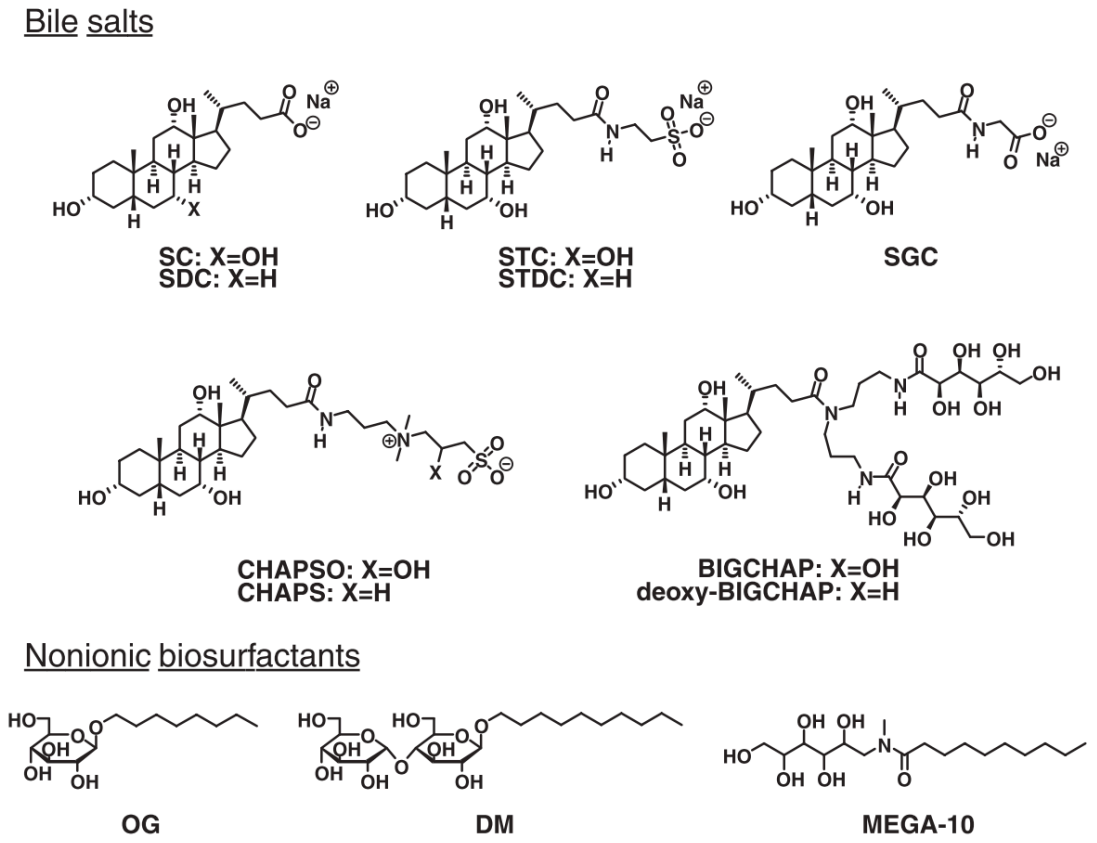

Figure 1-5. Chemical structures of bile salts and nonionic biosurfactants. Adapted from ref. 14 with kind permission. Copyright 2006 WILEY-VCH Verlag GmbH & Co.KGaA, Weinheim.

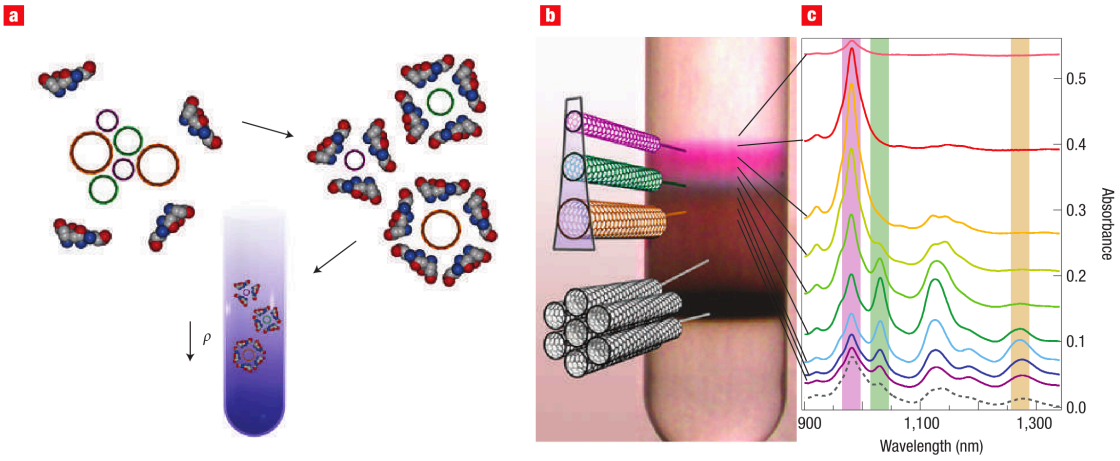

Figure 1-6. Sorting of SWNTs by diameter, bandgap and electronic type using density gradient ultracentrifugation. (a) Schematic of surfactant encapsulation and sorting, where ρ is density. (b) Photographs and (c) optical absorbance (1 cm path length) spectra after separation using density gradient ultracentrifugation. Adapted from ref. 14 with kind permission. Copyright 2015 Elsevier Ltd. All rights reserved.

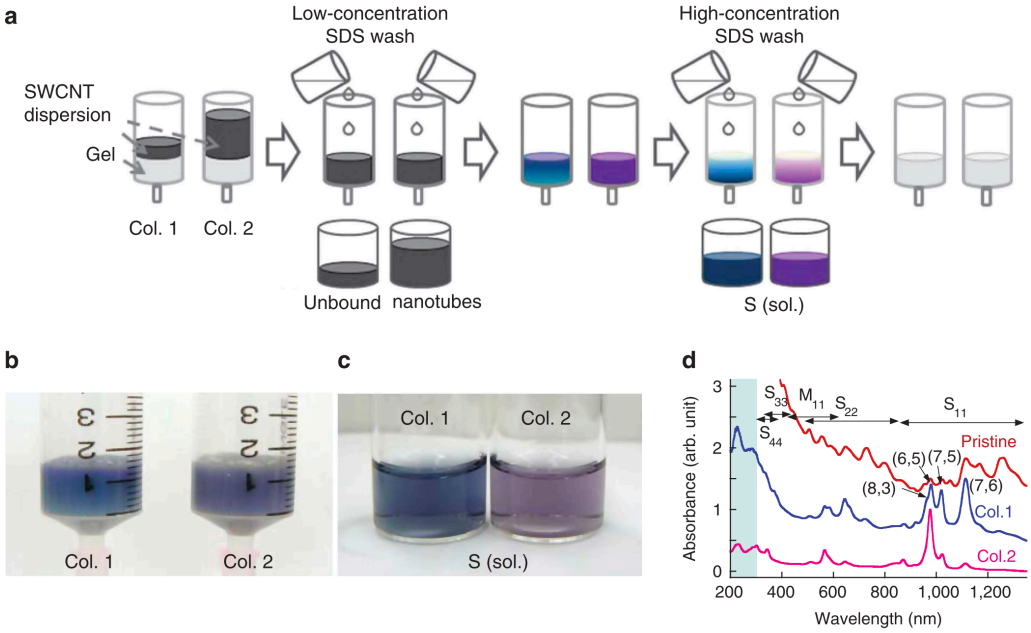

Figure 1-7. Effect of overloading single-wall carbon nanotubes (SWCNTs) on gel columns. Schematic diagram of overloading effect with SWCNTs in the gel columns. Adapted from ref. 19 with kind permission. Copyright 2011, Springer Nature.

1-3-2. Soring SWCNTs according to their chirality using natural polymers

Recently, several papers have described the separation of the chiral mixtures of semiconducting/metallic SWNTs using natural polymers such as deoxyribonucleic acid (DNA)[27-30] (Fig. 1-8). These reports confined the molecular recognition takes place on the surface of SWCNTs. DNA can take several possible states such as single-stranded and double stranded[31-33]. Both the single- and double- forms were individually proven to possible to solubilize SWCNTs especially for the semiconducting-parts by Nakashima[27] (double-stranded DNA, Fig. 1-8) and Zheng[28-30] (single-stranded DNA, Fig. 1-9), respectively. Furthermore, the components of DNA can influence the recognition of chirality and Zheng successfully performed the selective sorting of SWCNT chirality tuned by various sequences of DNA[31].

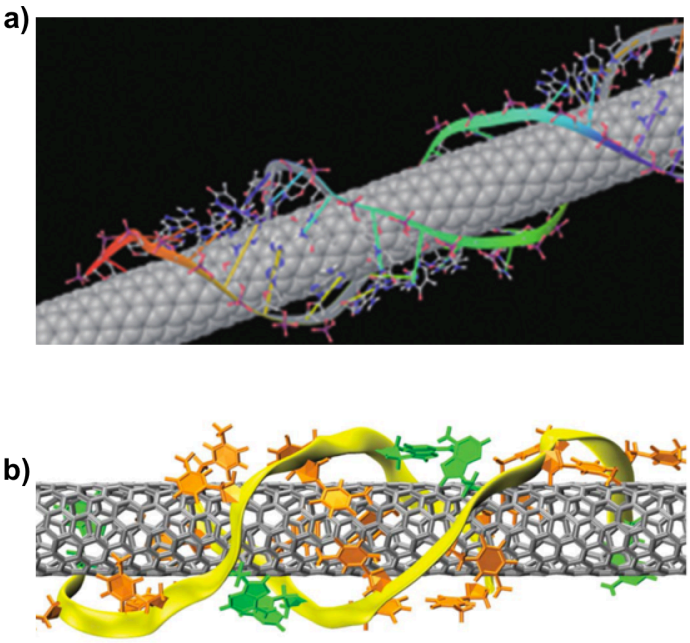

Figure 1-8. Energy-minimized structure of SWCNT wrapped by (a) double-stranded DNA and (b) single-stranded DNA. Adapted from ref. 14 with kind permission. Copyright 2015 Elsevier Ltd. All rights reserved.

Natural polymers are elegantly designed and ready for use in SWCNT sorting and, nowadays, it is accessible to prepared the arranged sequences[32-36]. Contrary to their limitless possibility to individually recognize the all individual chirality of SWCNT by DNA sequent, the problem is its time and cost for the preparation of DNA itself and the follow-up chirality separation using anion-changing gel-column chromatography[31]. For more efficient solubilization/separation of specific chirality of SWCNT, more facile and more cheap methods are still demanded.

1-3-3. Sorting semiconducting-SWCNTs using synthetic polymers

One of the important findings in the chirality-sorting methods is the selective extraction using artificially synthesized polymers[37-50]. As described in the previous section, molecular recognition is powerful tool for the chirality-sorting of SWCNTs and the key is the strategical design of the molecules. Poly(9,9-didodecylfluorene-2,7-diyl) (PFOs)[37-40], PFO derivatives,[41-46] polycarbazole[48] and region-regular polyalkylthiophene[49,50] are known to dissolve only semiconducting SWNTs. Especially, molecular recognition methods with (co)polymers are preferred by their facile, mild-conditioned and one-pot separation of semiconducting -SWNTs;

however, adsorbed molecules including general surfactants on the separated SWCNTs cannot be easily removed.[51] One other drawback is that these conventional methods require complicated synthesis or sophisticated machine tools setup. For a facile sorting of chemically pure semiconducting-SWCNTs, highly-efficient and low-cost purification method has been demanded.

1-4. Removable solubilizers for SWCNT based on supramolecular chemistry

The selective extraction is simple and powerful for the chirality-sorting; however, it is difficult that the removal of the polymers in the polymer/SWNT hybrids due to the strong polymer wrapping through molecular interactions.[52-55] The First demonstration for solubilization and release of SWCNTs using supramolecular polymers was reported by Stoddart using metal complex.[56] For the other weak-bond based supramolecular system, hydrogen-bond polymer is utilized for the is reversible solubilization/bundling of multi-walled carbon nanotubes by Bonifazi.[57] Unfortunately, both method showed no chirality selectivity along the solubilization procedures, probably because of the rack of intentionally designed chirali recognition moieties in the systems.

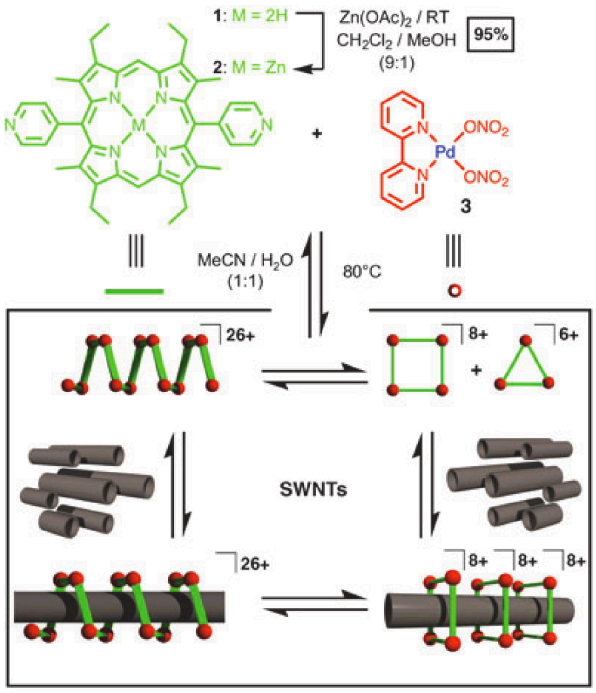

Figure 1-9. Schematic of dynamic coordination chemistry in action with SWNTs. Adapted from ref. 56 with kind permission. Copyright 2015 WILEY-VCH Verlag GmbH & Co. KGaA, Weinheim.

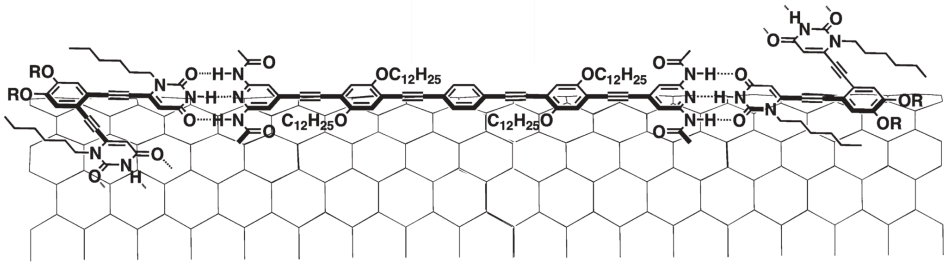

Figure 1-10. Schematic representation of the envisaged self-assembly processes taking place on the surface of carbon nanotube. Adapted from ref. 57 with kind permission. Copyright 2011, American Chemical Society.

Practical use of the SWCNTs in the next-generation devices requires the chirality purity of the SWCNTs. For the purpose, introduction of degradable moieties into the known chirality selective polymer is the nearest pathway. Recently, several reports for the removal of the wrapping chirality selective polymers are demonstrated,[58-62] but most of them are intended to ensure the polymer-bond-breaking, which usually realized on the sacrifice of the polymer. Furthermore, degradable moiety is not suitable for the recognition of the SWCNT chirality,

which decrease the purity of the SWCNTs. One more important requirement for the chirality selective SWCNT solubilizing polymers is the length of the polymer. Reducing the polymer length should weaken polymer/SWCNT interactions[63,64] and the effects of the polymer length to chirality selectivity and removability have been considered. Henrich et al. synthesized 9,9-dialkylfluorene oligomers (from dimer to octamer) and compared their dispersing properties toward SWNTs with those of the parent polymer PFO.[66] The octamer shows selectivity to near armchair semiconducting SWNTs and exchange with a conjugated polymer; however, the oligomers do not show clear semiconducting/metallic selectivity, and naked SWNTs have not been obtained.

Summarizing these knowledge, it is agreeable that in-situ growing polymers based on supramolecular mechanism are suitable for the chirality-selective separation/purification of SWCNTs.

1-5. **The aim of this research**

In the present research, I describe the sorting of the semiconducting- and the metallic-SWCNTs based on a supramolecular approach. Furthermore, the separation of the optical and the structural isomers of SWCNTs are targeted. In order to achieve this multiple functionalities, I designed supramolecular systems consist of metal-ligand coordination, hydrogen-bond, optical recognition molecules and bulky π-conjugated adducts. The non-covalent weak bonds are, furthermore, utilized to design external stimuli-responsive moieties to make the SWCNT solubilizers removable.

As the goal, we designed and synthesized solubilizer molecules that efficiently recognize/solubilize semiconducting-SWCNTs based on the difference in the SWCNT chirality recognition and solubility product between the semiconducting- and metallic-SWCNTs followed by detachment of the solubilizers from the SWNT surfaces. The chemical structures of these molecules are covalent polymers, coordination polymers and hydrogen-bond polymers composed of fluorene moieties and functional parts. The fluorene backbone acts as the

semiconducting-SWCNT recognition moiety and the functional parts connecting fluorene units with giving the polymer new features. Such a technique to combine conventional backbones and functional moieties are basic, but powerful tool to design efficient solubilizers for SWCNTs.

Especially, supramolecular coordination complex polymers with semiconducting-SWCNT selectivity is exhibited for the first time in the field, as far as I know, that opened up and deepens the cooperation between chemistry and carbon nanotube science. Therefore, such efficient combinations between SWCNTs and supramolecular systems have been investigated in this research.

1-6. **Content of the research**

I expected that the introduction of functional moieties in the conventional fluorene polymer might control the chirality selectivity and yield of the extracted SWCNTs. In the present research, thus, I investigated five fluorene based copolymers, which can be devided into three categories, the polymer carrying optical recognition units, bulky π-system and weak-bond based polymers. All the presented polymers interact with SWCNTs by supramolecular recognition and the results are described in four chapters as follows.

Synthesis, characterization and sorting optical isomers of SWCNTs using chiral-recognizing solubilizers are presented in Chapter 2.

Chapter 3 describes the sysnthesis, characterization and sorting SWCNTs using fullerene carrying solubilizers.

Coordination polymers for the selective separation of semiconducting-SWCNTs are presented in Chapter 4.

High chiral selective hydrogen-bond polymers are described in the Chapter 5.

Throughout these researches, I have discovered that the extracting highly chiral-pure extraction is possible using removable supramolecular solubilizers (Chapter 4 and 5). These are the first example in designing chiral selective SWCNT solubilizers.

References

[1] S. Iijima, *Nature* **1991**, *354*, 56.

[2] J. Azamat, A. Balaei, M. Gerami, *Comput. Mater. Sci.* **2016**, *113*, 66.

[3] Y. Y. Huang, E. M. Terentjev, *Polymers (Basel).* **2012**, *4*, 275.

[4] L. Vaisman, H. D. Wagner, G. Marom, *Adv. Colloid Interface Sci.* **2006**, *128–130*, 37.

[5] A. Vijayaraghavan, S. Blatt, D. Weissenberger, M. Oron-Carl, F. Hennrich, D. Gerthsen, H. Hahn, R. Krupke, *Nano Lett.* **2007**, *7*, 1556.

[6] F. J. Martín-Martínez, S. Melchor, J. a Dobado, *Phys. Chem. Chem. Phys.* **2011**, *13*, 12844.

[7] Q. Cao, S. Han, G. S. Tulevski, Y. Zhu, D. D. Lu, W. Haensch, *Nat. Nanotechnol.* **2013**, *8*, 180.

[8] J. E. Rossi, C. D. Cress, A. Merrill, K. J. Soule, N. D. Cox, B. J. Landi, *Carbon N. Y.* **2015**, *81*, 488.

[9] J. a Fagan, J. R. Simpson, B. J. Bauer, S. H. D. P. Lacerda, M. L. Becker, J. Chun, K. B. Migler, A. R. H. Walker, E. K. Hobbie, *J. Am. Chem. Soc.* **2007**, *129*, 10607.

[10] M. Ouyang, J.-L. Huang, C. M. Lieber, *Acc. Chem. Res.* **2002**, *35*, 1018.

[11] C. V. V. M. Gopi, M. Venkata-Haritha, S. K. Kim, H. J. Kim, *J. Power Sources* **2016**, *311*, 111.

[12] R. M. Jain, R. Howden, K. Tvrdy, S. Shimizu, A. J. Hilmer, T. P. McNicholas, K. K. Gleason, M. S. Strano, *Adv. Mater.* **2012**, *24*, 4436.

[13] A.-M. Dowgiallo, K. S. Mistry, J. C. Johnson, J. L. Blackburn, *ACS Nano* **2014**.

[14] Wang, H. & Bao, Z., *Nano Today* (2016). doi:10.1016/j.nantod.2015.11.008.

[15] V. Likodimos, T. A. Steriotis, S. K. Papageorgiou, G. E. Romanos, R. R. N. Marques, R. P. Rocha, J. L. Faria, M. F. R. Pereira, J. L. Figueiredo, A. M. T. Silva, P. Falaras, *Carbon N. Y.* **2014**, *69*, 311.

[16] Y. Hirana, G. Juhasz, Y. Miyauchi, S. Mouri, K. Matsuda, N. Nakashima, *Sci. Rep.* **2013**, *3*.

[17] S. Ghosh, S. M. Bachilo, R. B. Weisman, *Nat. Nanotechnol.* **2010**, *5*, 443.

[18] M. S. Arnold, A. A. Green, J. F. Hulvat, S. I. Stupp, M. C. Hersam, *Nat. Nanotechnol.* **2006**, *1*, 60.

[19] H. Liu, D. Nishide, T. Tanaka, H. Kataura, *Nat. Commun.* **2011**, *2*, 309.

[20] T. Tanaka, J. Hehua, Y. Miyata, H. Kataura, *Appl. Phys. express* **2008**, *1*, 1.

[21] C. Y. Khripin, J. a Fagan, M. Zheng, *J. Am. Chem. Soc.* **2013**, *135*, 6822.

[22] A. Nish, J. Hwang, J. Doig, R. Nicholas, *Nat. Nanotechnol.* **2007**, *2*, 640.

[23] F. Chen, B. Wang, Y. Chen, L.-J. Li, *Nano Lett.* **2007**, *7*, 3013.

[24] M. Zheng, A. Jagota, E. D. Semke, B. A. Diner, R. S. Mclean, S. R. Lustig, R. E. Richardson, N. G. Tassi, *Nat. Mater.* **2003**, *2*, 338.

[25] M. Zheng, E. D. Semke, *J. Am. Chem. Soc.* **2007**, *129*, 6084.

[26] A. Ishibashi, N. Nakashima, *Chem. - A Eur. J.* **2006**, *12*, 7595.

[27] N. Nakashima, S. Okuzono, H. Murakami, T. Nakai, K. Yoshikawa, *Chem. Lett.* **2003**, *32*, 456.

[28] X. Tu, A. R. Hight Walker, C. Y. Khripin, M. Zheng, *J. Am. Chem. Soc.* **2011**, *133*, 12998.

[29] L. Zhang, X. Tu, K. Welsher, X. Wang, M. Zheng, H. Dai, *J. Am. Chem. Soc.* **2009**, *131*, 2454.

[30] M. Zheng, E. D. Semke, *J. Am. Chem. Soc.* **2007**, *129*, 6084.

[31] X. Tu, S. Manohar, A. Jagota, M. Zheng, *Nature* **2009**, *460*, 250.

[32] F. Schöppler, C. Mann, T. C. Hain, F. M. Neubauer, G. Privitera, F. Bonaccorso, D. Chu, A. C. Ferrari, T. Hertel, *J. Phys. Chem. C* **2011**, *115*, 14682.

[33] M. Zheng, A. Jagota, M. S. Strano, A. P. Santos, P. Barone, S. G. Chou, B. a Diner, M. S. Dresselhaus, R. S. McLean, G. B. Onoa, G. G. Samsonidze, E. D. Semke, M. Usrey, D. J. Walls, *Science* **2003**, *302*, 1545.

[34] B. Koh, J. B. Park, X. Hou, W. Cheng, *J. Phys. Chem. B* **2011**, *115*, 2627.

[35] R. Sharifi, M. Samaraweera, J. a Gascón, F. Papadimitrakopoulos, *J. Am. Chem. Soc.* **2014**, *136*, 7452.

[36] C. F. Chiu, W. A. Saidi, V. E. Kagan, A. Star, *J. Am. Chem. Soc.* **2017**, *139*, 4859.

[37] X. Tu, S. Manohar, A. Jagota, M. Zheng, *Nature* **2009**, *460*, 250.

[38] J. Zhang, A. a Boghossian, P. W. Barone, A. Rwei, J.-H. Kim, D. Lin, D. a Heller, A. J. Hilmer, N. Nair, N. F. Reuel, M. S. Strano, *J. Am. Chem. Soc.* **2011**, *133*, 567.

[39] T.-G. Cha, J. Pan, H. Chen, J. Salgado, X. Li, C. Mao, J. H. Choi, *Nat. Nanotechnol.* **2014**, *9*, 39.

[40] S.-Y. Ju, D. C. Abanulo, C. A. Badalucco, J. A. Gascon, F. Papadimitrakopoulos, *J. Am. Chem. Soc.* **2012**, *134*, 13196.

[41] T. Shiraki, A. Tsuzuki, F. Toshimitsu, N. Nakashima, *Chemistry* **2016**, *22*, 4774.

[42] S.-Y. Ju, D. C. Abanulo, C. A. Badalucco, J. A. Gascon, F. Papadimitrakopoulos, *J. Am. Chem. Soc.* **2012**, *134*, 13196.

[43] X. Wang, C. Wang, L. Cheng, S.-T. Lee, Z. Liu, *J. Am. Chem. Soc.* **2012**.

[44] Y. Kato, A. Inoue, Y. Niidome, N. Nakashima, *Sci. Rep.* **2012**, *2*, 1.

[45] Y. Noguchi, T. Fujigaya, Y. Niidome, N. Nakashima, *Chem. Phys. Lett.* **2008**, *455*, 249.

[46] S.-Y. Ju, D. C. Abanulo, C. A. Badalucco, J. A. Gascon, F. Papadimitrakopoulos, *J. Am. Chem. Soc.* **2012**, *134*, 13196.

[47] D. Roxbury, J. Mittal, A. Jagota, *Nano Lett.* **2012**, *12*, 1464.

[48] M. Ito, Y. Ito, D. Nii, H. Kato, K. Umemura, Y. Homma, *J. Phys. Chem. C* **2015**, 150828160259001.

[49] M. Zheng, E. D. Semke, *J. Am. Chem. Soc.* **2007**, *129*, 6084.

[50] F. Sen, A. A. Boghossian, S. Sen, Z. W. Ulissi, J. Zhang, M. S. Strano, *ACS Nano* **2012**, *6*, 10632.

[51] R. R. Johnson, a T. C. Johnson, M. L. Klein, *Nano Lett.* **2008**, *8*, 69.

[52] A. N. G. Parra-Vasquez, N. Behabtu, M. J. Green, C. L. Pint, C. C. Young, J. Schmidt, E. Kesselman, A. Goyal, P. M. Ajayan, Y. Cohen, Y. Talmon, R. H. Hauge, M. Pasquali, *ACS Nano* **2010**, *4*, 3969.

[53] S. K. Samanta, M. Fritsch, U. Scherf, W. Gomulya, S. Z. Bisri, M. A. Loi, *Acc. Chem. Res.* **2014**, *47*, 2446.

[54] A. H. Bae, T. Hatano, N. Nakashima, H. Murakami, S. Shinkai, *Org. Biomol. Chem.* **2004**, *2*, 1139.

[55] Y. Noguchi, T. Fujigaya, Y. Niidome, N. Nakashima, *Chem. - A Eur. J.* **2008**, *14*, 5966.

[56] K. S. Chichak, A. Star, M. V. P. Altoé, J. F. Stoddart, *Small* **2005**, *1*, 452.

[57] A. Llanes-Pallas, K. Yoosaf, H. Traboulsi, J. Mohanraj, T. Seldrum, J. Dumont, A. Minoia, R. Lazzaroni, N. Armaroli, D. Bonifazi, *J. Am. Chem. Soc.* **2011**, *133*, 15412.

[58] M. Imit, A. Adronov, *Polym. Chem.* **2015**, *6*, 4742.

[59] A. Graf, Y. Zakharko, S. P. Schießl, C. Backes, M. Pfohl, B. S. Flavel, J. Zaumseil, **2016**, *105*, 593.

[60] K. S. Mistry, B. a Larsen, J. L. Blackburn, *ACS Nano* **2013**, *7*, 2231.

[61] L. Hong, F. Toshimitsu, Y. Niidome, N. Nakashima, *J. Mater. Chem. C Mater. Opt. Electron. Devices* **2014**, *2*, 5223.

[62] L. Hong, F. Toshimitsu, Y. Niidome, N. Nakashima, *J. Mater. Chem. C* **2014**, *2*.

[63] H. Ozawa, T. Fujigaya, Y. Niidome, N. Nakashima, *Chem. Asian J.* **2011**, *6*, 3281.

[64] M. Tange, T. Okazaki, S. Iijima, *ACS Appl. Mater. Interfaces* **2012**, *4*, 6458.

[65] A. Nish, J.-Y. Hwang, J. Doig, R. J. Nicholas, *Nanotechnology* **2008**, *19*, 95603.

[66] S. D. Stranks, A. M. R. Baker, J. a Alexander-Webber, B. Dirks, R. J. Nicholas, *Small* **2013**, 1.

[67] Akazaki, K., Toshimitsu, F., Ozawa, H., Fujigaya, T. & Nakashima, N., *J. Am. Chem. Soc.* **134,** 12700–12707 (2012).

Chapter 2

Recognition and separation of optical isomers of SWCNTs using synthetic polymers

2-1. Introduction

As-synthesized SWCNTs are usually mixed isomers of semiconducting- and metallic-SWCNTs with more than several chirality indices (*n*,*m*), and furthermore, they are also racemic mixtures consist of equal amount of enantiomers with left- or right-handed winding alignment of carbon atoms along with chirality index.[1,2] These SWCNT enantiomers should exhibit corresponding circular dichroism (CD)[11,12] as seen in bio, pharmaceutical and chemical compounds, however, neither detailed properties nor differences of SWCNTs enantiomers have not been accessed deeply owing to the absence of suitable separation/purification technique. Although many techniques and approaches toward chirality separation of SWCNTs have been developed, it still needs a breakthrough to extract/separate right- or left-handed SWCNT enantiomers from their racemic chiral mixtures.

Recently, several challenges describing the separation of the racemic mixtures of SWCNTs into each enantiomer have been reported. Komatsu et al. [12,13] used chiral diporphyrin molecules to separate the left- and right- racemic mixtures. Hersam et al. applied the density gradient ultracentrifugation (DGU) [14,15] technique for sorting SWCNTs and Weisman et al.[16] sorted enantiomers of the SWCNTs by improved nonlinear DGU gradient using mixed surfactants of sodium cholate and sodium dodecyl sulphate. However, regarding cost and efficiency of the

system, simultaneous resolution of SWCNTs according to their metallic or semiconducting chirality and left- or right-handed helicity is still remains as a big challenge.

Polyfluorene-based copolymers are intensively focused due to their highly specific sorting ability toward semiconducting SWCNTs.[17,18] I have previously demonstrated a rational method for the selective recognition and solubilization of specific chirality of (*n*,*m*)SWCNTs with a series of systematically designed and synthesized fluorene-based copolymers,[19] in which I revealed the flexible and controllable selectivity of the copolymers over the SWCNT chirality. In that research, I used chiral moieties as side chains of the polyfluorene, but no significant enantiomer selectivity was obserbed.

With this insight, here I developed the strategy to separate semiconducting, left- or right-handed SWCNT enantiomers with newly designed and synthesized chiral fluorene-based copolymers (Figure 2-1). The approach was introduction of chiral binaphthol moiety, (*R*)- and (*S*)-2,2'-dimethoxy-1,1'-binaphthyl-6,6'-diyl (RBN and SBN), into the fluorene polymers (poly-9,9-dioctyl-2,7-fluorene, PFO), which was based on the fundamental idea of hybridizing chirality sorting and enantio-selective extraction. PFO and their derivatives[20-26] are known to dissolve only semiconducting SWCNTs and RBN and SBN are so-called BINAP family that possess powerful enantiomer recognizing ability.[27-29]

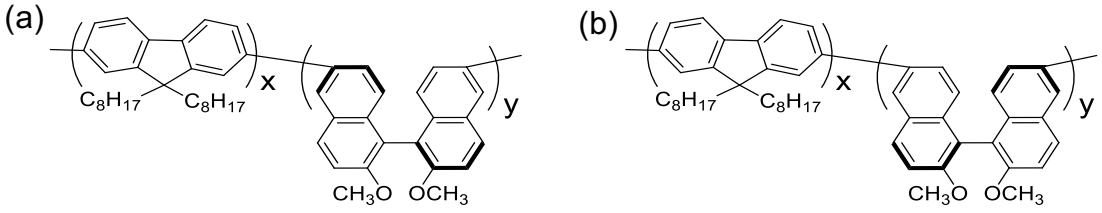

Figure. 2-1. Chemical structures of copolymers of Poly{(9,9-dioctylfluorenyl-2,7-diyl)-*ran*-[(R)-2,2'-dimethoxy-1,1'-binaphthyl-6,6'-diyl]} **(PFO)x(RBN)y** (a) and Poly{(9,9-dioctylfluorenyl-2,7-diyl)-*ran*-[(S)-2,2'-dimethoxy-1,1'-binaphthyl-6,6'-diyl]} (PFO)x(SBN)y (b). Adapted from ref. 35 with kind permission. Copyright 2012 American Chemical Society.

To realize this concept, I synthesized 12 novel copolymers denoted as **(PFO)x(RBN)y** and **(PFO)x(SBN)y**, where **x** and **y** are the copolymer composition ratios. The copolymers successfully extracted only semiconducting SWCNT enantiomers by simple sonication in toluene, and no further purifications were needed. In particular, I find that the proportion of chiral binaphthol moiety exhibited dramatic influence on the recognition/extraction of SWCNT enantiomers.

To verify the selectivity features of our copolymers, I simulated the conformation of each copolymer on SWCNTs in accordance with typical experimental conditions. The calculation well elucidated that the driving force of enantio-selective sorting was governed not only by chiral interactions but also by copolymers' wrapping fashion, those cooperatively altered upon changing composition ratio of the copolymers.

2-2. Experimental

2-2-1. Synthesis of copolymers. (*R*)- and (*S*)-6,6'-dibromo-2,2'-dimethoxy-1,1'-binaphthalene were synthesized according to the literature.[32] Chiral copolymers, **(PFO)x(RBN)y** and **(PFO)x(SBN)y** were synthesized via Yamamoto coupling reaction.[33,34] Briefly, the synthesis procedure of **(PFO)61(RBN)39** is described as following. $Ni(COD)_2$ (100 mg, 0.36 mmol), 2,2'-dipyridyl (62 mg, 0.40 mmol), 1,5-cyclooctadiene (0.1 mL), dried DMF (1.5 mL) and dried toluene (3.0 ml) were placed in a flask and heated at 80 °C for 30 min under a nitrogen flow to obtain a dark purple complex to which a mixed solution of 2,7-dibromo-9,9'-dioctylfluorene (55 mg) and (*R*)-6,6'-dibromo-2,2'-dimethoxy-1,1'-binaphthalene (39 mg) in dried DMF (0.5 mL) and dried toluene (0.5 mL) was added, and then reacted at 80 °C for 24 h. After the reaction, the solution was poured into a mixed solution (150 mL) of 2M HCl (50 mL), acetone (50 mL), and methanol (50 mL) to produce a precipitate, which was collected by filtration, and then rinsed with acetone.

The obtained solid was dissolved in chloroform, and then reprecipitated from methanol to produce a yellowish solid (52 mg). ^{1}H NMR ($CDCl_3$, 300 MHz) : δ 8.30-7.40 (m, 3.2H), 3.80 (m, 1H), 2.04 (m, 1H), 1.35-0.936 (m, 5.2H), 0.916-0.437 (m, 2.6H). Yeild: 52%. M_n = 5377, M_w = 20658, PDI = 3.84. Other 11 different **(PFO)x(RBN)y** and **(PFO)x(SBN)y** were synthesized by a similar way. The composition ratios (x,y) of the copolymers were determined by their ^{1}H NMR spectra. **(PFO)86(RBN)14**: ^{1}H NMR ($CDCl_3$, 300 MHz): δ 8.3-7.40 (m, 10.2H), 3.80 (m, 1H), 2.04 (m, 4H), 1.35-0.936 (m, 35.7H), 0.916-0.437 (m, 38.9H). Yeild: 52%, M_n = 28514, M_w = 55618, PDI = 1.95. **(PFO)76(RBN)24**: ^{1}H NMR ($CDCl_3$, 300 MHz): δ 8.30-7.40 (m, 5.66H), 3.80 (m, 1H), 2.04 (m, 2.07H), 1.35-0.936 (m, 14.1H), 0.916-0.437 (m, 6.11H). Yeild: 86%, M_n = 23962, M_w = 85831, PDI = 3.58. **(PFO)71(RBN)29**: ^{1}H NMR ($CDCl_3$, 300 MHz): δ 8.30-7.40 (m, 5.36H), 3.80 (m, 1H), 2.04 (m, 1.62H), 1.35-0.936 (m, 8.88H), 0.916-0.437 (m, 4.3H). Yeild: 63%, M_n = 16328, M_w = 42775, PDI = 2.62. **(PFO)68(RBN)32**: ^{1}H NMR ($CDCl_3$, 300 MHz): δ 8.30-7.40 (m, 3.94H), 3.80 (m, 1H), 2.04 (m, 1.44H), 1.35-0.936 (m, 7.89H), 0.916-0.437 (m, 3.73H). Yeild: 46%, M_n = 9029, M_w = 30383, PDI = 3.37. **(PFO)44(RBN)56**: ^{1}H NMR ($CDCl_3$, 300 MHz): δ 8.30-7.40 (m, 2.19H), 3.80 (m, 1H), 2.04 (m, 0.533H), 1.35-0.936 (m, 2.85H), 0.916-0.437 (m, 1.55H). Yeild: 37%, M_n = 2055, M_w = 11565, PDI = 5.63. (**PFO)85(SBN)15**: ^{1}H NMR ($CDCl_3$, 300 MHz): δ 8.30-7.40 (m, 7.61H), 3.80 (m, 1H), 2.04 (m, 3.7H), 1.35-0.936 (m, 21.5H), 0.916-0.437 (m, 9.63H). Yeild: 82%, M_n = 20923, M_w = 51138, PDI = 2.44. **(PFO)72(SBN)28**: ^{1}H NMR ($CDCl_3$, 300 MHz): δ 8.30-7.40 (m, 4.4H), 3.80 (m, 1H), 2.04 (m, 1.73H), 1.35-0.936 (m, 9.48H), 0.916-0.437 (m, 4.46H). Yeild: 49%, M_n = 12461, M_w = 36663, PDI = 2.94. **(PFO)65(SBN)35**: ^{1}H NMR ($CDCl_3$, 300 MHz): δ 8.30-7.40 (m, 3.76H), 3.80 (m, 1H), 2.04 (m, 1.25H), 1.35-0.936 (m, 6.73H), 0.916-0.437 (m, 3.33H). Yeild: 56%, M_n = 9966, M_w = 24790, PDI = 2.49.**(PFO)55(SBN)45**: ^{1}H NMR ($CDCl_3$, 300 MHz): δ 8.30-7.40 (m, 2.90H), 3.80 (m, 1H), 2.04 (m, 0.804H), 1.35-0.936 (m,

5.67H), 0.916-0.437 (m, 3.22H). Yeild: 53%, M_n = 4489, M_w = 14086, PDI = 3.14. **(PFO)51(SBN)49**: ^{1}H NMR ($CDCl_3$, 300 MHz): δ 8.30-7.40 (m, 2.63H), 3.80 (m, 1H), 2.04 (m, 0.692H), 1.35-0.936 (m, 3.69H), 0.916-0.437 (m, 1.78H). Yeild: 45%, M_n = 3818, M_w = 24110, PDI = 6.31. **(PFO)47(SBN)53**: ^{1}H NMR ($CDCl_3$, 300 MHz): δ 8.30-7.40 (m, 2.33H), 3.80 (m, 1H), 2.04 (m, 0.584H), 1.35-0.936 (m, 3.14H), 0.916-0.437 (m, 1.55H). Yeild: 47%, M_n = 3292, M_w = 16873, PDI = 5.13.

2-2-2. Enantio-selective separation of (*n*,*m*)SWCNTs. CoMoCAT-SWCNTs (SWeNT®SG65, SouthWest NanoTechnologies, Co.) were purchased from Aldrich and used as received. A typical procedure for the SWCNT dissolution using the copolymers is as follows. The SWCNTs (1 mg) and the copolymer (3 mg) were sonicated in toluene (3 ml) for 1 h and the dispersion was centrifuged at 10000 g for 1 h followed by collection of the supernatant (upper 80%) for measurements. Vis-NIR absorption, circular dichroism and PL spectra were measured using a spectrophotometer (JASCO, type V-570), a circular dichroism spectropolarimeter (JASCO, type J-820), and a spectrofluorometer equipped with a liquid-nitrogen-cooled InGaAs near-IR detector (Horiba-Jobin Yvon, SPEX Fluorolog-3-NIR), respectively. The excitation and emission wavelengths for PL measurements were in the range of 500–850 and 900–1400 nm, respectively.

2-2-3. Molecular mechanical simulations. The molecular mechanics simulations were carried out using MacroModel (Infocom, version 8.6) with the OPLS-2005 force field. Dielectric constants were kept at 2.3. Minimization on the calculation was carried out using the Polak-Ribiere conjugate gradient with a convergence threshold on the gradient of 0.05 $kJmol^{-1}$. Default values were used for all other parameters.

2-3. Results and discussion

2-3-1. Selective recognition/extraction of SWCNTs by chiral copolymers

Twelve copolymers were synthesized with different compositions by means of altering copolymerization ratios through Yamamoto coupling reaction. The resulting ratio between PFO(x) and RBN/SBN(y) was determined quantitatively by ^{1}H NMR spectroscopy, that is, For **(PFO)x(RBN)y**, (x:y) = (86:14), (76:24), (71:29), (68:32), (61:39) and (44:56), and for **(PFO)x(SBN)y**, (x:y) = (85:15), (72:28), (65:35), (55:45), (51:49) and (47:53), respectively. Throughout this thesis the copolymers are named based on the percentage of each comonomer units.

The UV-Vis absorption and circular dichroism (CD) spectra of typical copolymers in toluene are shown in Figure 2-2 (a, b), in which **(PFO)x(RBN)y** and **(PFO)x(SBN)y** showed almost mirror-image CD spectra (Fig. 2-3 and 2-4). The introduction of bulky binaphthol moiety caused blue shift due to the decreased effective conjugation, which suggests that copolymers were allowed to have various conformations compared to normal PFOs. CD intensity also reflected the amount of chiral BN moiety as shown in Figure 2-2 (c, d) in which CD intensity was plotted as a function of RBN or SBN ratios (y).

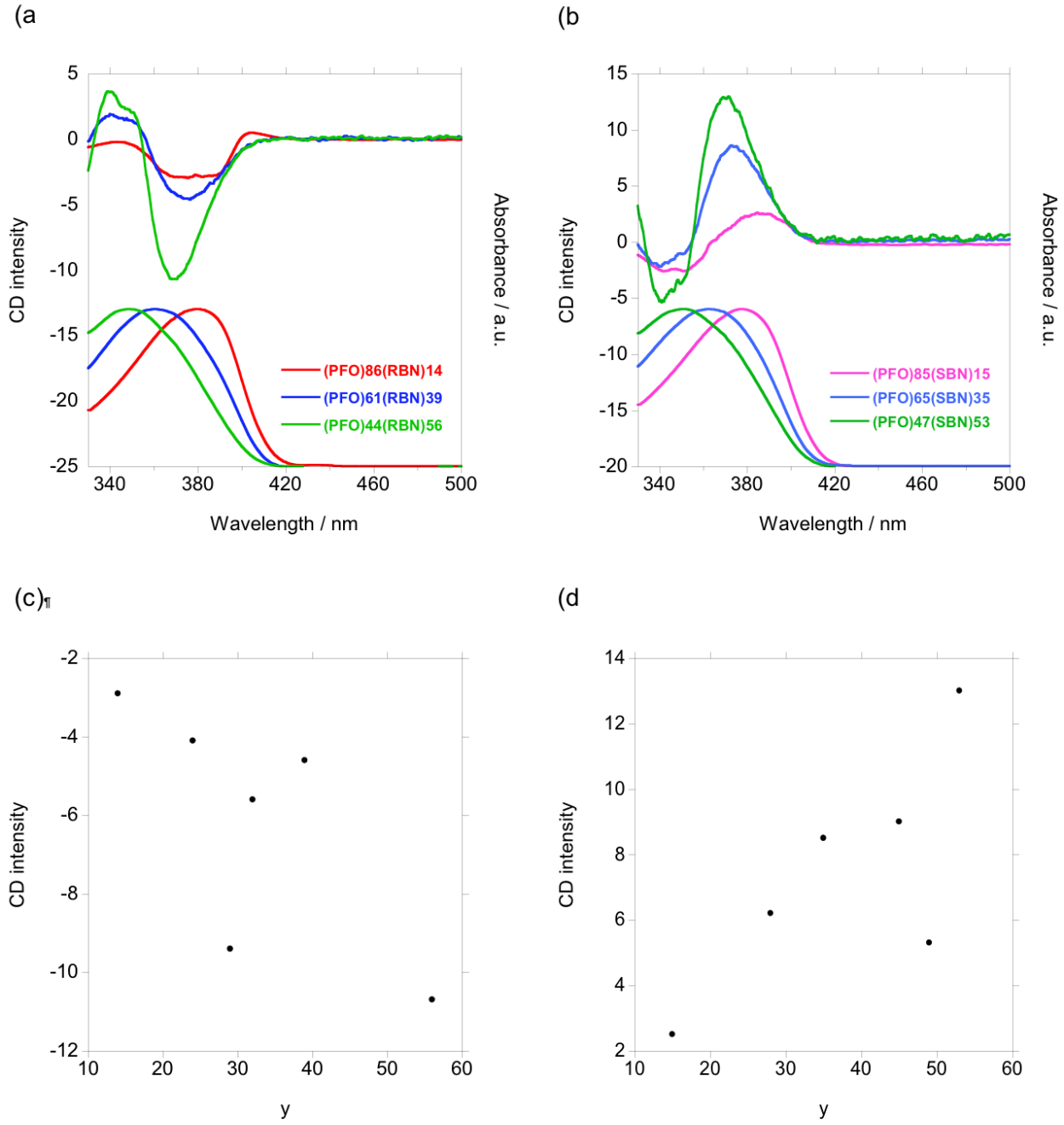

Figure 2-2. UV-Vis absorption and CD spectra of **(PFO)x(RBN)y** (x: y; 86: 14, 61: 39, 44: 56) (a) and **(PFO)x(SBN)y** (x: y; 85: 15, 65: 35, 47: 53) (b). CD spectra are normalized based on the absorbance intensity of the copolymers at maximum wavelength. The CD intensity are plotted as a function of RBN (c) and SBN ratios (d). Adapted from ref. 35 with kind permission. Copyright 2012 American Chemical Society.

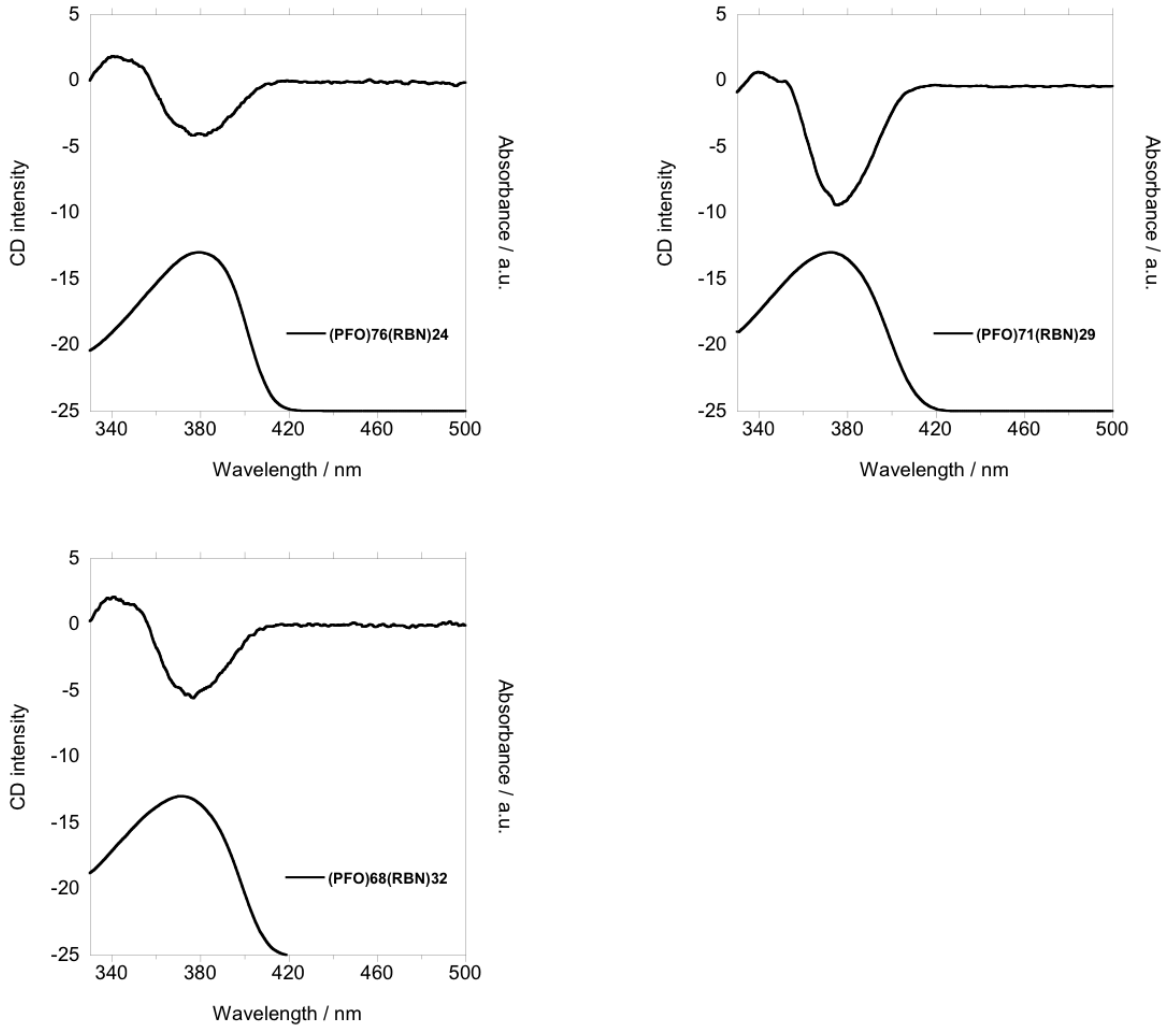

Figure 2-3. Absorption and CD spectra of (PFO)x(RBN)y (x: y; 86: 14, 76: 24, 71 : 29, 68 : 32, 61 : 39, 44: 56). Adapted from ref. 35 with kind permission. Copyright 2012 American Chemical Society.

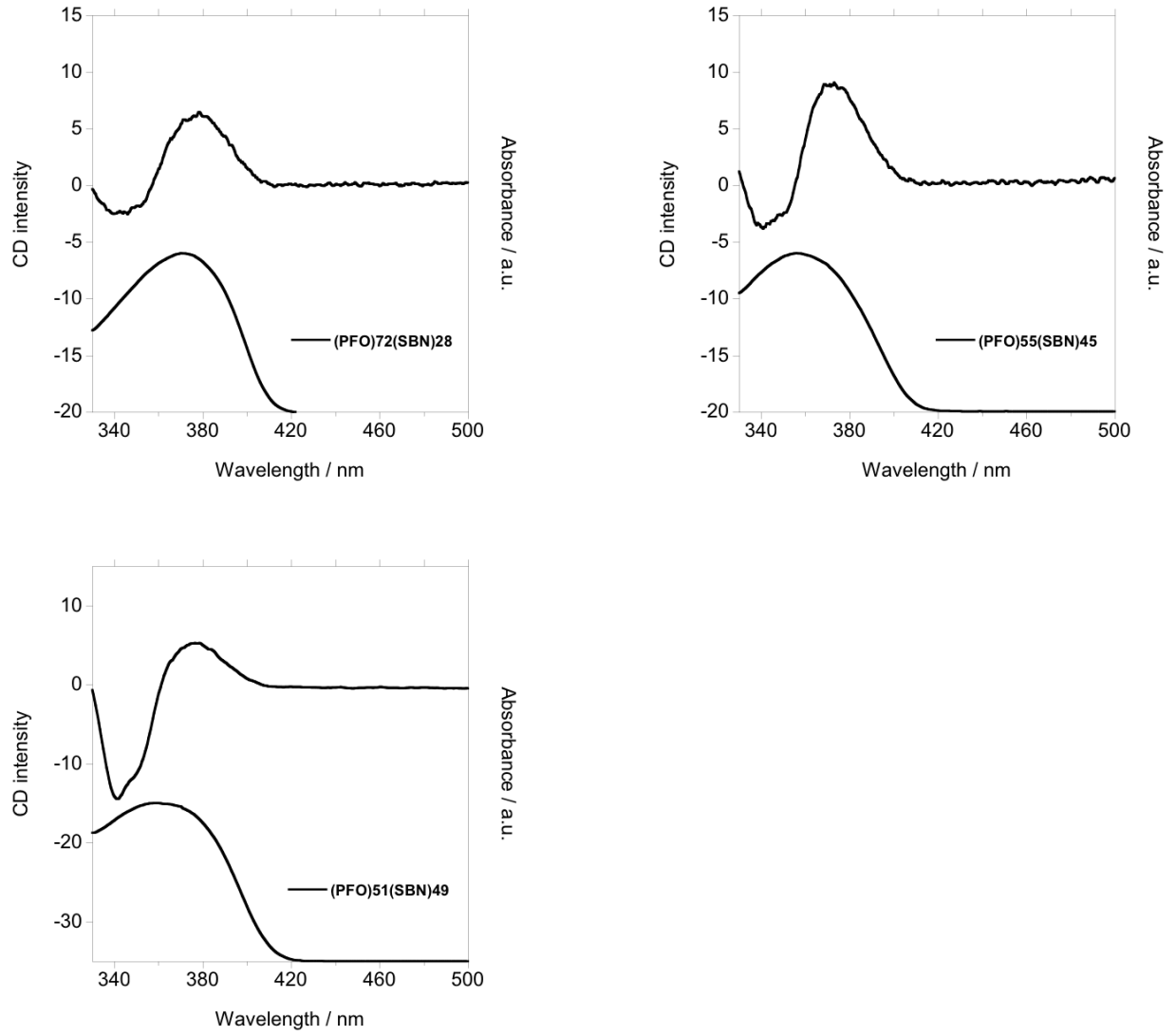

Figure 2-4. Absorption and CD spectra of (PFO)x(SBN)y (x: y; 85: 15, 72: 28, 65: 35, 55: 45, 51: 49, 47: 53). Adapted from ref. 35 with kind permission. Copyright 2012 American Chemical Society.

The Vis-NIR absorption spectra of the solubilized SWCNTs using the copolymers are shown in Figure 2-5, in which I observe the first (E^s_{11}) and second (E^s_{22}) semiconducting bands of the SWCNTs, and almost no metallic band appeared in the range of 400-550 nm. The results clearly indicate that all the used copolymers dissolved semiconducting SWCNTs with a high selectivity like normal PFO. Furthermore, the introduction of RBN or SBN into the PFO gradually altered the preferred chirality indices (*n*,*m*) of the extracted SWCNTs as compared to normal PFO, depending on the composition ratios of the copolymers.

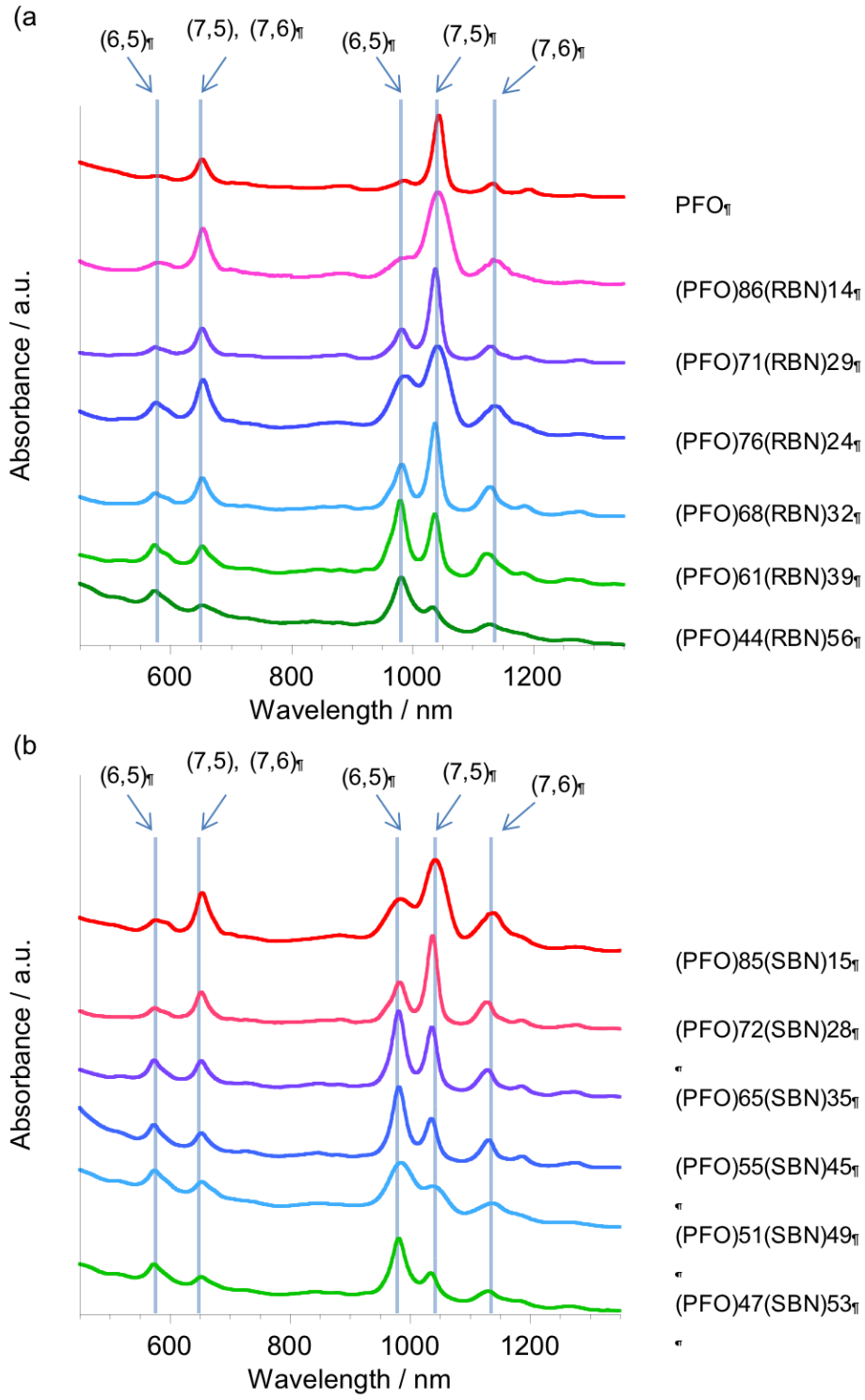

Figure 2-5. Absorption spectra of SWCNTs solubilized by **PFO**, **(PFO)x(RBN)y** (x: y; 90: 10, 86: 14, 76: 24, 71 : 29, 61 : 39, 44 : 56) (a) and **(PFO)x(SBN)y** (x: y; 85: 15, 72: 28, 65: 35, 55: 45, 51: 49, 47: 53) (b). Adapted from ref. 35 with kind permission. Copyright 2012 American Chemical Society.

In order to assign the precise chirality index and the relative amount of solubilized SWCNT species, photoluminescence (PL) spectroscopy was measured on all the twelve samples. The typical two-dimensional PL mapping of the copolymer-solubilized SWCNTs is shown in Figure 2-6 and calibrated content of the SWCNT species assessed from the PL mappings are summarized in Table 2-1 and 2-2. It is evident that the composition ratio of each comonomer units plays an important roll in sorting SWCNT chirality, as seen in our previous report on fluorene-based copolymers.[19] In the present **(PFO)x(RBN/SBN)y** copolymers, higher content of PFO enriched (7,5)SWCNT, whereas the increase of RBN/SBN composition ratio enabled extraction of (6,5), (7,6) and (8,6) species.

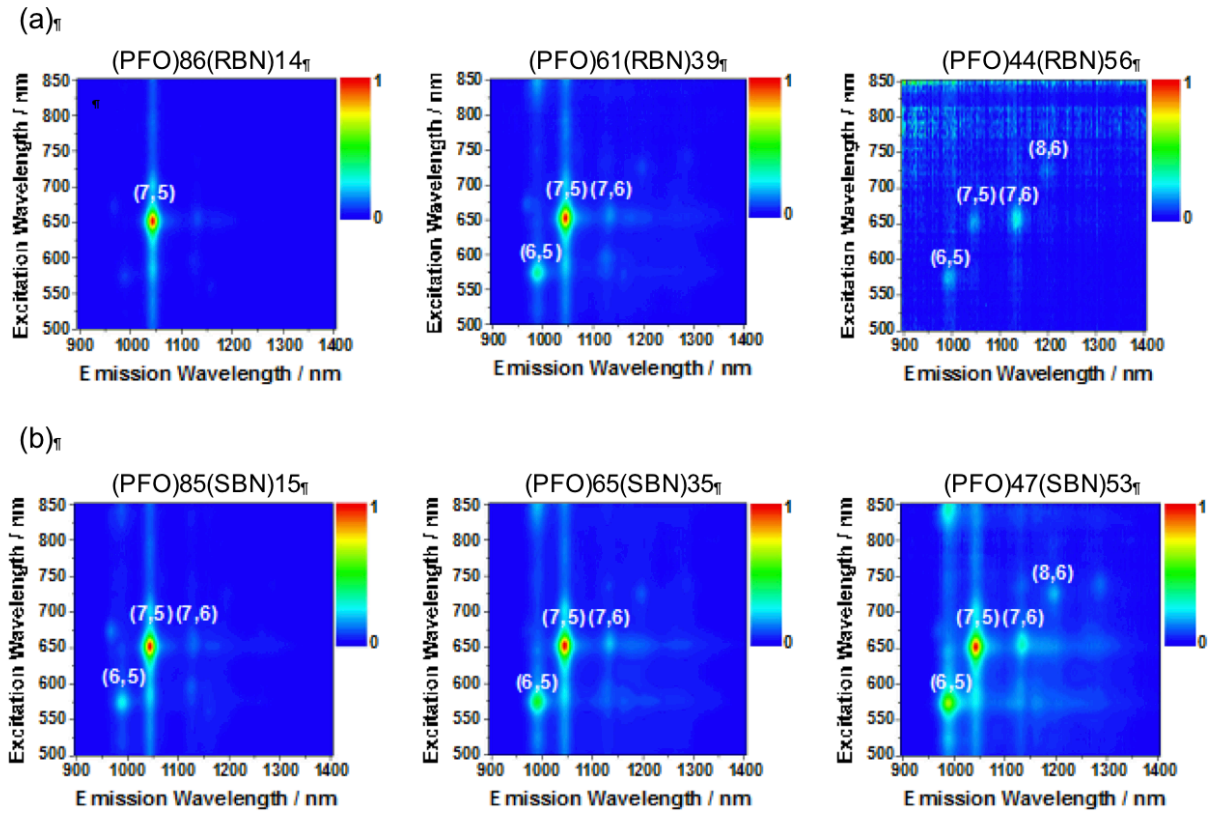

Figure 2-6. Two-dimensional Photoluminescence (PL) mapping of SWCNTs solubilized by copolymers (PFO)x(RBN)y (x: y; 86: 14, 61 : 39, 44: 56) (a) and (PFO)x(SBN)y (x: y; 85: 15, 65: 35, 47: 53) (b). Adapted from ref. 35 with kind permission. Copyright 2012 American Chemical Society.

Table 2-1. Calibrated content of the SWCNT species deduced from the PL mappings of the samples prepared using copolymers (PFO)x(RBN)y or (PFO)x(SBN)y in toluene. Adapted from ref. 35 with kind permission. Copyright 2012 American Chemical Society.

chiral index (n,m)	calibrated content/ %[a]		
	(PFO)86(RBN)14	**(PFO)61(RBN)39**	**(PFO)44(RBN)56**
(6,5)	4.27	27.2	18.3
(7,5)	82.7	39.6	18.7
(7,6)	10.6	23.4	39.0
(8,6)	2.46	9.76	24.0

chiral index (n,m)	calibrated content/ %[a]		
	(PFO)85(SBN)15	**(PFO)65(SBN)35**	**(PFO)47(SBN)53**
(6,5)	38.0	25.9	23.1
(7,5)	48.7	50.7	44.5
(7,6)	9.88	16.4	19.4
(8,6)	3.39	6.98	13.1

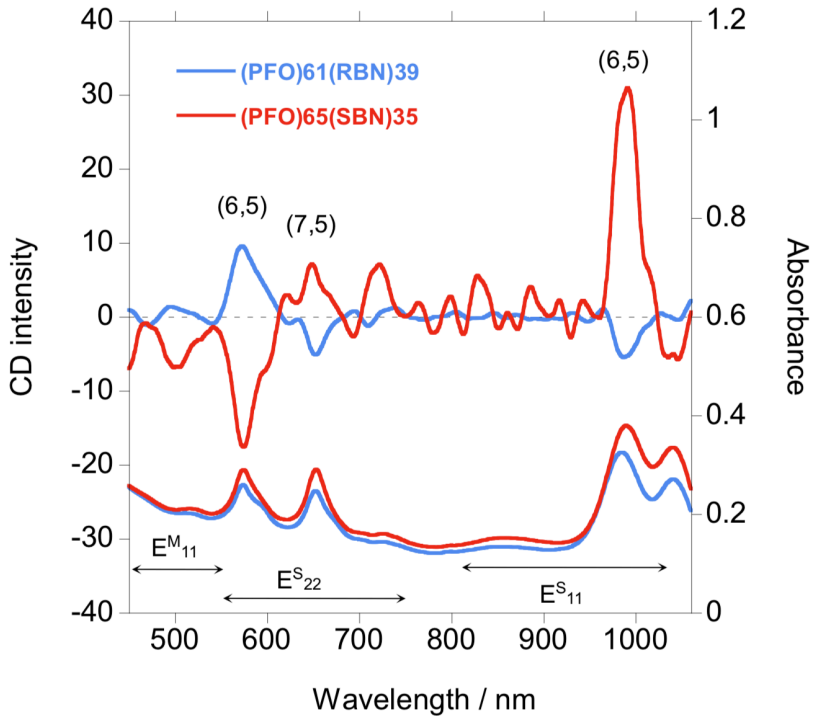

Figure 2-7. Absorption and CD spectra of SWCNTs extracted with (PFO)61(RBN)39 (blue) and (PFO)65(SBN)35 (red). CD spectra are normalized based on the absorbance intensity of the SWCNTs at 574 nm. Adapted from ref. 35 with kind permission. Copyright 2012 American Chemical Society.

Figure 2-7 shows the Visible-NIR absorption and CD spectra (intensity is normalized at 574 nm) of the SWCNTs solubilized by **(PFO)61(RBN)39** and **(PFO)65(SBN)35**, in which evident CD peaks are observed in the region of the second (E^s_{22}) and the first (E^s_{11}) semiconducting bands of the SWCNTs (for absorption and CD spectra of the SWCNTs solubilized with the other copolymers, see Fig. 2-8 and 2-9). To eliminate the possibility of induced CD[30] from chiral copolymers on SWCNT/copolymers composites, in-situ copolymer exchange reaction with the incorporation of optically neutral copolymer was conducted. Here, as an achiral copolymer, poly(9,9-dioctylfluorene 2,2'-bipyridine) (**PFO-Bpy**) was used to replace the chiral copolymers on solubilized (6,5)SWCNTs because it has stronger affinity especially to (6,5)SWCNT and causes indicative absorption peak shift (~9 nm) relative to the pristine (6,5)SWCNT in the NIR

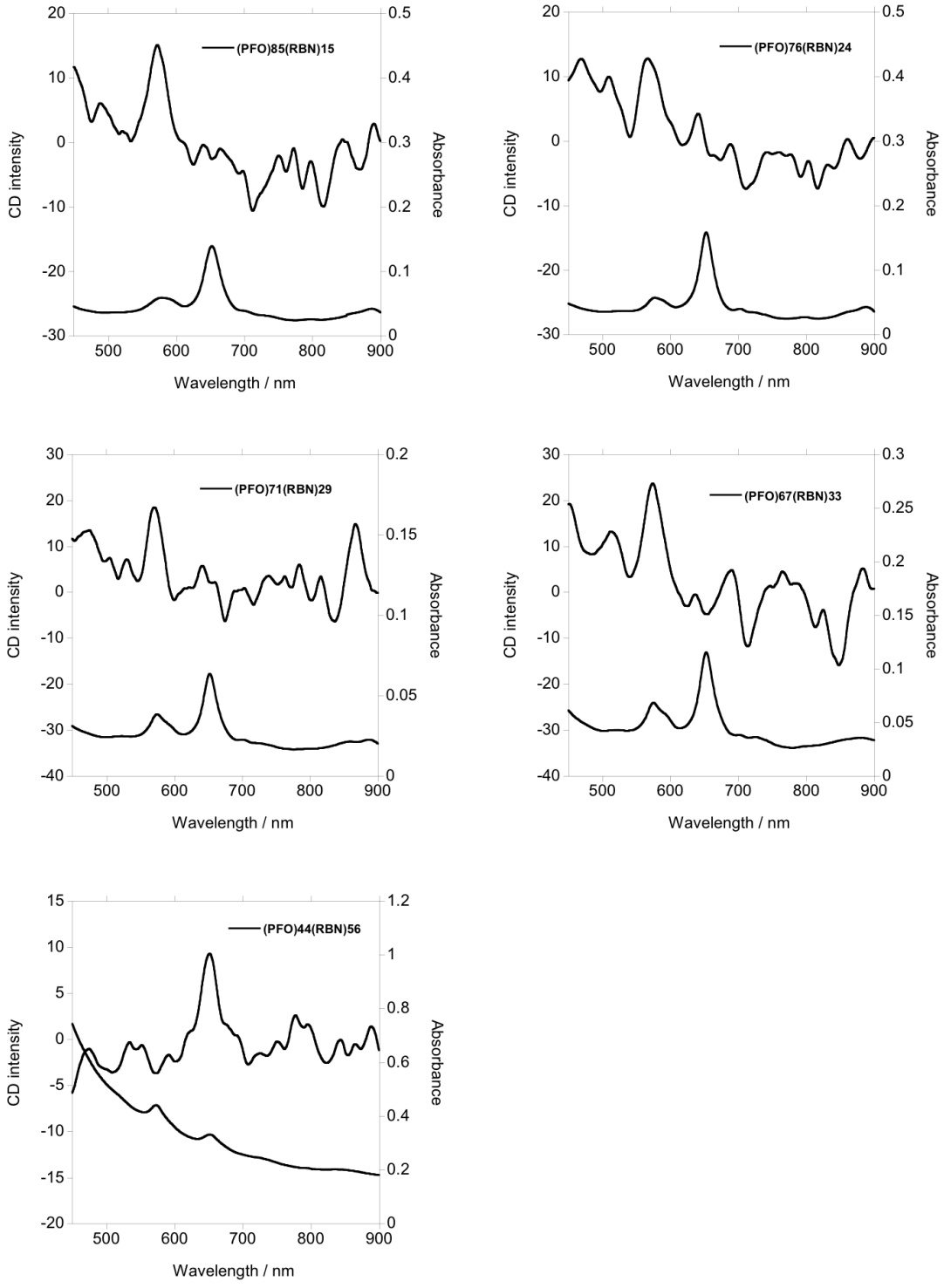

Figure 2-8. Absorption and CD spectra of SWCNTs extracted with (PFO)x(RBN)y (x: y; 86: 14, 76: 24, 71 : 29, 67 : 33, 44: 56). CD spectra are normalized based on the absorbance intensity of the SWCNTs at 574 nm. Adapted from ref. 35 with kind permission. Copyright 2012 American Chemical Society.

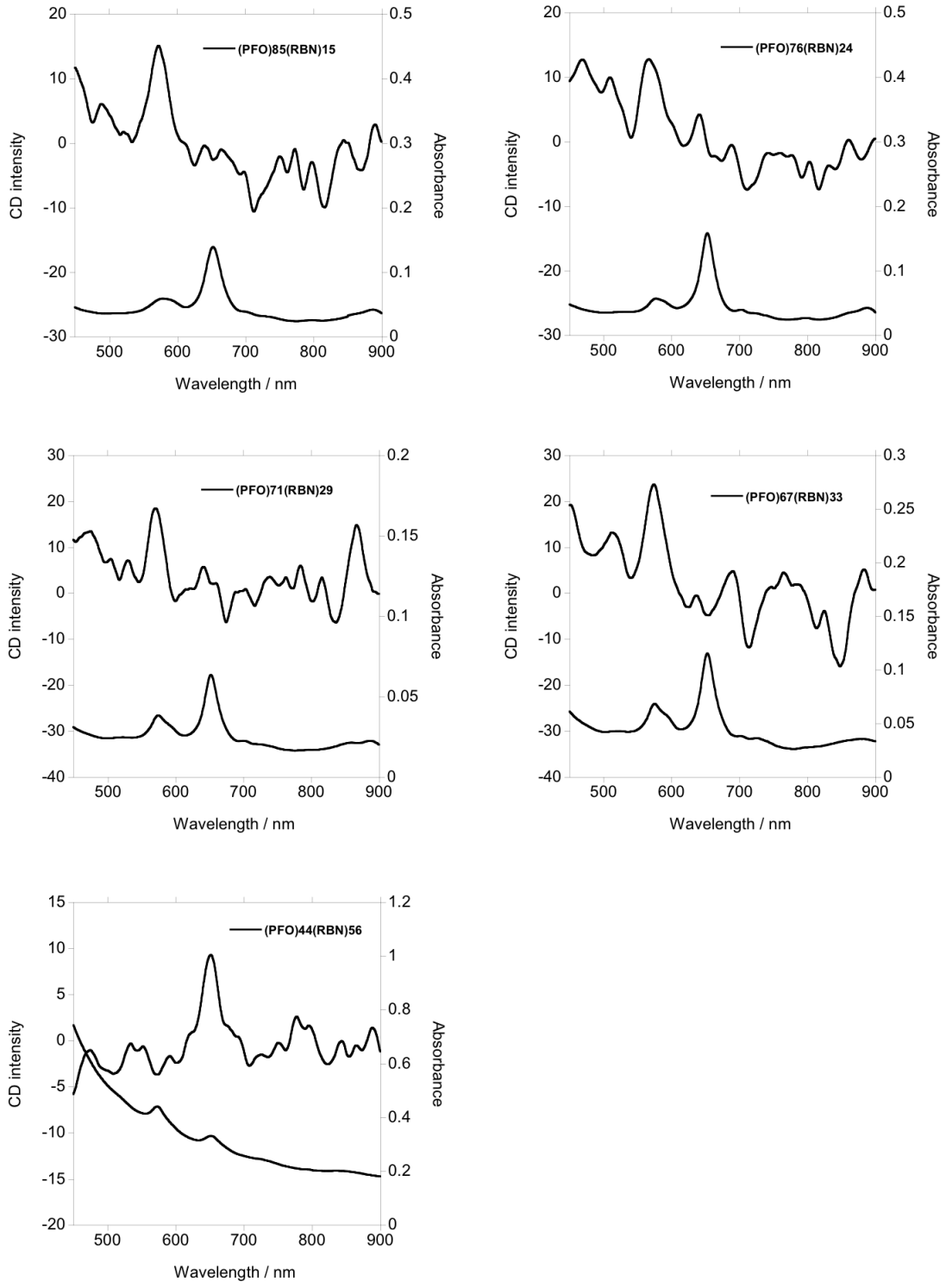

Figure 2-9. Absorption and CD spectra of SWCNTs extracted with (PFO)x(SBN)y (x: y; 82: 18, 72: 28, 60: 40, 55 : 45, 52: 48, 48: 52). CD spectra are normalized based on the absorbance intensity of the SWCNTs at 574 nm. Adapted from ref. 35 with kind permission. Copyright 2012 American Chemical Society.

region, which I reported previously.[23] As a control, I found no optical activity over the same spectral range in PFO-Bpy-solubilized SWCNTs, in which I confirmed that PFO-Bpy extracts racemic (6,5)SWCNTs. The obtained Vis-NIR absorption spectra of E^s_{11} region of the (6,5)SWCNT after copolymer exchange in SWCNTs/**(PFO)61(RBN)39** solution was almost identical to that obtained with **PFO-Bpy** (See the Figure 2-10). These demonstrated that the solubilizing copolymers on (6,5) SWCNT were successfully exchanged from the original chiral copolymer to **PFO-Bpy**. On the other hand, the CD spectral change was not significant after the addition of **PFO-Bpy** to the solution, namely, before and after addition of **PFO-Bpy**, CD intensity around 574 and 653 nm was 9.52 and 9.35, respectively. Consequently, it is evident that the observed spectra was not induced CD but real ones arose from the E^s_{22} band of the enantiomers of the semiconducting (6,5)SWCNTs (around 574 nm), and (7,5)SWCNTs (around 653 nm).

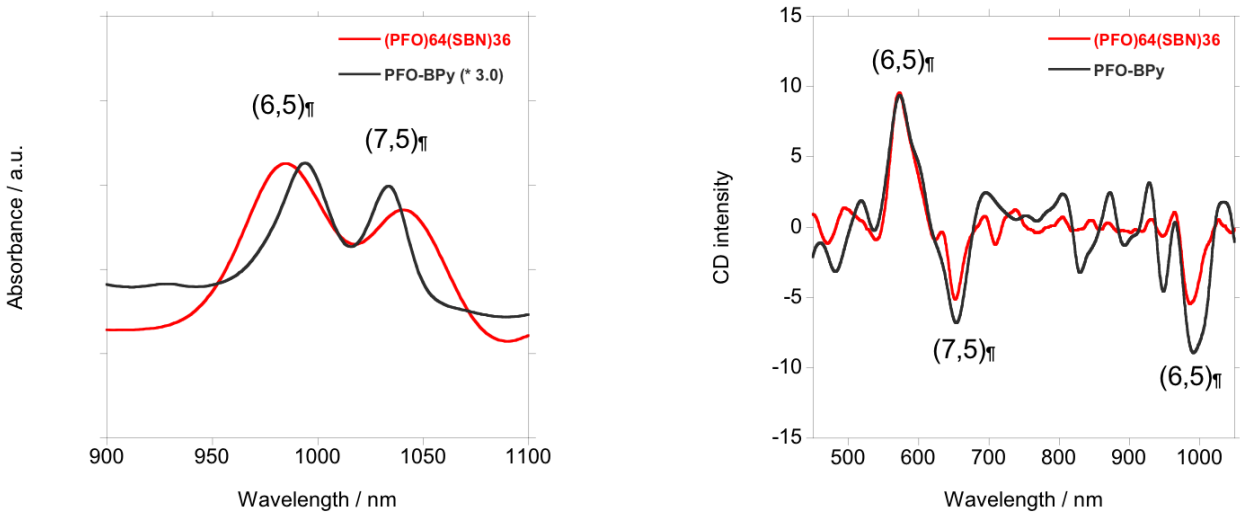

Figure 2-10. Absorption (left) and CD (right) spectra of SWCNTs extracted with (PFO)64(RBN)36 and PFO-BPy. Absorption spectra normalized at their maximum absorption wavelength. CD spectra are normalized based on the absorbance intensity of the SWCNTs at 574 nm. Adapted from ref. 35 with kind permission. Copyright 2012 American Chemical Society.

2-3-2. The effect of composition ratios of solubilizing copolymers.

The effect of composition ratios of **(PFO)x(RBN)y** and **(PFO)x(SBN)y** is now discussed based on the CD intensity of the extracted SWCNT enantiomers. This result is shown in Figure 2-11 as a plot of CD intensity at 574 nm of the extracted SWCNTs versus composition ratios (y) of RBN or SBN in the copolymers. In this thesis, SWCNT enantiomers are labeled as (+) or (-) according to whether their CD signals at the E^{s}_{22} band are positive or negative. It was to our surprise that the CD intensity of solubilized SWCNT enantiomers was not simply proportional to the amount of chiral binaphthol in the copolymers. In the case with **(PFO)x(RBN)y**, during the ratio of RBN moiety (y) in the copolymer was up to 39%, the (+)SWCNTs were enriched, whereas CD signal dramatically inverted at higher y values ending up at (-)SWCNTs enrichment with the copolymer **(PFO)44(RBN)56**. Comparable behavior was also observed when **(PFO)x(SBN)y** was used, namely, with the y value in the **(PFO)x(SBN)y** was 15 to 35, the amount of (-)SWCNTs were multiplied, while the other copolymers with higher y values extracted (+)SWCNTs. Considering the large structural change of the copolymers upon altering the composition ratio, as indicated by the blue shift in Figure 2-2(a, b), it was suggested that the amount of chiral moiety and the conformation of the copolymers cooperatively determine the affinity to the handedness of SWCNT enantiomers. These chiral copolymers' drastic but still controllable preference on extracting both SWCNT enantiomers allows the relevant separation parameters to be identified and optimized. For the origin of crossover observed for the recognition of enantiomer according to the composition ratios of the copolymer is discussed using molecular mechanics simulation in the section 2-3-3.

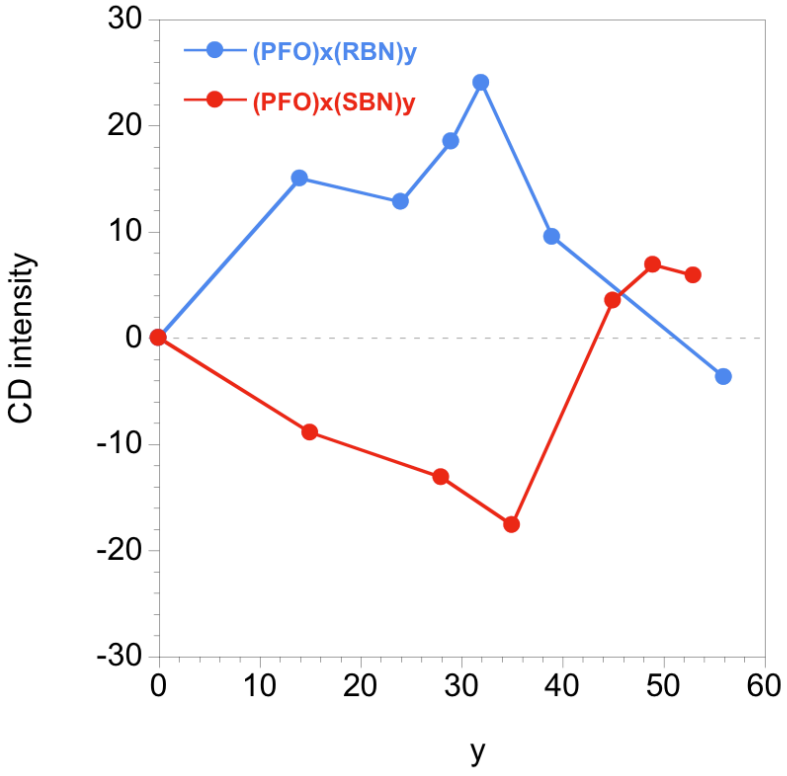

Figure 2-11. CD intensity at 574 nm of the extracted SWCNTs plotted as a function of composition ratios of RBN or SBN in the copolymers. Adapted from ref. 35 with kind permission. Copyright 2012 American Chemical Society.

To estimate the performance of enantio-selective extraction of SWCNTs by our chiral copolymers, I applied the following equation (1), which was presented by Wang et al.[13], placing optical purity of the extracted enantiomer as CD_{norm},

$$CD_{norm} = (CD_{raw} / L_{CD}) / (A_{E22} / L_{abs}) \qquad (1)$$

where CD_{raw} is the CD intensity at 574 nm of the E^s_{22} transition, A_{E22} is the background-corrected absorption intensity at 574 nm of the E^s_{22} transition, and L_{CD} and L_{abs} are the path lengths of the optical cell used in the measurements. Our result and other reported values obtained by different method are summarized in Table 2-2. In our study so far, the maximum enantiomer purity (CD_{norm}) of 24 mdeg was obtained by using **(PFO)68(RBN)32** toward (+)(6,5)SWCNT, and this recorded the equivalent value to molecular recognition method by Komatsu et al.[13] This value is lower than those obtained by Hersam et al.[14,15] and Weisman et al.[16] using DGU methods. Nevertheless, our copolymer method still has room for improving purity and selectivity of enantiomer recognition by optimizing the composition ratios and molecular weight of the copolymer.

Table 2-2. Comparison of Enantiomer Purity of (6,5)SWCNTs Extracted by Four Different Methods. Adapted from ref. 35 with kind permission. Copyright 2012 American Chemical Society.

method	CD_{raw} / mdeg	L_{CD} / cm	A_{E22}	L_{abs} / cm	CD_{norm} / mdeg	reference
DGU	-41.6	1.0	0.77	1.0	54	Ref 15
DGU	20	1.0	0.55	1.0	36	Ref 16
Molecular recognition	4.0	10	0.017	1.0	24	Ref 13
Enantiomer separation using (PFO)68(RBN)32	0.60	1.0	0.025	1.0	24	This study

2-3-3. Molecular mechanics simulations

In this study, our copolymers exhibited two intriguing SWCNT recognition/extraction behavior, one is specific enantiomer recognition and the other is drastic inversion of preference between copolymer (*R*) or (*S*) to SWCNT (+) or (-) depending on the copolymer composition ratios. In an effort to understand the origin of these enantiomer recognition behavior of the copolymers toward the SWCNTs, molecular mechanics simulations using the OPLS2005 force field[27] were utilized to model the interactions between (6,5)SWCNT enantiomers with the copolymers, and as a comparison, PFO was also employed. The initial structure of the polymers were reflected the composition ratio and the average molecular weight of the synthesized polymers, and the length were set around 86 nm. (6,5)SWCNTs in the calculation were 172 nm long so as to keep copolymers to stay around the center of SWCNT surface, and enantiomers are identical except for helicity. The binding energy (E_{bind}) of the wrapped SWCNT is calculated by using equation (2),

$$E_{bind} = E_{complex} - (E_{SWCNT} + E_{polymer}) \qquad (2)$$

Where $E_{complex}$, $E_{polymer}$, and E_{SWCNT} represent the potential energies of the complex, polymer, and SWCNTs, respectively. Assuming same energy would be obtained from identical conformation, and neglecting periodic heterogeneous fluctuation on the surface of calculated SWCNTs induced by their edge structure, resulting binding energy could be considered as an indicator of chiral interactions between copolymers and SWCNTs. As the representative copolymer of lower content of RBN/SBN, **(PFO)60(RBN)40** and **(PFO)60(SBN)40** were modeled to simulate the copolymers which extracted SWCNT enantiomers most efficiently in the experiment. The calculated potential energies using **(PFO)60(RBN)40** are summarized in Table

2-3 showing greater binding energies (-632.547 kcal mol^{-1}) was obtained with left-handed (6,5)SWCNT compared to that with right-handed one (-621.032 kcal mol^{-1}). Contrastive behavior was observed when **(PFO)60(SBN)40** were applied, anmely, the binding energy with right-handed SWCNT was greater (-634.383 kcal mol^{-1}) than that with left-handed SWCNT (-618.727 kcal mol^{-1}) (Table 2-4**)**. In order to confirm this values to be distinguished, **PFO** were applied in the calculation with each SWCNT enantiomers. The E_{bind} of left-handed SWCNT with the **PFO** was -623 kcal mol^{-1}, meanwhile, E_{bind} of right-handed SWCNT with the **PFO** was -625 kcal mol^{-1}. The difference (~2 kcal mol^{-1}) is relatively smaller compared to that obtained with chiral copolymers. Considering that the same energies were obtained for each enantiomers of SWCNT and also **(PFO)60(RBN)40** and **(PFO)60(SBN)40** showed negligible difference among their $E_{polymer}$, all those results indicate the distinct enantiomer recognition of **(PFO)60(RBN)40** and **(PFO)60(SBN)40** on the (6,5)SWCNT enantiomers. A further calculations were carried out for the (6,5)SWCNT enantiomers with **(PFO)44(RBN)56** and **(PFO)44(SBN)56** in order to explain the enantiomer recognition inversion by changing the composition ratios of the copolymers. The E_{bind} of the complex of **(PFO)44(RBN)56** with right-handed SWCNT was -635 kcal mol^{-1}, and with left-handed SWCNT resulted in lower value of -627 kcal mol^{-1}. Opposite behavior was observed when **(PFO)44(SBN)56** were applied, namely, the E_{bind} were -648 and -634 kcal mol^{-1} for the complex with left-handed SWCNT and right-handed SWCNT, respectively (Table 2-5, Table 2-6). These contrastive behaviors of the copolymers depending on their composition ratio agreed well to the experimental results. I sought the reason for the energy change of the complexes from comparing their wrapping conformations shown in Figure 2-12 and Figure 2-13. It is remarkable that the wrapping direction of the copolymers flipped by altering the composition ratios even though they have same chiral moieties, in other words, for the complex with (+)(6,5)SWCNT,

(PFO)60(RBN)40 showed clockwise winding, while **(PFO)44(RBN)56** wrapped the SWCNT in anticlockwise direction, and the other copolymers behaved in the same manner. Such dramatic conformation change could be the trigger to adapt the preferential interaction between the chiral copolymers and the SWCNTs cooperatively with the degree of the embedded chirality. To the best of our knowledge, the relationship between SWCNT's handedness and optical activity is still in discussion, therefore, I could not simply conclude that these simulations explain the realistic situations, nevertheless, I believe this approach and result might be a help to understand and design the interaction between copolymers and SWCNTs.

Table 2-3. Calculated potential and binding energies between (6,5)SWCNT enantiomers with **(PFO)60(RBN)40**. Adapted from ref. 35 with kind permission. Copyright 2012 American Chemical Society.

(6,5)SWNTs	potential energy of SWNT (E_{SWNT}) / kcal mol^{-1}	potential energy of (PFO)60(RBN)40 ($E_{polymer}$) / kcal mol^{-1}	total potential energy ($E_{polymer} + E_{SWNT}$) / kcal mol^{-1}	potential energy of complex ($E_{complex}$) / kcal mol^{-1}	binding energy $E_{bind} = E_{complex} - (E_{polymer} + E_{SWNT})$ / kcal mol^{-1}
Left-handed	88163	1437	89600	88967	-633
Right-handed	88163	1437	89600	88979	-621

Table 2-4. Calculated potential and binding energies between (6,5)SWCNT enantiomers with **(PFO)60(SBN)40**. Adapted from ref. 35 with kind permission. Copyright 2012 American Chemical Society.

(6,5)SWNTs	potential energy of SWNT (E_{SWNT}) / kcal mol^{-1}	potential energy of (PFO)60(SBN)40 ($E_{polymer}$) / kcal mol^{-1}	total potential energy ($E_{polymer} + E_{SWNT}$) / kcal mol^{-1}	potential energy of complex ($E_{complex}$) / kcal mol^{-1}	binding energy $E_{bind} = E_{complex} - (E_{polymer} + E_{SWNT})$ / kcal mol^{-1}
Left-handed	88163	1437	89600	88981	-619
Right-handed	88163	1437	89600	88965	-635

Table 2-5. Calculated potential and binding energies between (6,5)SWCNT enantiomers with the **(PFO)44(RBN)56**. Adapted from ref. 35 with kind permission. Copyright 2012 American Chemical Society.

(6,5)SWNTs	potential energy of SWNT (E_{SWNT}) / kcal mol^{-1}	potential energy of (PFO)44(RBN)56 ($E_{polymer}$) / kcal mol^{-1}	total potential energy ($E_{polymer} + E_{SWNT}$) / kcal mol^{-1}	potential energy of complex ($E_{complex}$) / kcal mol^{-1}	binding energy $E_{bind} = E_{complex} - (E_{polymer} + E_{SWNT})$ / kcal mol^{-1}
Left-handed	88163	1566	89729	89102	-627
Right-handed	88163	1566	89729	89094	-635

Table 2-6. Calculated potential and binding energies between (6,5)SWCNT enantiomers with **(PFO)44(SBN)56**. Adapted from ref. 35 with kind permission. Copyright 2012 American Chemical Society.

(6,5)SWNTs	potential energy of SWNT (E_{SWNT}) / kcal mol^{-1}	potential energy of (PFO)44(SBN)56 ($E_{polymer}$) / kcal mol^{-1}	total potential energy ($E_{polymer} + E_{SWNT}$) / kcal mol^{-1}	potential energy of complex ($E_{complex}$) / kcal mol^{-1}	binding energy $E_{bind} = E_{complex} - (E_{polymer} + E_{SWNT})$ / kcal mol^{-1}
Left-handed	88163	1566	89729	89081	-648
Right-handed	88163	1566	89729	89095	-634

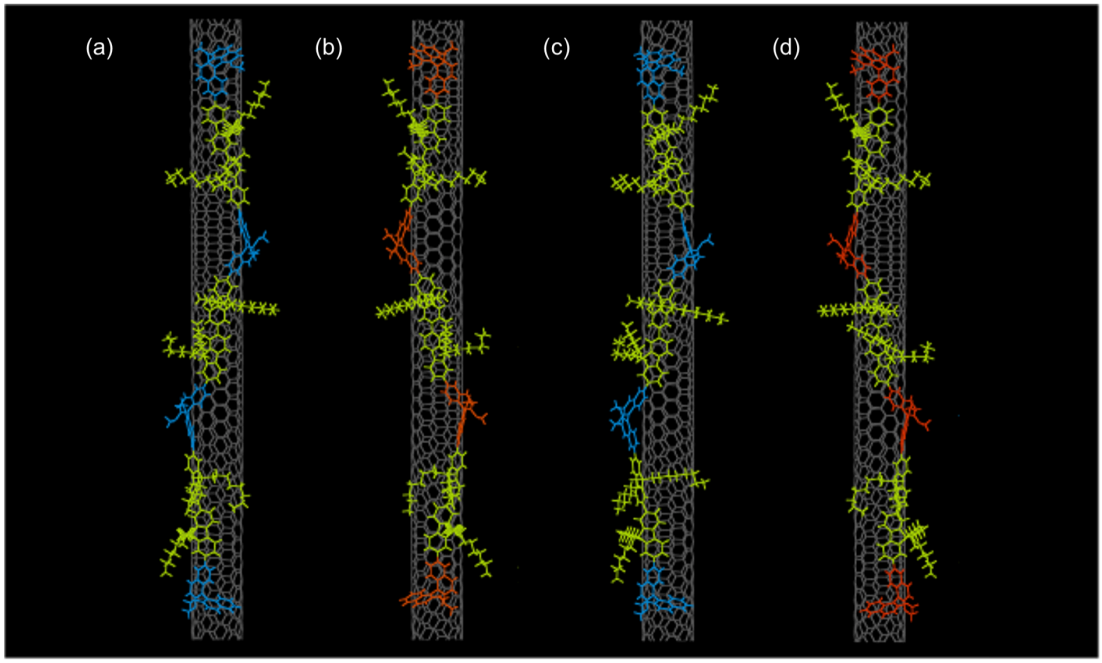

Figure 2-12. Modeled structures of left-handed SWCNT with **(PFO)60(RBN)40** (a), left-handed SWCNT with **(PFO)60(SBN)40** (b), right-handed SWCNT with **(PFO)60(RBN)40** (c), and right-handed SWCNT with **(PFO)60(SBN)40** (d). Adapted from ref. 35 with kind permission. Copyright 2012 American Chemical Society.

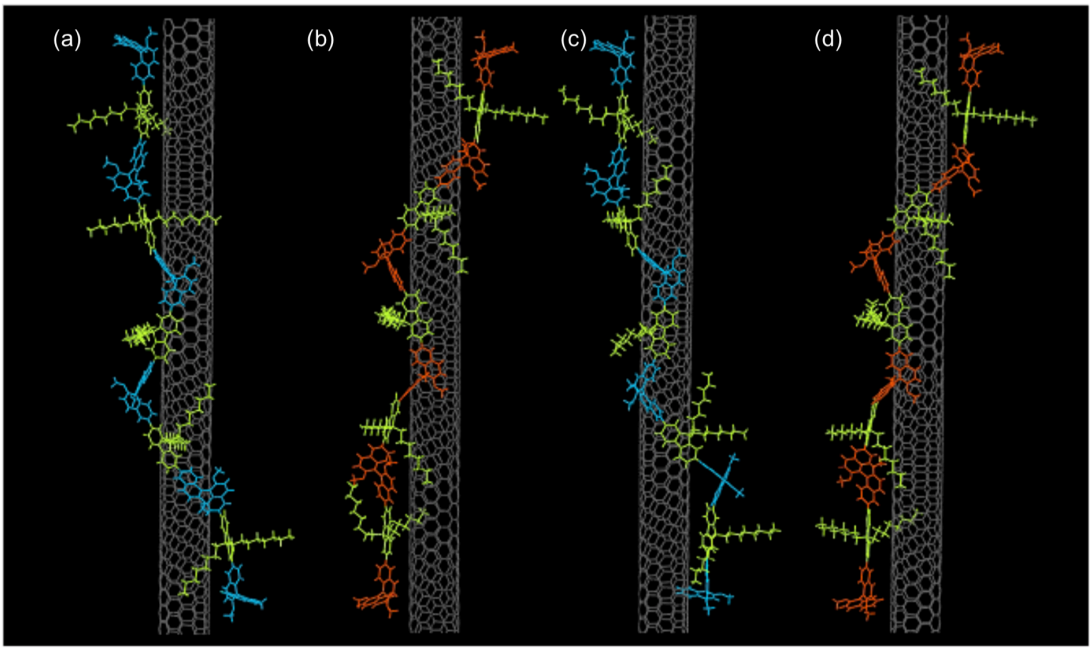

Figure 2-13. Modeled structures of left-handed SWCNT with the **(PFO)44(RBN)56** (a), left-handed SWCNT with **(PFO)44(SBN)56** (b), right-handed SWCNT with **(PFO)44(RBN)56** (c), and right-handed SWCNT with **(PFO)44(SBN)56** (d). Adapted from ref. 35 with kind permission. Copyright 2012 American Chemical Society.

2-4. Conclusions

In summary, I have rationally extended the ability of fluorene-based copolymer family for sorting semiconducting SWCNTs with enantio-selective separation/extraction. The key factor was introducing bulky (*R*)- or (*S*)- chiral binaphtol moieties. All of our chiral copolymers separated the SWCNT enantiomers successfully, and the maximum separation efficiency was obtained with **(PFO)68(RBN)32** toward (+) (6,5)SWCNT. With the systematically synthesized twelve copolymers with various composition ratios between fluorene and binaphthol, I have disclosed that the synthesized (*R*)- or (*S*)- chiral copolymers extract both right- and left-handed SWCNT enantiomers by altering the composition ratios of the copolymers. This recognition inversion behavior was moderately accounted by the cooperative effect of chiral and conformational interactions, which was revealed by molecular mechanics simulation based on binding energies. The basic idea of this study will accelerate further improvement of strategic molecular design for enantio-selective SWCNT sorting with a selected or single chirality. Additional investigations for improving this method including the newly designed and synthesized copolymers with various chiral moieties are now undergoing.

REFERENCES

(1) Dai, H. *Acc. Chem. Res.* **2002**, *35*, 1035-1044.

(2) Gao, X.; Li, K. *International Journal of Solids and Structures* **2003**, *40*, 7329-7337.

(3) Zhao, X. Lu, X. Tze, W. T. Y.; Wang, P. *Biosensors and Bioelectronics* **2010**, *25*, 2343-2350.

(4) Fujigaya, T. Okamoto, M.; Nakashima, N. *Carbon* **2009**, *47*, 3227-3232.

(5) Okamoto, M. Fujigaya, T.; Nakashima, N. *small* **2009**, *5*, 735-740.

(6) Hong, H. Gao, T.; Cai, W. *Nano Today* **2009**, *4*, 252-261.

(7) Odom, T. W.; Huang, J.-lin, Kim, P.; Lieber, C. M. *Nature* **1998**, *391*, 62-64.

(8) Ouyang, M. I. N. Huang, J.-lin; Lieber, C. M. *Acc. Chem. Res.* **2002**, *35*, 1018-1025.

(9) Tasaki, S.; Maekawa, K.; Yamabe, T. *Phys. Rev. B* **1998**, *57*, 9301–9318.

(10) Samsonidze, G.; Grüneis, A.; Saito, R.; Jorio, A.; Souza Filho, A.; Dresselhaus, G.; Dresselhaus, M. *Phys. Rev. B* **2004**, *69*, 205402-1-205402-11.

(11) Sa´nchez-Castillo, A.; Roma´n-Velazquez, C. E.; Noguez, C. *Phys. Rev. B*, **2006**, *73*, 045401-1-045401-7.

(12) Peng, X.; Komatsu, N.; Bhattacharya, S.; Shimawaki, T.; Aonuma, S.; Kimura, T.; Osuka, A. *Nature nanotechnology*, **2007**, *2*, 361-5.

(13) Wang, F.; Matsuda, K.; Rahman, a F. M. M.; Peng, X.; Kimura, T.; Komatsu, N. *J. Am. Chem. Soc.* **2010**, *132*, 10876-10881.

(14) Green, A. ; Duch, M. C.; Hersam, M. C. *Nano Res* **2009**, *2*, 69-77.

(15) Green, A. A.; Hersam, M. C. *Adv. Mater.* **2011**, *23*, 2185-2190.

(16) Ghosh, S.; Bachilo, S. M.; Weisman, R. B. *Nat. Nanotechnol.* **2010** *5* 443-450.

(17) Nish, A.; Hwang, J.; Doig, J.; Nicholas, R. J. *Nat. Nanotechnol.* **2007**, *2*, 640-646.

(18) Chen, F.; Wang, B.; Chen, Y.; Li, L.-J. *Nano lett.* **2007**, *7*, 3013-3017.

(19) Ozawa, H.; Fujigaya, T.; Niidome, Y.; Hotta, N.; Fujiki, M.; Nakashima, N. *J. Am. Chem. Soc.* **2011**, *133*, 2651-2657.

(20) Hwang, J.-Y.; Nish, A.; Doig, J.; Douven, S.; Chen, C.-W.; Chen, L.-C.; Nicholas, R. J. *J. Am. Chem. Soc.* **2008**, *130*, 3543-3553.

(21) Stürzl, N.; Hennrich, F.; Lebedkin, S.; Kappes, M. M. *J. Phys. Chem. C* **2009**, *113*, 14628-14632.

(22) Berton, N.; Lemasson, F.; Tittmann, J.; St, N.; Hennrich, F.; Kappes, M. M.; Mayor, M. *Chem. Mater.* **2011**, 2237-2249.

(23) Ozawa, H.; Ide, N.; Fujigaya, T.; Niidome, Y.; Nakashima, N. *Chem. Lett.* **2011**, *40*, 239-241.

(24) Ozawa, H.; Fujigaya, T.; Song, S.; Suh, H.; Nakashima, N. *Chem. Lett.* **2011**, *40*, 470-472.

(25) Gao, J.; Loi, M. A.; Carvalho, E. J. F. D. C.; Santos, M. C. D. *ACS NANO* **2011**, *5*, 3993-3999.

(26) Imin, P.; Imit, M.; Adronov, A. *Macromolecules* **2011**, *44*, 9138–9145.

(27) Hopkins, J.; M. Dalrymple, S. A.; Parvez, M.; Keay, B. A. *Org. Lett*, **2005**, *7*, 3765-3768.

(28) Canac, Y.; Chauvin, R. *Eur. J. Inorg. Chem.* **2010**, *2010*, 2325-2335.

(29) Turlington, M.; Du, Y.; Ostrum, S. G.; Santosh, V.; Wren, K.; Lin, T.; Sabat, M.; Pu, L. *J. Am. Chem. Soc.* **2011**, *133*, 11780-11794.

(30) Dukovic, G.; Balaz, M.; Doak, P.; Berova, N. D.; Zheng, M.; Mclean, R. S.; Brus, L. E. *J. Am. Chem. Soc.* **2006**, *128*, 9004–9005.

(31) Fariborz, M.; Nigel, G. J. R.; Wayne, C. G.; Rob, L.; Mark, L.; Craig, C.; George, C.; Thomas, H.; Still, W. C. *J. Comput. Chem.* **1990**, *11*, 440–467.

(32) Es, J. J. G. S. V.; Biemans, H. A. M.; Meijier, E. W. *Tetrahedron: Asymmetry* **1997**, *8*, 1825-1831.

(33) Lee, J.-Ik; Chu, H. Y.; Lee, H.; Oh, J.; Do, L.-Mi; Zyung, T.; Lee, J.; Shim, H.-Ku *ETRI Journal* **2005**, *27*, 181-187.

(34) Grisorio, R.; Mastrorilli, P.; Nobile, C. F.; Romanazzi, G.; Suranna, G. P.; Gigli, G.; Piliego, C.; Ciccarella, O. G.; Cosma, P.; Acierno, D.; Amendola, E. *Macromolecules* **2007**, *40*, 4865-4873.

(35) Akazaki, K., Toshimitsu, F., Ozawa, H., Fujigaya, T. & Nakashima, N., *J. Am. Chem. Soc.* **134,** 12700–12707 (2012).

Chapter 3

Recognition and separation of semiconducting-SWCNTs using fullerene carrying copolymers

3-1. Introduction

Single-walled carbon nanotubes (SWCNTs) possess remarkable electronic and photophysical properties[1] that surpass conventional organic electronic materials. The combination of the SWCNTs and fullerenes[2] is one of the desirable systems for the development of nanotube-based electronic devices, such as organic photovoltaic and optoelectronic devices.[3] Highly purified semiconducting-SWCNTs (semiconducting-SWCNTs) without containing metallic-SWCNTs (met-SWCNTs) are suitable for near-IR (NIR) light harvesting photovoltaic applications.[4] However, the efficiency of the semiconducting-SWCNT-based optoelectronic devices has been limited due to coexistence of the met-SWCNTs[5] and random molecular orientations in such composites, in which the semiconducting-SWCNTs and the acceptor, such as fullerenes, do not form suitable conducting pathways.[6] Although hybrid materials of covalent-modified SWCNTs and fullerenes with high power conversion efficiencies (PCE) have been developed,[7] the covalent nanotube modification lowers the intrinsic properties of the SWCNTs, which leads to lower efficiency than the theoretical value.[8] While, in case of non-covalent bonding, the interaction of fullerenes and the SWCNTs is only Van der Waals interaction, which is too weak to fix the molecular orientation of the fullerene moieties on the surfaces of the SWCNTs. Various

methods such as graphene sheet wrapping[9] and bulk-heterojunction formation[10] have been developed in order to increase the interactions between the SWCNTs and the fullerenes. However, they did not control the semiconducting- or met-SWCNT separation and molecular orientation of the composites simultaneously. Recently, Arnold et al. reported that an organic photovoltaic device with a bulk-heterojunction structure prepared by a simple mixture of fullerene (C_{60}) and pure semiconducting-SWCNTs extracted using poly(9,9-di-n-octylfluorenyl-2,7-diyl (PFO) showed high PCE values.[11] However, the molecular orientation between the semiconducting-SWCNTs and the fullerenes are still not controlled in such a simple mixture system.

In this study, I describe the design and synthesis of three different new copolymers (**1**-**3**, Figure 1) that are composed of fullerene-carrying carbazole and fluorene units with the composition ratios (fluorene unit : carbazole unit = x:y) of 1:1 (Copolymer **1**), 5:1 (Copolymer **2**) and 10:1 (Copolymer **3**). The SWCNT sorting using these copolymers were examined using vis-NIR absorption, photoluminescence (PL) and Raman spectroscopies and atomic force microscopy (AFM), and found that i) all these copolymers acted as semiconducting-SWCNT solubilizers, and ii) the amounts of the solubilized semiconducting-SWCNTs depended on the copolymer composition ratios. Furthermore, I propose optimized molecular structures and orientations between the fullerene moieties, copolymer's main chains and semiconducting-SWCNTs based on molecular mechanics calculations.

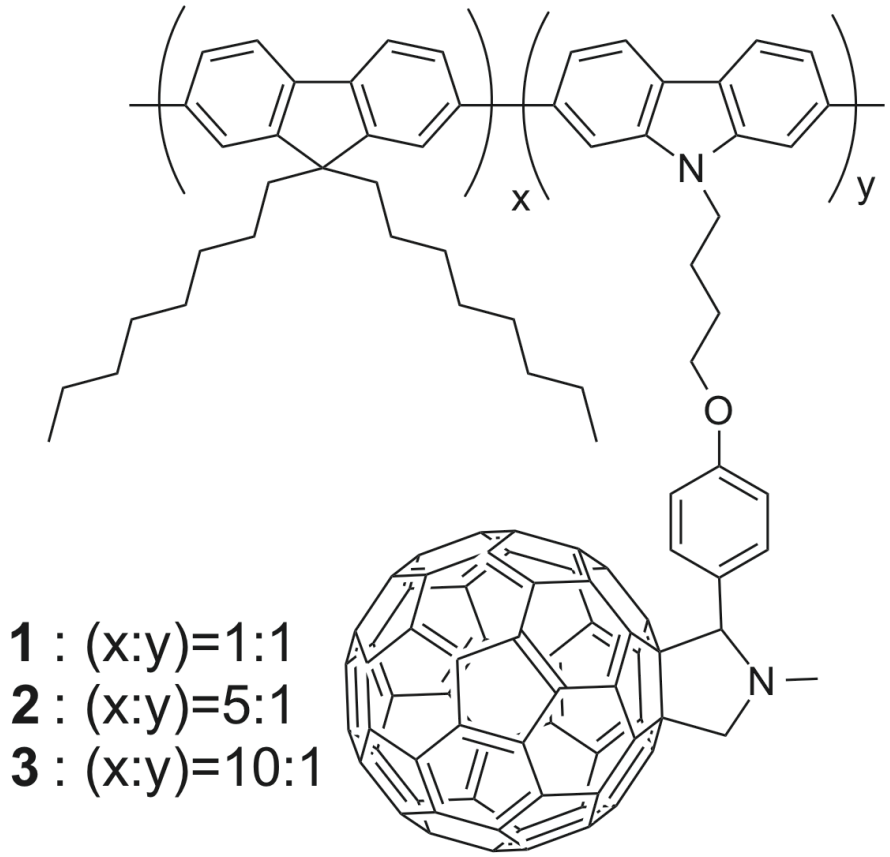

Figure 3-1. Chemical structures of copolymers **1**, **2** and **3.** Adapted from ref. 21with kind permission. Copyright 2015 John Wiley and Sons.

Polyfluorenes (PFs), such as PFO, are known to selectively extract only semiconducting-SWCNTs,[12] and resulted highly isolated PFs/SWCNT composites can educe potential high PL quantum yield and radiative lifetime of semiconducting-SWCNTs. I have previously determined a structural effect of the PFs for the selective recognition and solubilization of a specific chirality of semiconducting-SWCNTs using a series of systematically designed and synthesized PF-based copolymers[13] and demonstrated enhanced switching FET properties of the polymer-wrapped semiconducting-SWCNTs by the complexation with metal nanoparticles.[14] Such synthetic introduction of functional groups into the wrapping polymer is very beneficial because both selective semiconducting-SWCNT-sorting and the molecular orientation of introduced functional groups can be regulated at the same time by a suitable polymer design.

3-2. Experimental

3-2-1. Instruments. ^{1}H NMR spectra were recorded on a Bruker AV300M spectrometer. High-resolution mass spectra (HRMS) were obtained using Bruker MicroTOF-QIII electrospray ionization time-of-flight (ESI-TOF) mass spectrometer. Analytical gel permeation chromatography (GPC) measurements were recorded using a Jasco MD-2015 Plus with the use of Toso TSK-GEL α-3000 and TSK-GEL α-M in THF as the mobile phase at the flow rate of 0.5 ml /min, in which calibration was carried using the polystyrene standard. The UV-vis-NIR absorption and PL spectra, and two-dimensional (2D) PL mapping were recorded using a V-670 (Jasco) and a Horiba Jobin Yvon spectrofluorometer (FluorologR-3 with FluorEssence), respectively. The Raman spectra at excitation of 633-nm were recorded using a RAMANtouch

(Nanophoton Corporation). AFM images were recorded using an Agilent Technologies Agilent5500. The molecular mechanics simulations were carried out using MacroModel (Schrodinger, version 9.7) with the OPLS-2005 force field [20]. Dielectric constant (2.3) of toluene was used in calculations. Minimization on the calculation was carried out using the Polak-Ribiere conjugate gradient (PRCG) with a convergence threshold on the gradient of 0.05 kJ/mol. Default values were used for all the other parameters.

3-2-2. Synthesis of a carbazole derivative (4). A mixture of 2,6-dibromo-9-(6'-bromobutyl)carbazole (500 mg, 1.09 mmol), and 4-hydroxybenzaldehyde (240 mg, 2 mmol), and potassium carbonate (1 g, 7.24 mmol) in DMF (20 mL) was heated at 95 C° under flowing nitrogen for 24 h. After cooling, dichloroethane (200 mL) was poured into the crude reaction mixture. The organic phase was washed with 2×100 mL portions of water, and then the organic layers were collected followed by drying in the presence of Na_2SO_4. A solid by solvent evaporation was washed with ethylacetate to provide compound **4** (400 mg, 73%) as a white solid. ^{1}H-NMR (300 MHz, $CDCl_3$):δ 9.88 (s, 1 H, CHO), 7.90 (d, *J* = 8.30 Hz, 2H, Arcar), 7.82 (d, *J* = 8.7 Hz, 2 H, Ar), 7.55 (s, 2 H, Arcar), 7.36 (m, *J* = 8.30 Hz, 2 H, Arcar), 6.97 (d, *J* = 8.7 Hz, 2 H, Ar), 4.32 (t, *J* = 7.1 Hz, 2 H, CH_2N), 4.06 (t, *J* = 5.97 Hz, 2H, CH_2OAr), 2.09 (m, 2 H, CH_2) and 1.88 (m, 2 H, CH_2). ^{13}C-NMR (75 MHz, $CDCl_3$):δ 190.32, 165.33, 130.98, 129.28, 124.72, 122.49, 121.49, 121.35, 118.92, 114.54, 112.61, 70.11, 68.00, 28.16, 24.51. FTIR (thin film): 2942, 2830, 1690, 1604, 1584, 1578, 1449, 1425, 1253, 1161, 997, 866, 828, 801 and 790 cm^{-1}. HRMS (ESI): calcd. for $C_{23}H_{19}Br_2NO_2$ ([M]+) 498.9783 found 498.9785. Elemental analysis: calcd. for $C_{23}H_{19}Br_2NO_2$ C 55.12 H 3.82 N, 2.79 found C 54.91 H 3.77 N 2.52.

3-2-3. Synthesis of fullerene-carrying carbazole derivative (5). A mixture of compound **4** (100 mg, 0.2 mmol), C_{60} (125 mg, 0.138 mmol), and sarcosine (80 mg, 0.898 mmol) in dry toluene (200 mL) was refluxed under nitrogen for 24 h. After cooling, the resulting solution was evaporated, then drying. After purification by column chromatography (silica gel, eluent solvent; *n*-hexane/dichloromethane 4:1) provided compound **5** (37 g, 21%) as a brown solid. ^{1}H-NMR (300 MHz, $CDCl_3$): δ 7.89 (d, *J* = 8.30 Hz, 2H, Arcar), 7.72 (m, 2 H, Ar), 7.55 (s, 2 H, Arcar), 7.36 (m, *J* = 8.30 Hz, 2 H, Arcar), 6.97 (d, *J* = 8.7 Hz, 2 H, Ar), 4.98 (d, *J* = 9.94 Hz, 1 H), 4.88 (s, 1 H), 4.30 (t, *J* = 7.1 Hz, 2 H, CH_2N), 4.24 (d, *J* = 9.53 Hz, 1 H),4.00 (t, *J* = 5.97 Hz, 2H, CH_2OAr), 2.07 (m, 2 H, CH_2), 1.85 (m, 2 H, CH_2). ^{13}C-NMR (75 MHz, $CDCl_3$):δ 158.81, 156.38, 154.11, 153.64, 147.30, 146.80, 146.52, 146.35, 146.27, 146.13, 145.94, 145.78, 145.54, 145.46, 145.31, 145.27, 145.23, 145.14, 144.70, 144.60, 144.39, 143.10, 142.98, 142.68, 142.53, 142.28, 142.16, 142.09, 141.99, 141.79, 141.68, 141.53, 141.29, 140.16, 140.12, 139.90, 139.55, 136.79, 135.80, 135.75, 130.56, 129.16, 129.05, 128.24, 125.31, 122.68, 121.55, 121.34, 119.81, 114.55, 112.02, 93.40, 83.15, 69.99, 68.97, 67.27, 43.07, 26.74, 25.75. FTIR (thin film) 2948, 2777, 1735, 1587, 1510, 1450, 1426, 1244, 1182, 1056, 839 cm^{-1}. HRMS (ESI): calcd. for $C_{85}H_{24}Br_2N_2O$ ([M]+) 1246.0255 found 1246.0255. Elemental analysis: calcd. for $C_{85}H_{24}Br_2N_2O+2H_2O$ C 79.45 H 1.94 N, 2.18 found C 79.41 H 2.28 N 2.27.

3-2-4. General procedure for the synthesis of copolymers 1-3. Typical procedure (Scheme 1) for the synthesis of Copolymer **1** is as follows. $Ni(COD)_2$ (100 mg, 0.36 mmol), 2,2'-dipyridyl (57 mg, 0.36 mmol), 1,5-cyclooctadiene (0.2 mL), dried DMF (1 mL) and dried toluene (10 ml) were placed in a two-necked round bottle flask under nitrogen and heated at 80 °C for 30 min to obtain a dark purple complex, to which 2,7-dibromo-9,9'-dioctylfluorene

(54 mg, 0.1 mmol) and compound **5** (124 mg, 0.1 mmol) dissolved in dried toluene (10 mL) were added, then the mixture was heated at 80 °C for 48 h, and then poured into methanol (50 mL) and filtrated. The solution was precipitated in a mixture of methanol/acetone/conc. hydrochloric acid to obtain a solid, which was collected and then dissolved in toluene, in which an undissolved solid was removed by filtration. After removing ~90 vol% of toluene under reduced pressure, the concentrated solution was poured into methanol (50 mL) to produced a precipitate, which was filtered, then dried under vacuum at room temperature to provide a brown solid (31 mg) as Copolymer **1**. Copolymer **1**: ^{1}HNMR ($CDCl_3$, 300 MHz):δ 9.31-8.8 (m, β-position), 8.34-7.94 (m, ph), 7.94-7.68 (m, fluorene), 6.9-6.75 (m, ph), 4.06 (m, OCH_2), 2.11 (m, CH_2), 1.84 (m, CH_2), 1.1-1.5 (m, CH_2), 0.85-0.80 (m, CH_3). UV-vis (toluene): λmax = 386 nm. Fluorescence (toluene, λex = 350 nm), λem = 413, 438 nm. FTIR (thin film) 2926, 2854, 1607, 1458, 1252, 1062, 885, 757 and 722 cm^{-1}. Copolymers **2** and **3** were synthesized by a similar manner, in which 2,7-dibromo-9,9'-dioctylfluorene (54 mg, 0.1 mmol) and compound **5** (25 mg, 0.02 mmol) and 2,7-dibromo-9,9'-dioctylfluorene (54 mg, 0.1 mmol) and compound **5** (12 mg, 0.01 mmol) were used for the synthesis of Copolymers **2** and **3**, respectively. Copolymer **2**: ^{1}HNMR ($CDCl_3$, 300 MHz):δ 9.31-8.8 (m, β-position), 8.34-7.94 (m, ph), 7.94-7.68 (m, fluorene), 6.9-6.75 (m, ph), 4.06 (m, OCH_2), 2.11 (m, CH_2), 1.84 (m, CH_2), 1.1-1.5 (m, CH_2), 0.85-0.80 (m, CH_3). UV-vis (toluene): λmax = 386 nm. Fluorescence (toluene, λex = 350 nm), λem = 413, 438 nm. FTIR (thin film) 2926, 2854, 1607, 1458, 1252, 1062, 885, 757 and 722 cm^{-1}. Copolymer **3**: ^{1}HNMR ($CDCl_3$, 300 MHz):δ 9.31-8.8 (m, β-position), 8.34-7.94 (m, ph), 7.94-7.68 (m, fluorene), 6.9-6.75 (m, ph), 4.06 (m, OCH_2), 2.11 (m, CH_2), 1.84 (m, CH_2), 1.1-1.5 (m, CH_2), 0.85-0.80 (m, CH_3). UV-vis (toluene): λmax = 386 nm. Fluorescence (toluene, λex = 350 nm), λem = 413, 438 nm. FTIR (thin film) 2926, 2854, 1607,

1458, 1252, 1062, 885, 757 and 722 cm^{-1}. The molecular weights and Mw/Mn values deduced using analytical GPC for the Copolymers **1**, **2** and **3** were: 98,400 and 2.4, 65,900 and 2.1 and 70,200 and 1.7, respectively.

3-2-5. Solubilization and resolubilization of SWCNTs using Copolymers 1-3

Purified SWCNTs (HiPco; the length and diameter of the pristine SWCNTs were 100-1000 nm and 0.8-1.2 nm, respectively) was purchased from Unidym (Lot. No. P0261) and used as received. The SWCNTs (1 mg) were added to Copolymer **1** (or **2** or **3**) (3 mg) dissolved in toluene (3 mL) and sonicated with a bath-type ultrasonic cleaner (Branson 2210) for 1 h, followed by centrifugation at 10,000 *g* for 1 h (Hitachi himac CS 100GXL). The collected supernatant was then passed through a filter (Advantec Inc., PTFE; pore size 1 μm) to obtain a solid, which was washed with toluene to remove any excess Copolymers **1** (or **2** or **3**). The obtained hybrids were added to toluene (3 ml) and then resonicated for 30 min to obtain three different resolubilized hybrid solutions.

3-3. Results and discussion

3-3-1. Synthesis of copolymers

As shown in Scheme 3-1, the copolymers were synthesized by Yamamoto coupling of a fullerene-containing Bromo-terminated carbazole **5** and dibromofluorene monomer, in which compound **5** was synthesized according to Prato reaction, and the products were characterized using ^{1}H NMR, UV-Vis absorption, FT-IR and fluorescence spectroscopies and GPC analysis.

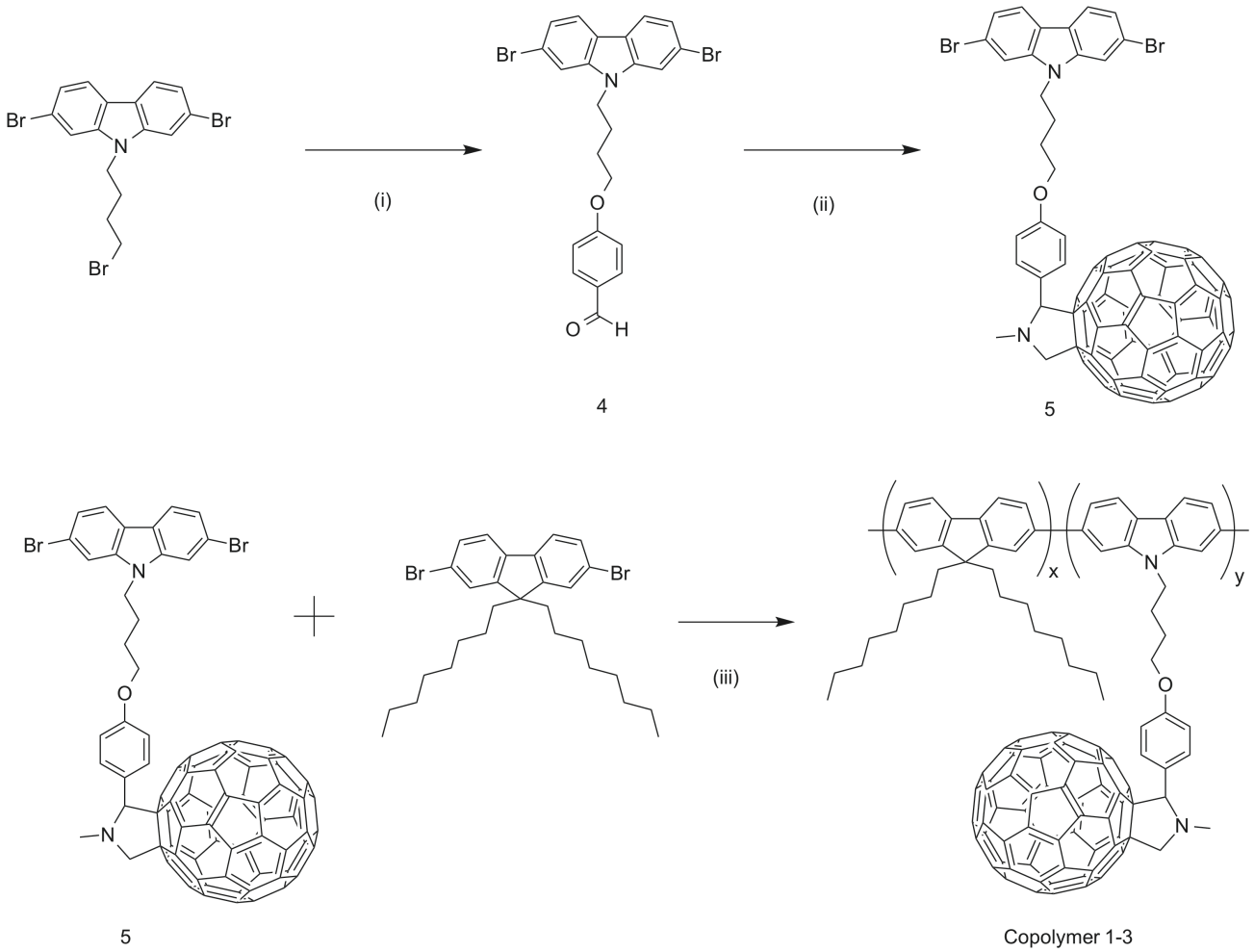

Scheme 3-1. Synthetic route of copolymers **1-3**. Reagents and conditions: (i) K_2CO_3, DMF, 95 °C, 24h; (ii) C_{60}, sarcosine, toluene, 120 °C, 24h; (iii) $Ni(COD)_2$, 2,2'-dipyridyl, 1,5-cyclooctadiene, 2,7-dibromo-9,9'-dioctylfluorene, DMF, toluene, 85°C, 24h. Adapted from ref. 21with kind permission. Copyright 2015 John Wiley and Sons.

3-3-2. Solubilization of SWCNTs using the copolymers

All the three copolymers were found to successfully solubilize the SWCNTs as shown in Figure 3-2. Figure 3-3 and 3-4 show AFM images of the three different copolymer-wrapped SWCNTs and PFO-wrapped SWCNTs (for comparison) on mica. I recognized no bundled SWCNTs in many different areas in the AFM images. Their height distributions were obtained from selected 200 points of their AFM images. The average height of the Copolymer **1**-wrapped SWCNTs (Figure 3-3E) was 2.9 ± 0.5 nm, which was ~2.3-nm higher than that of the PFO-wrapped SWCNTs (1.6 ± 0.3 nm, Figure 3-3H), which indicated that the fullerene moiety in the Copolymer **1** aligned along the sidewalls of the SWCNTs. For Copolymer **2** and **3**, the observed height were 2.0 ± 0.6 nm for Copolymer **2** (Figure 3-3F) and 1.7 ± 0.4 nm for Copolymer **3** (Figure 3-3G), and the height difference from the PFO-wrapped SWCNTs was smaller than of the expected height of C_{60} (diameter = 0.67 nm), which would be due to the low content of the C_{60} units in the Copolymers **2** and **3**. All these results suggest successful individual solubilization of the SWCNTs using Copolymers **1-3**.

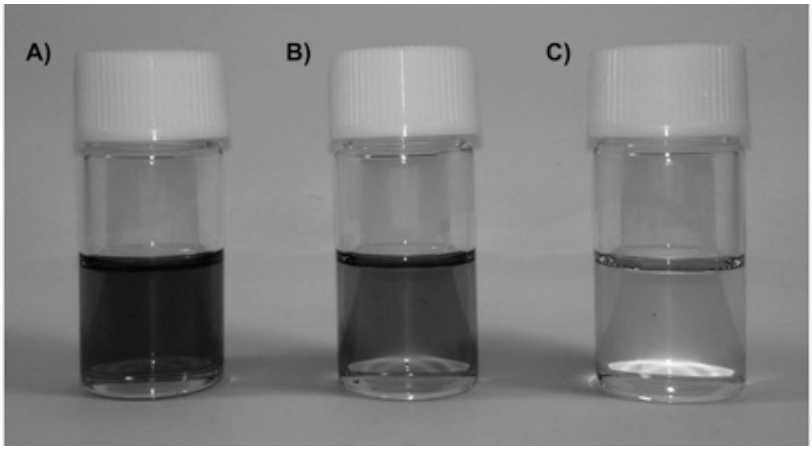

Figure 3-2. Photos of the solubilized SWCNTs using (A) Copolymer **1**, (B) Copolymer **2** and (C) Copolymer **3** in toluene. Adapted from ref. 21with kind permission. Copyright 2015 John Wiley and Sons.

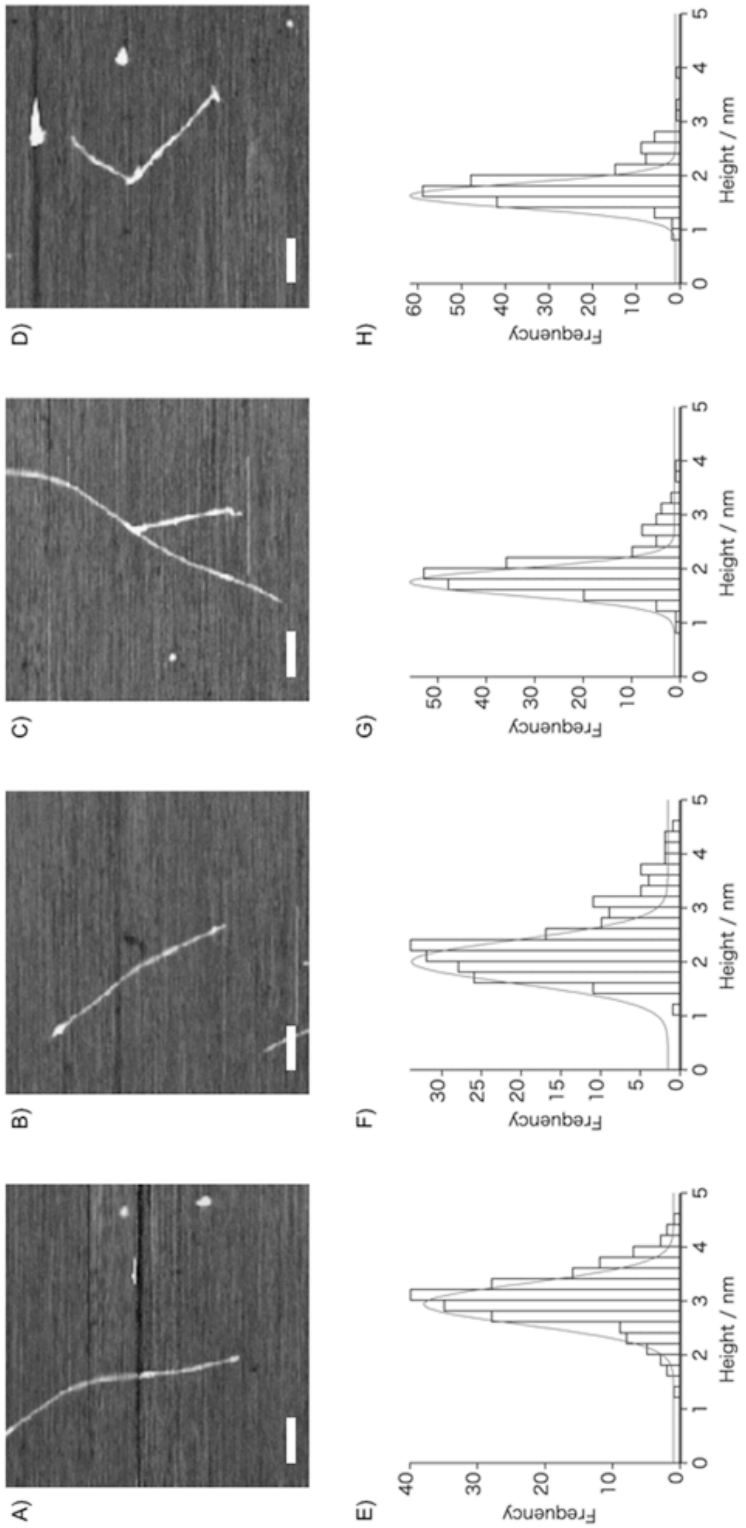

Figure 3-3. AFM images of the SWCNTs wrapped with (A) Copolymer **1**, (B) Copolymer **2**, (C) Copolymer **3** and (D) PFO. Scale bar is 20 nm. Histograms show height profiles for the SWCNTs wrapped with (E) Copolymer **1**, (F) Copolymer **2**, (G) Copolymer **3** and (H) PFO. Adapted from ref. 21with kind permission. Copyright 2015 John Wiley and Sons.

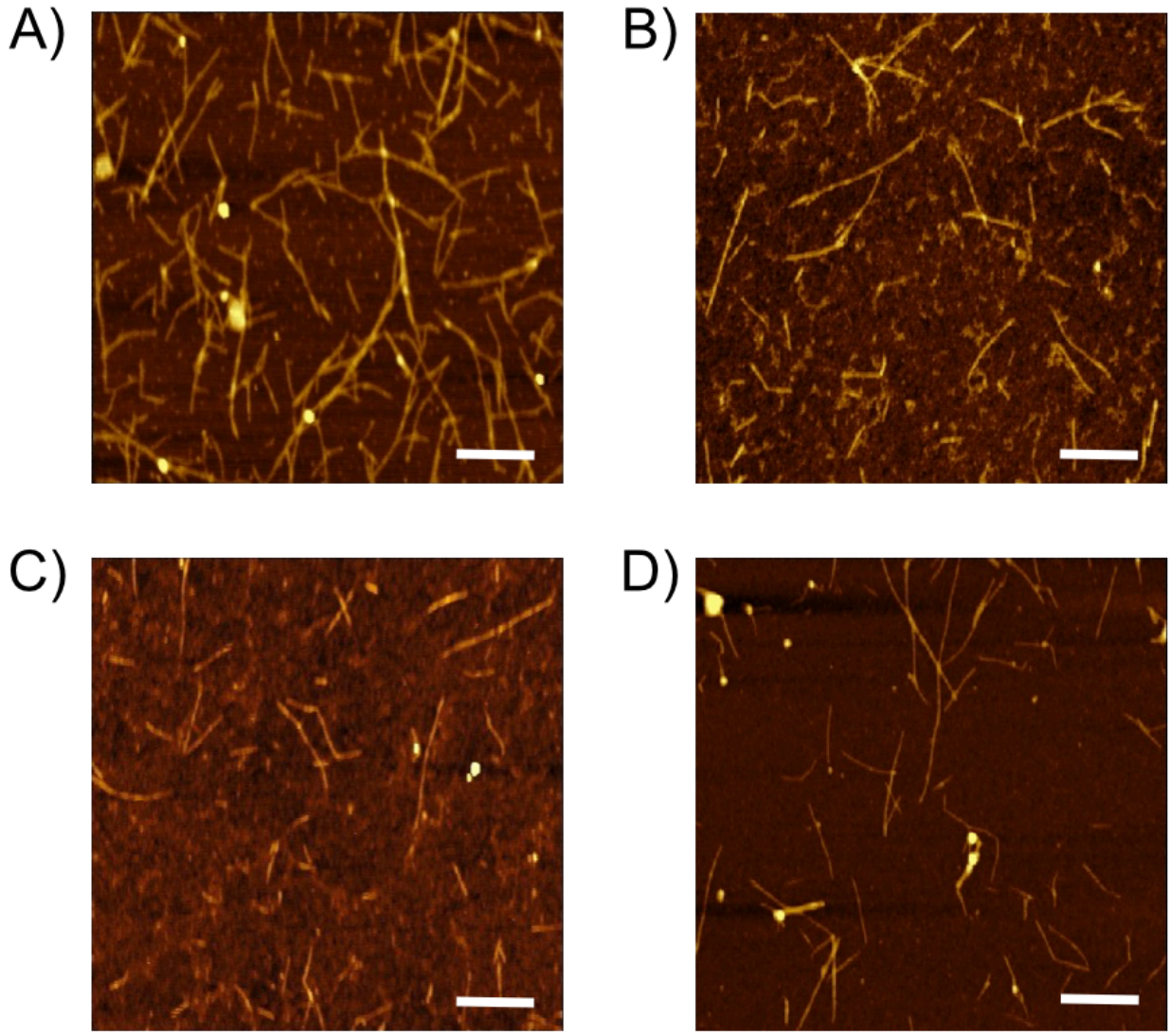

Figure 3-4. AFM images of the SWCNTs wrapped with (A) Copolymer 1, (B) Copolymer 2, (C) Copolymer 3 and (D) PFO. Scale bar is 200 nm. Adapted from ref. 21with kind permission. Copyright 2015 John Wiley and Sons.

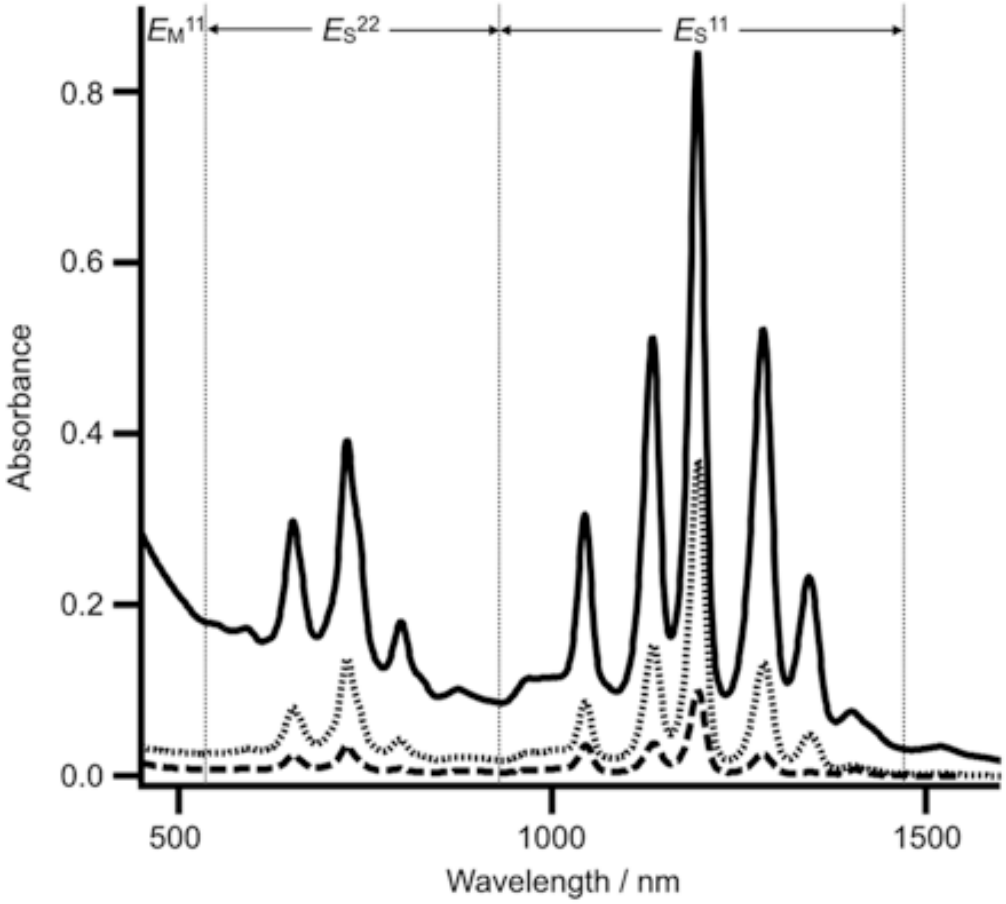

Figure 3-5. UV-vis-NIR absorption spectra of solubilized SWCNTs using Copolymer **1** (solid line), Copolymer **2** (dotted line) and Copolymer **3** (broken line) in toluene (optical length, 1 cm). E_m^{11}, E_s^{11} and E_s^{22} are the energy optical levels of the first transition of met-SWCNTs and the first and the second transitions of semiconducting-SWCNTs, respectively. Adapted from ref. 21with kind permission. Copyright 2015 John Wiley and Sons.

Figure 3-5 shows the vis-NIR absorption spectra of the Copolymer-wrapped SWCNTs in toluene, in which I observe characteristic absorption bands in the ranges of 600-800 (E_S^{22}) and 1000-1400 nm (E_S^{11}). The observed peaks at 1044, 1134, 1194, 1282 and 1343 nm are ascribable to the SWCNTs with chiralities of (7,5), (7,6), (8,6), (8,7) and (9,7), respectively. For Copolymer **1**, I recognized absorption tailing due to higher copolymer composition ratio of the carbazole-C_{60} moieties. Notably, all the copolymers shows no met-SWCNT absorption peak in the range of 400-600 nm (E_M^{11}), indicating that the copolymers extracted only the

semiconducting-SWCNTs with high selectively, whose behavior resembles previously reported results using PFOs[12a] and related copolymers.[13a,d] I will discuss the chiral selectivity in extracted SWCNTs using the copolymers later.

As can be seen in Figure 3-5, the density of C_{60} moiety in the copolymers affects the amounts of extracted semiconducting-SWCNTs; namely, higher C_{60} density in the copolymers resulted in larger concentration of the extracted semiconducting-SWCNTs, which would be due to a strong interaction between the SWCNT surfaces and C_{60} moieties on the Copolymers.

The Radial Breathing Mode (RBM) in the Raman spectra of SWCNTs in the range of 150-350 cm^{-1} is useful to recognize met- and semiconducting-SWCNTs.[12a,13,15] As shown in Figure 3-6, the Raman spectra of the three different copolymer-wrapped SWCNTs measured at a 633 nm excitation, no significant RBM signal from the met-SWCNTs (150-230 cm^{-1}) was recognized. For the three different samples, the obtained semiconducting-SWCNT selectivity deduced from the Raman spectra was up to ~99%, which is comparable to that using PFO.[12a] Although, as described, Copolymer **1**-wrapped SWCNTs showed a shoulder peak in the range of 400-550 nm in its absorption spectrum (see in Figure 3-5), the Raman spectrum of the sample shows no existence of met-SWCNTs, which is an evidence that the shoulder peak is not derived from the SWCNTs, but the carbazole-C_{60} moiety in the Copolymer **1**. I like to emphasize that the introduction of 50-mol% bulky carbazole-C_{60} moiety in the polyfluorene chains remained semiconducting-SWCNTs sorting ability.

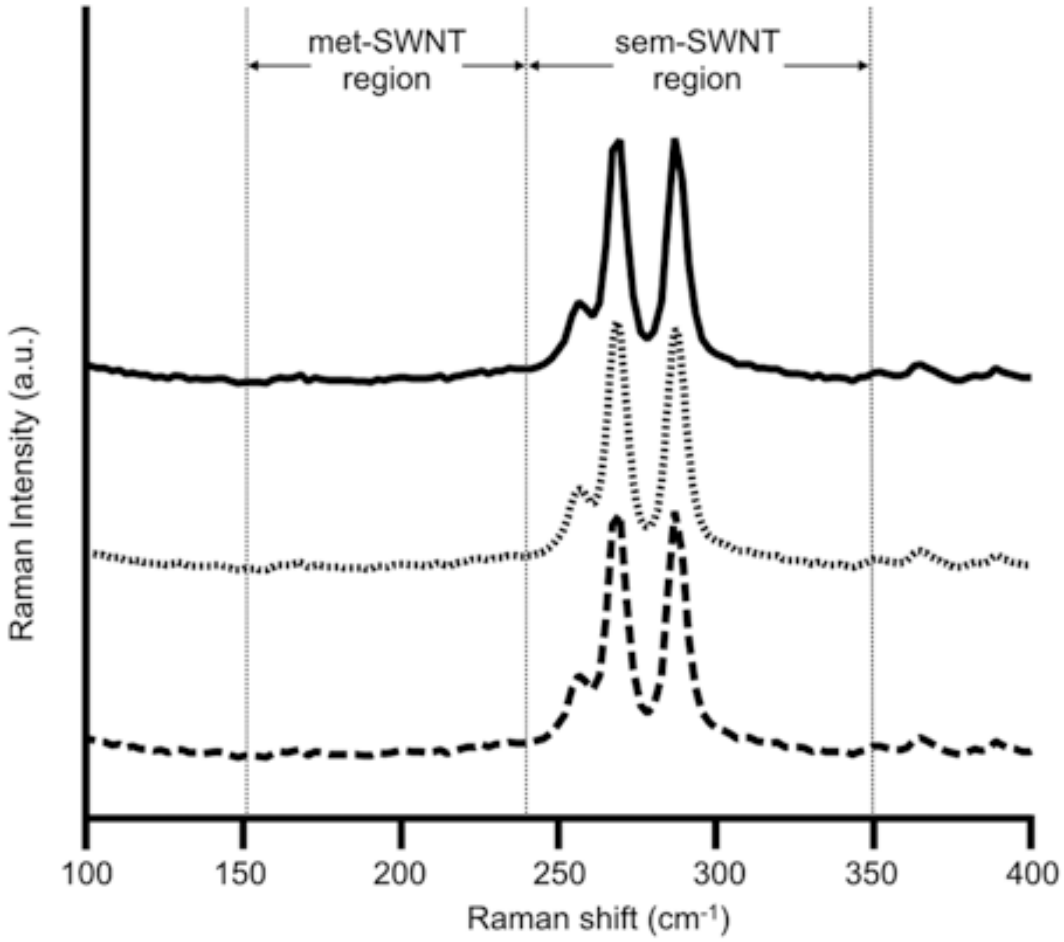

Figure 3-6. Raman spectra of extracted SWCNTs using Copolymer **1** (solid line), Copolymer **2** (dotted line) and Copolymer **3** (broken line). Excitation wavelength: 633 nm. Adapted from ref. 21with kind permission. Copyright 2015 John Wiley and Sons.

I then measured the fluorescence spectra of the Copolymer **1**-wrapped SWCNTs together with that of single component of Copolymer **1**, and the result is shown in Figure 3-7, in which the Copolymer **1**-wrapped SWCNTs shows peaks at 413 and 438 nm, which were almost identical to those (414 and 439 nm) of the Copolymer **1** (single component). However, the fluorescence was quenched dramatically when the Copolymer **1** was complexed with the semiconducting-SWCNTs. Such quenching would be caused by energy transfer from the copolymers to the SWCNTs as previously reported for other polymer-SWCNT composites.[12] In order to investigate the emission from the SWCNTs with each chirality, I also carried out two-dimensional photoluminescence (2D-PL) mapping spectroscopy measurements. Figure 3-8A shows a 2D-PL mapping for the Copolymer **1**-wrapped SWCNTs, in which only five SWCNT chiralities including (7,5), (7,6), (8,6), (8,7), and (9,7) are observed, which is similar to the conventional PFO [12] (Figure 3-8B).

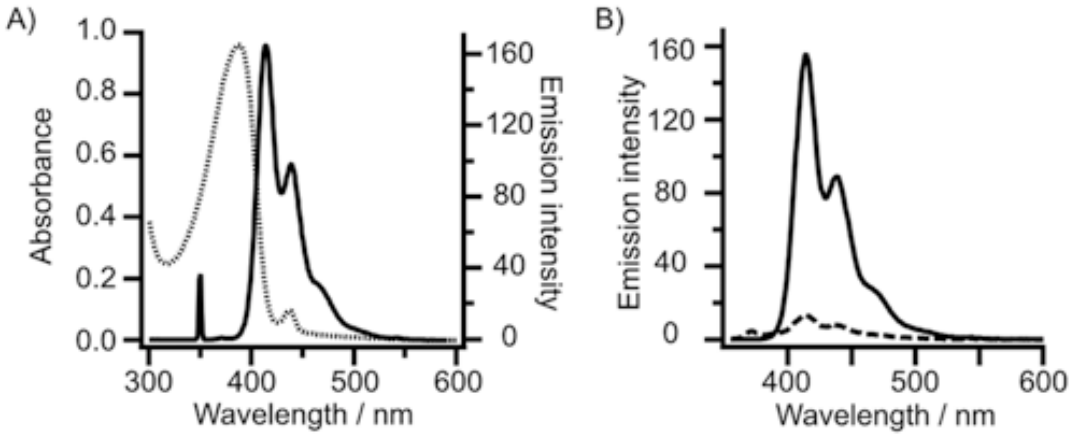

Figure 3-7. (A) UV-vis absorption (dotted line) and emission (excitation at 350 nm) spectra (solid line) of Copolymer **1**. (B) Emission spectra of Copolymer **1** (solid line) and Copolymer **1**-wrapped SWCNTs (broken line) in toluene. Excitation wavelength: 350 nm. Adapted from ref. 21with kind permission. Copyright 2015 John Wiley and Sons.

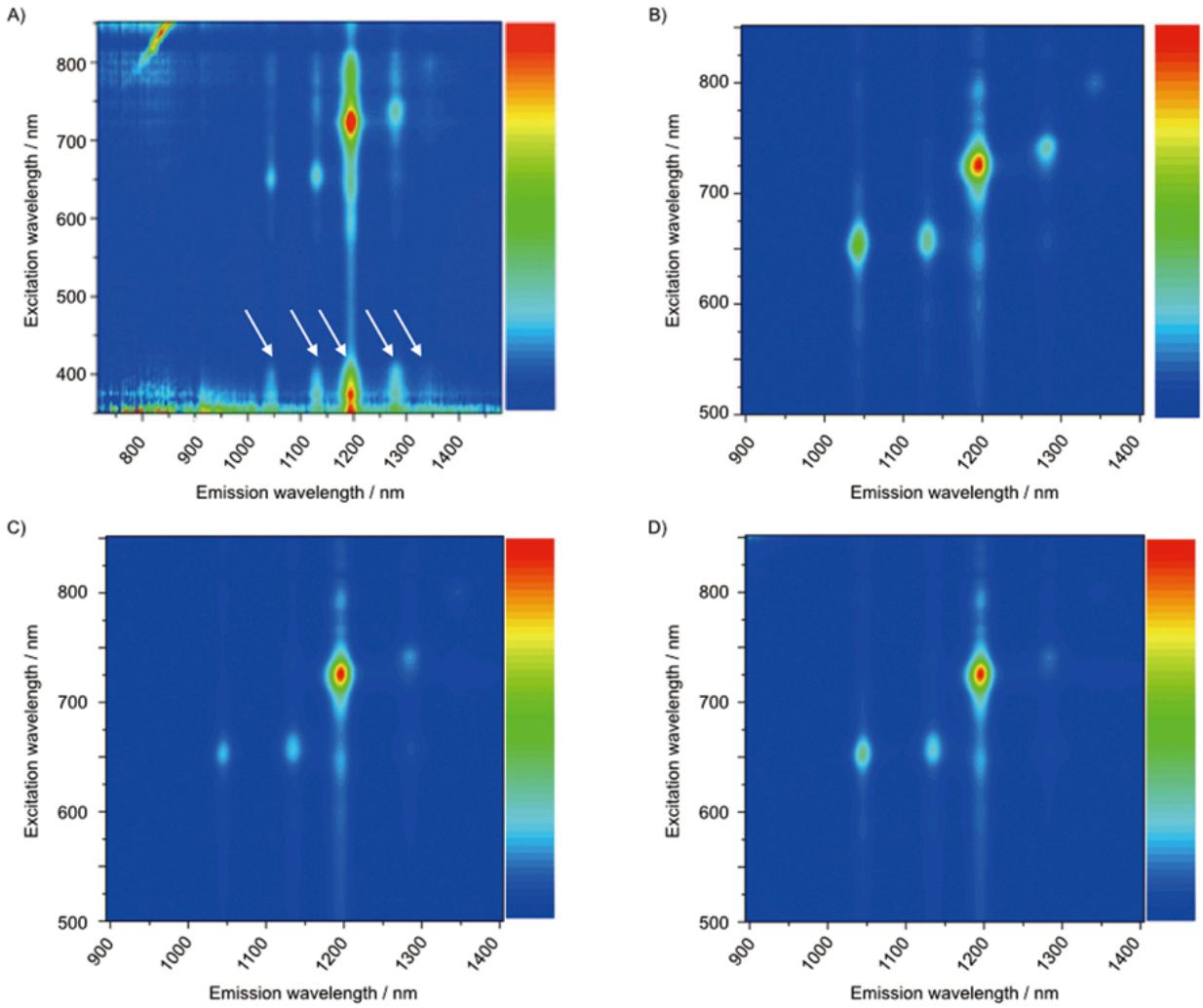

Figure 3-8. 2D-PL mapping of the solubilized SWCNTs using (A) Copolymer **1**, (B) PFO, (C) Copolymer **2** and (D) Copolymer **3** (for the white arrows in the PL-mapping (A), see the text). Adapted from ref. 21with kind permission. Copyright 2015 John Wiley and Sons.

As indicated by the white arrows in Figure 3-8A, when excited at around the absorption region (350- 400 nm) of the Copolymer **1**, I see emission from the SWCNTs with the five different (n,m) chiralities. These results suggest that the Copolymer **1** behaved as a light absorber that transfers energy to the SWCNTs with the specific chiralities. The energy transfer from polymers to SWCNTs is known to be the Förester mechanism.[16] Similar mechanism is suggested in this study, and thus, the obtained result indicates that the energy transfer from the fluorene moiety to the C_{60} moiety in the copolymers is not significant. The Copolymers **2** and **3** also selectively extracted five chiralities (Figures 3-8C and 3-8D) similar to that of Copolymer **1.** In order to evaluate the efficiency for each chirality of the tubes, I then calculated the relative content of each SWCNT based on the calibrated PL intensity using the method reported by Saito et al.[17] As shown in Table 1, all the copolymers are found to preferentially (~60%) extract the (8,6) semiconducting-SWCNTs, which suggests that chiral selectivity is controlled dominantly by the introduction of carbazole moieties into the PF.

3-3-3. Molecular mechanics simulations

In an effort to understand the chirality-selective semiconducting-SWCNT extraction using the copolymers, molecular mechanics simulations were used to evaluate the optimized molecular orientations of the copolymer-wrapped SWCNTs. In order to understand the efficiency of the extraction yield, which related to the contents of C_{60} moiety, the Copolymers **1-3** and the most abundant (8,6) semiconducting-SWCNTs were modeled to visualize the structures and energies of the hybrids. The length of the SWCNT was set to 20 nm, which is longer than that of one-units (10 nm) of the copolymers. Considering the surface area of the SWCNTs that is adequately covered by the copolymers, the numbers of wrapping copolymers

were decided to be three strips. Taking into account that the copolymer length directly affects the interaction between the copolymers and the SWCNT surfaces, the number of □-conjugated elements in the main chain was matched by placing contents ratio between the fluorene moiety (x) and fullerene-carrying carbazole part (y) to be 6:6, 10:2 and 11:1, for Copolymers **1**, **2** and **3**, respectively. The fullerene moieties are rather flexible compared to the □-conjugated main chains so that the following two possible initial structures were examined; that is, all the fullerene are in contact with SWCNT surfaces (Figure 3-9) (**structure 1**), and placed outlying to the SWCNTs (with no contact, Figure 3-10) (**structure 2**). To predict the binding interactions[18] between the copolymers and the (8,6) SWCNT, the stabilizing energies ($E_{\text{stabilizing}}$) of the SWCNT with each structure was calculated as:

$$E_{\text{stabilizing}} = E_{\text{complex}} - (E_{\text{SWCNT}} + E_{\text{Copolymer}}) \qquad (1)$$

where E_{complex}, E_{SWCNT} and $E_{\text{Copolymer}}$ are the energies of the SWCNT/Copolymer complexes, SWCNT and the copolymer, respectively.[12a,13c,d,e]

The results are summarized in Table 3-2 for the calculated potential and stabilizing energy of the copolymers of the **structures 1** and **2**. By comparing the $E_{\text{stabilizing}}$ obtained in both structures, clear difference was observed; namely, **structure 1** was stabilized by -1170 kcal/mol, -312 kcal/mol and -192 kcal/mol for Copolymer **1,** Copolymer **2** and Copolymer **3**, respectively. These values strongly suggest that solubilized SWCNTs are taking the molecular orientation of **structure 1**. Furthermore, the $E_{\text{stabilizing}}$ in **structure 1** drastically increased along with the number of introduced fullerene moieties, which marks distinct contrast to the behavior of the **structure 2**, which well agrees with experimental result obtained by absorption spectroscopy

results (see Figure 3-5). The fullerenes in optimized **structure 1** keep the minimal distance of ~0.32 nm to SWCNT surfaces, which satisfies effective π-π interactions.[19] Together with all the spectral results, solubilization of the SWCNTs using these fullerene-carrying copolymers exhibited the influence of the density of fullerene in the copolymers. Such a result is important for strategical design of new hybrid materials with the semiconducting-SWCNTs with a specific chirality as well as the design and fabrication of a nanotube/fullerene hybrid-based photoactive nanomaterials and devices.

Table 3-1. Calibrated content of the SWCNT species deduced from the PL mapping of the extracted semiconducting-SWCNTs using the copolymers in this study and PFO. Adapted from ref. 21with kind permission. Copyright 2015 John Wiley and Sons.

Copolymer	Chiral index of SWCNTs (n,m)	Calculated PL intensity	Emission peak shift	PL peak intensity	Calibrated PL peak intensity	Calibrated content
Copolymer **1**	(7,5)	0.71	1045.0	5548.6	3939.5	18.5
	(7,6)	0.47	1135.1	5822.0	2736.3	12.8
	(8,6)	0.49	1197.0	26368.5	12920.6	60.6
	(8,7)	0.30	1285.7	4244.2	1273.3	6.0
	(9,7)	0.27	1347.3	1691.6	456.7	2.1
Copolymer **2**	(7,5)	0.71	1045.0	3558.9	2526.8	28.1
	(7,6)	0.47	1136.1	2573.1	1209.4	13.4
	(8,6)	0.49	1197.0	9801.7	4802.8	53.4
	(8,7)	0.30	1283.7	1240.8	372.2	4.1
	(9,7)	0.27	1346.3	300.0	81.0	0.9
Copolymer **3**	(7,5)	0.71	1045.9	174.2	123.7	19.0
	(7,6)	0.47	1134.4	156.2	73.4	11.3
	(8,6)	0.49	1198.7	780.5	382.4	58.6
	(8,7)	0.30	1283.6	175.8	52.7	8.1
	(9,7)	0.27	1346.5	73.8	19.9	3.0
PFO	(7,5)	0.71	1043.0	14167	19953	15.0
	(7,6)	0.47	1131.1	9304	19796	14.8
	(8,6)	0.49	1197.0	25459	51958	38.9
	(8,7)	0.30	1284.7	7924	26415	19.8
	(9,4)	0.70	1131.1	1926	2751	2.1
	(9,7)	0.27	1342.3	3390	12557	9.4
	(10,5)					

Table 3-2. Calculated potential and stabilizing energies between the (8,6) SWCNT with Copolymers **1** to **3** in **structures 1** and **2**. The energies are given in average out of three simulation trials. $E_{Copolymer}$ represents sum of the three copolymers' potential energies. Adapted from ref. 21with kind permission. Copyright 2015 John Wiley and Sons.

structure	Copolymer	potential energy of SWCNT E_{SWCNT} (kcal/mol)	potential energy of Copolymers $E_{Copolymer}$ (kcal/mol)	total potential energy (E_{SWCNT} +$E_{Copolymer}$) (kcal/mol)	potential energy of Copolymer-wrapped SWCNTs $E_{complex}$ (kcal/mol)	stabilizing energy $E_{stabilizing}$ = $E_{complex}$ – (E_{SWCNT} + $E_{Copolymer}$) (kcal/mol)
structure 1	**1**	101321	7066	122398	118695	-3703
	2	101321	12376	138311	135987	-2324
	3	101321	34229	203861	201897	-1964
structure 2	**1**	101321	7066	122398	119865	-2533
	2	101321	12376	138311	136299	-2012
	3	101321	34229	203861	202089	-1772

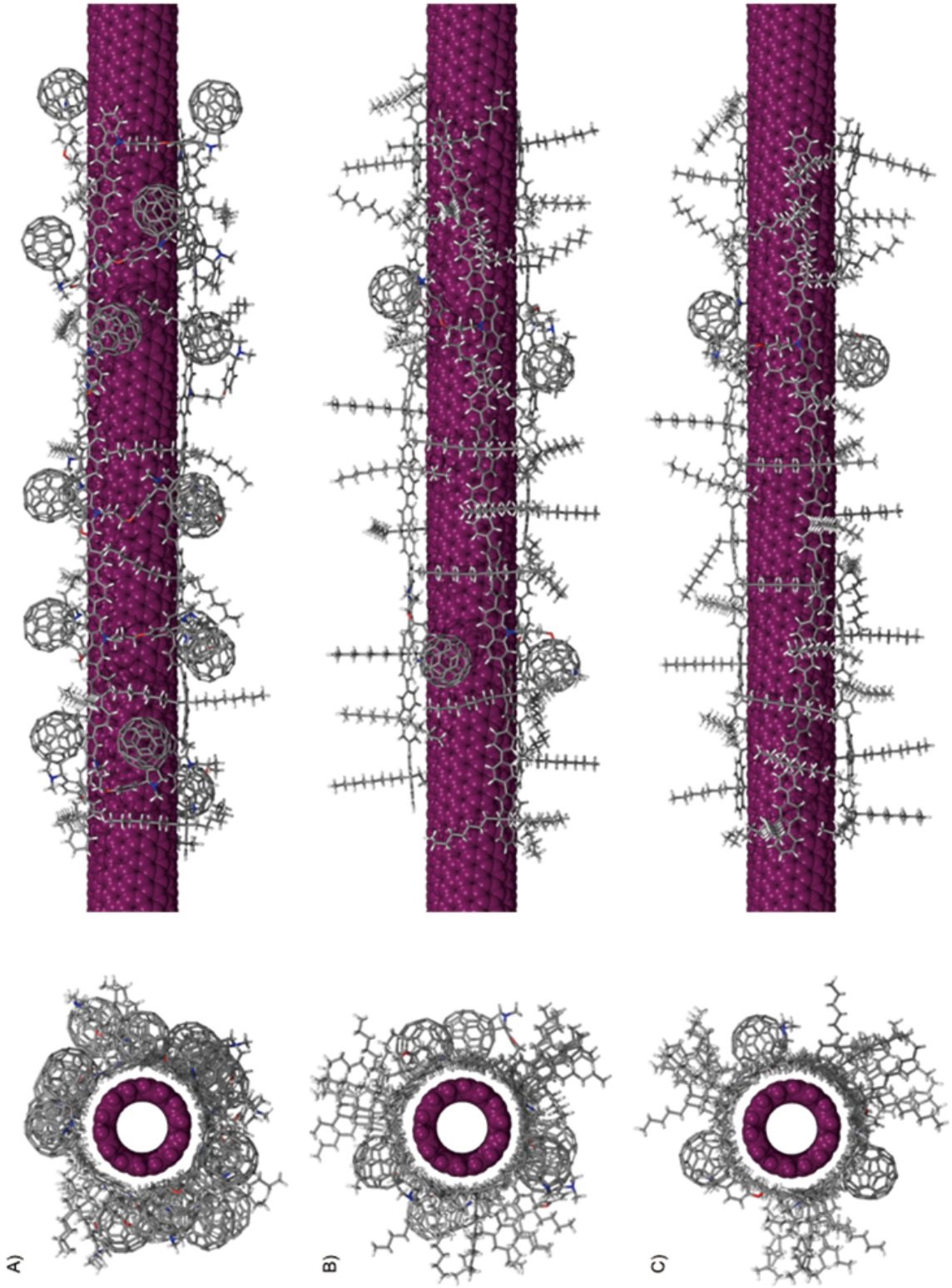

Figure 3-9. Optimized structures of the simulated complexes of **structure 1** using three copolymer strips on the semiconducting-(8,6)SWCNTs. The images of (A), (B) and (C) are the top views (left) and the side views (right) of Copolymer **1**/semiconducting-(8,6)-SWCNT, Copolymer **2**/semiconducting-(8,6)-SWCNT and Copolymer **3**/ semiconducting-(8,6)-SWCNT, respectively. Adapted from ref. 21with kind permission. Copyright 2015 John Wiley and Sons.

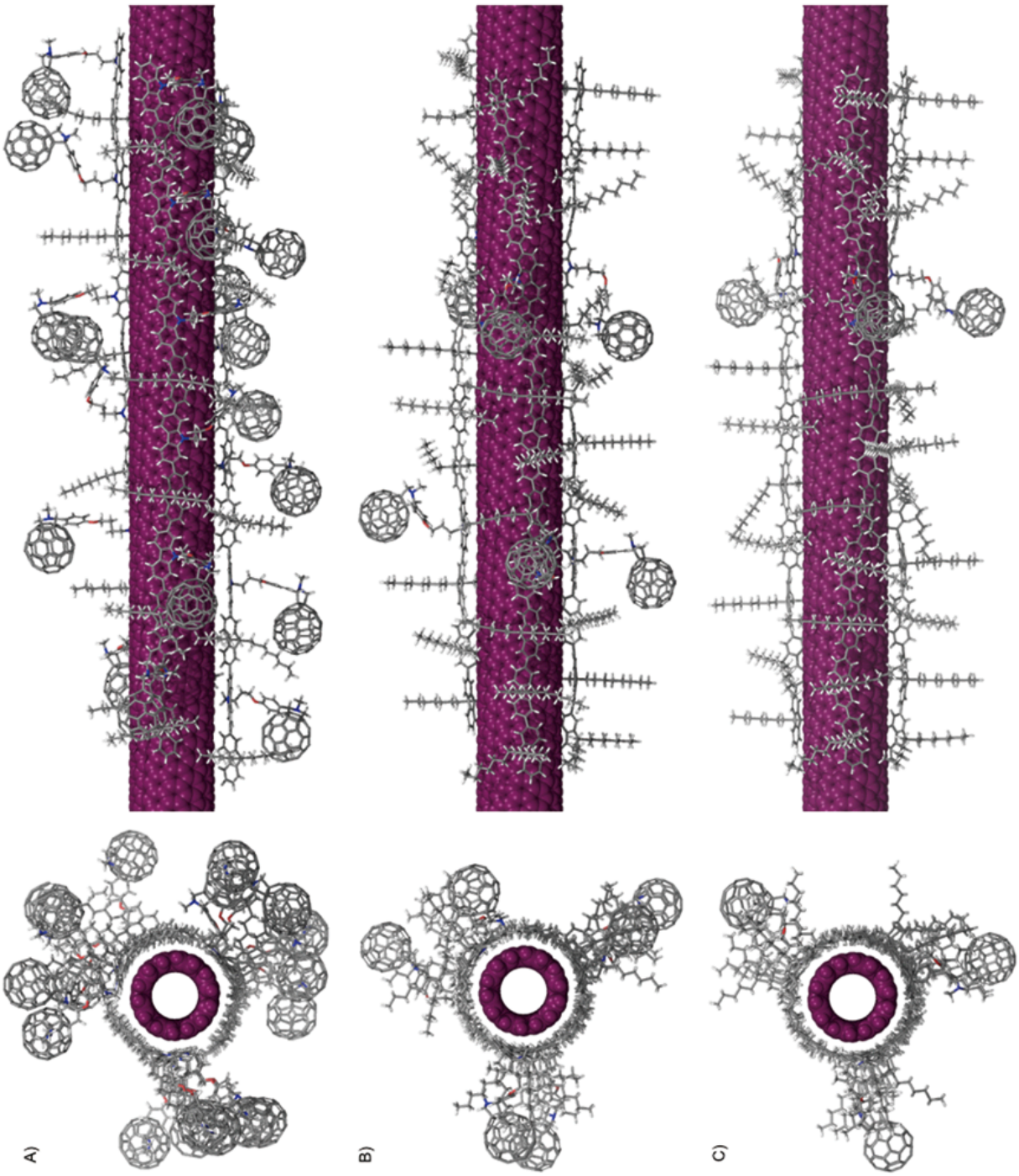

Figure 3-10. Optimized structures of the simulated complexes of **structure 2** using three copolymer strips on the semiconducting-(8,6)-SWCNTs. The images of (A), (B) and (C) are the top views (left) and the side views (right) of Copolymer **1**/semiconducting-(8,6)-SWCNT, Copolymer **2**/semiconducting-(8,6)-SWCNT and Copolymer **3**/semiconducting-(8,6)-SWCNT, respectively. Adapted from ref. 21with kind permission. Copyright 2015 John Wiley and Sons.

3-4. Conclusions

In conclusion, I designed and synthesized Copolymers **1**-**3**, and prepared the hybrid nanomaterials of the semiconducting-SWCNTs with the copolymers, in which the C_{60}-moieties on the copolymers aligned one-dimensionally along the sidewalls of the SWCNTs. These copolymers selectively solubilized only semiconducting-SWMTs with five different (n,m) chiralities, and the increase in the C_{60}-moiety density in the copolymers increased the amounts of solubilized SWCNTs. The PL spectroscopic studies suggested the energy transfer from the C_{60}-moieties to the SWCNTs. Based on the molecular mechanics simulation, I proposed two possible hybrid structures, **structure 1** and **structure 2**, in which the interactions between the copolymers and semiconducting-SWCNTs were influenced by the copolymer composition ratios, and energetically, the **structure 1** was found to be a preferred hybrid structure. The fabrication and evaluation of the photoelectric properties of the devises using the hybrids are currently under investigation.

References

[1] a) *Carbon Nanotubes Synthesis, Structure, Properties and Applications*. (Eds.: M. S. Dresselhaus, G. Dresselhaus & P. Avouris), Springer, **2001**; b) S. M. Bachilo, M. S. Strano, C. Kittrell, R. H. Hauge, R. E. Smalley and R. B. Weisman, *Science*, **2002**, *298*, 2361– 2366; c) Q. Cao and J. A. Rogers, *Adv. Mater.*, **2009**, *21*, 29–53; d) P. M. Ajayan, *Chem. Rev.*, **1999**, *99*, 1787–1799.

[2] a) A. J. Moulé, K. Meerholz, *Adv. Mater.* **2008**, *20*, 240–245; b) R. Charvet, S. Acharya, J. P. Hill, M. Akada, M. Liao, S. Seki, Y. Honsho, A. Saeki, K. Ariga, *J. Am. Chem. Soc.* **2009**, *131*, 18030–18031; c) M. Li, S. Ishihara, M. Akada, M. Liao, L. Sang, J. P. Hill, V. Krishnan, Y. Ma, K. Ariga, *J. Am. Chem. Soc.* **2011**, *133*, 7348–7351; d) C. Gu, Z. Zhang, S. Sun, Y. Pan, C. Zhong, Y. Lv, M. Li, K. Ariga, F. Huang, Y. Ma, *Adv. Mater.* **2012**, *24*, 5727–5731; e) Y. Sun, G. C. Welch, W. L. Leong, C. J. Takacs, G. C. Bazan, A. J. Heeger, *Nat. Mater.* **2012**, *11*, 44–48; f) H. Li, B. C.-K. Tee, J. J. Cha, Y. Cui, J. W. Chung, S. Y. Lee, Z. Bao, *J. Am. Chem. Soc.* **2012**, *134*, 2760–2765.

[3] a) A. Du Pasquier, H. E. Unalan, A. Kanwal, S. Miller, M. Chhowalla, *Appl. Phys. Lett.* **2005**, *87*, 203511; b) A. G. Nasibulin, P. V Pikhitsa, H. Jiang, D. P. Brown, A. V Krasheninnikov, A. S. Anisimov, P. Queipo, A. Moisala, D. Gonzalez, G. Lientschnig, et al., Nat Nano 2007, 2, 156–161; c) C. Li, Y. Chen, Y. Wang, Z. Iqbal, M. Chhowalla, S. Mitra, *J. Mater. Chem.* **2007**, *17*, 2406–2411.

[4] a) E. Maligaspe, A. S. D. Sandanayaka, T. Hasobe, O. Ito, F. D'Souza, *J. Am. Chem. Soc.* **2010**, *132*, 8158–8164; b) B. Pradhan, K. Setyowati, H. Liu, D. H. Waldeck, J. Chen, *Nano Lett.* **2008**, *8*, 1142–1146; c) S. Barazzouk, S. Hotchandani, K. Vinodgopal, P. V Kamat, *J. Phys. Chem. B* **2004**, *108*, 17015–17018.

[5] J. L. Blackburn, T. M. Barnes, M. C. Beard, Y.-H. Kim, R. C. Tenent, T. J. McDonald, B. To, T. J. Coutts, M. J. Heben, *ACS Nano* **2008**, *2*, 1266–1274.

[6] a) R. Ulbricht, X. Jiang, S. Lee, K. Inoue, M. Zhang, S. Fang, R. Baughman, A. Zakhidov, *Phys. status solidi* **2006**, *243*, 3528–3532; b) A. J. Hilmer, K. Tvrdy, J. Zhang, M. S. Strano, *J. Am. Chem. Soc.* **2013**, *135*, 11901–11910; c) F. D. Souza, R. Chitta, A. S. D. Sandanayaka, N. K. Subbaiyan, L. D. Souza, Y. Araki, O. Ito, **2007**, 15865–15871; d) P. V

Kamat, K. G. Thomas, S. Barazzouk, G. Girishkumar, K. Vinodgopal, D. Meisel, *J. Am. Chem. Soc.* **2004**, *126*, 10757–10762.

[7] a) N. J. Alley, K. S. Liao, E. Andreoli, S. Dias, E. P. Dillon, A. W. Orbaek, A. R. Barron, H. J. Byrne, S. a. Curran, *Synth. Met.* **2012**, *162*, 95–101; b) T. Umeyama, N. Tezuka, S. Seki, Y. Matano, M. Nishi, K. Hirao, H. Lehtivuori, N. V Tkachenko, H. Lemmetyinen, Y. Nakao, et al., *Adv. Mater.* **2010**, *22*, 1767–1770; c) T. Umeyama, N. Tezuka, F. Kawashima, S. Seki, Y. Matano, Y. Nakao, T. Shishido, M. Nishi, K. Hirao, H. Lehtivuori, et al., *Angew. Chemie Int. Ed.* **2011**, *50*, 4615–4619.

[8] M. Bernardi, J. Lohrman, P. V Kumar, A. Kirkeminde, N. Ferralis, J. C. Grossman, S. Ren, *ACS Nano* **2012**, *6*, 8896–8903.

[9] a) C. Tang, T. Oppenheim, V. C. Tung, A. Martini, *Carbon* **2013**, *61*, 458–466; b) C. M. Isborn, C. Tang, A. Martini, E. R. Johnson, A. Otero-de-la-Roza, V. C. Tung, *J. Phys. Chem. Lett.* **2013**, *4*, 2914–2918; c) D. Kuzmicz, S. Prescher, F. Polzer, S. Soll, C. Seitz, M. Antonietti, J. Yuan, *Angew. Chemie Int. Ed.* **2014**, *53*, 1062–1066.

[10] a) R. M. Jain, R. Howden, K. Tvrdy, S. Shimizu, A. J. Hilmer, T. P. McNicholas, K. K. Gleason, M. S. Strano, *Adv. Mater.* **2012**, *24*, 4436–4439; b) G. Kalita, S. Adhikari, H. R. Aryal, M. Umeno, R. Afre, T. Soga, M. Sharon, *Appl. Phys. Lett.* **2008**, *92*, 063508; c) C. Li, Y. Chen, Y. Wang, Z. Iqbal, M. Chhowalla, S. Mitra, *J. Mater. Chem.* **2007**, *17*, 2406-2411.

[11] a) D. J. Bindl, M.-Y. Wu, F. C. Prehn, M. S. Arnold, *Nano Lett.* **2011**, *11*, 455–460; b) D. J. Bindl, A. S. Brewer, M. S. Arnold, *Nano Res.* **2011**, *4*, 1174–1179.

[12] a) A. Nish, J. Hwang, J. Doig, R. Nicholas, *Nat. Nanotechnol.* **2007**, *2*, 640-646; b) F. Chen, B. Wang, Y. Chen, L.-J. Li, *Nano Lett.* **2007**, *7*, 3013–3017.

[13] a) H. Ozawa, T. Fujigaya, Y. Niidome, N. Hotta, M. Fujiki, N. Nakashima, *J. Am. Chem. Soc.* **2011**, *133*, 2651–2657; b) H. Ozawa, N. Ide, T. Fujigaya, Y. Niidome, N. Nakashima, *Chem. Lett.* **2011**, *40*, 239–241; c) K. Akazaki, F. Toshimitsu, H. Ozawa, T. Fujigaya, N. Nakashima, *J. Am. Chem. Soc.* **2012**, *134*, 12700–12707; d) T. Fukumaru, F. Toshimitsu, T. Fujigaya, N. Nakashima, *Nanoscale* **2014**, *6*, 5879–5886; e) F. Toshimitsu, N. Nakashima, *Nat. Comm.,* **2014**, *5*, 5041.

[14] a) H. Ozawa, N. Ide, T. Fujigaya, Y. Niidome, N. Nakashima, *Chem. Eur. J.* **2011**, *17*, 13438–13444; b) H. Ozawa, X. Yi, T. Fujigaya, Y. Niidome, T. Asano, N. Nakashima, *J. Am. Chem. Soc.* **2011**, *133*, 14771–14777.

[15] a) N. Izard, S. Kazaoui, K. Hata, T. Okazaki, T. Saito, S. Iijima, N. Minami, *Appl. Phys. Lett.* **2008**, *92*, 243112; b) W. Z. Wang, W. F. Li, X. Y. Pan, C. M. Li, L.-J. Li, Y. G. Mu, J. a Rogers, M. B. Chan-Park, *Adv. Funct. Mater.* **2011**, *21*, 1643–1651; c) D. Chattopadhyay, I. Galeska, F. Papadimitrakopoulos, *J. Am. Chem. Soc.* **2003**, *125*, 3370–3375.

[16] a) J.-H. Ahn, J.-H. Kim, N. F. Reuel, P. W. Barone, A. A. Boghossian, J. Zhang, H. Yoon, A. C. Chang, A. J. Hilmer, M. S. Strano, *Nano Lett.* **2011**, *11*, 2743–2752; b) F. Chen, W. Zhang, M. Jia, L. Wei, X.-F. Fan, J.-L. Kuo, Y. Chen, M. B. Chan-Park, A. Xia, L.-J. Li, *J. Phys. Chem. C* **2009**, *113*, 14946–14952.

[17] Y. Oyama, R. Saito, K. Sato, J. Jiang, G. G. Samsonidze, a. Grüneis, Y. Miyauchi, S. Maruyama, a. Jorio, G. Dresselhaus, et al., *Carbon* **2006**, *44*, 873–879.

[18] L. Y. Yan, W. F. Li, X. F. Fan, L. Wei, Y. Chen, J. L. Kuo, L. J. Li, S. K. Kwak, Y. G. Mu, M. B. Chan-Park, *Small* **2010**, *6*, 110.

[19] T. Kawase, H. Kurata, *Chem. Rev.* **2006**, *106*, 5250–5273.

[20] F. Mohamadi, N. G. J. Richards, W. C. Guida, R. Liskamp, M. Lipton, C. Caufield, G. Chang, T. Hendrickson, W. C. Still, *J. Comput. Chem.* **1990**, *11*, 440–467.

[21] Toshimitsu, F., Ozawa, H. & Nakashima, N., *Chem. - A Eur. J.* **21,** 3359–3366 (2015).

Chapter 4

Chirality separation of semiconducting- and metallic-SWCNTs using coordination polymers

4-1. Introduction

SWNTs possess a unique one-dimensional structure with remarkable electronic, mechanical, thermal and photophysical properties. Not only their structural characteristics, but also opto-electronic properties derived from their diameters and chiral indices, denoted as (n,m)SWNTs, are important for a deep understanding of their fundamental intrinsic properties[1-10]. Highly purified semiconducting-SWNTs (semiconducting-SWNTs) not containing metallic-SWNTs (met-SWNTs) are specifically required for electronic devices, such as field-effect transistors and photovoltaic applications[11, 12] because the met-SWNTs decrease and reduce the efficiency of their associated devices[13, 14]. Hence, the separation/purification of SWNTs according to their chirality is one of the most important issues in the science of carbon nanotubes. Such approaches can be simply classified into two ways containing the covalent- and non-covalent functionalization of the SWNT sidewalls[15]. In order to preserve the intrinsic SWNT properties, the latter method has an advantage over the former one. Recently, various methods for the separation of sem- and met-SWNTs including: i) wrapping by SWNT solubilizers, such as DNAs[16, 17] and π-conjugated copolymers[18], ii) density gradient ultracentrifugation (DGU)[19, 20] and iii) gel chromatography techniques[21-23] have been reported. However, the reported techniques are rather complex and the efficiency is not very high.

Polyfluorene-based copolymers (PFOs)[24, 25] have been intensively studied because they dissolve/extract only semiconducting-SWNTs in toluene by a simple sonication method. I have previously demonstrated a rational method for the selective extraction of a specific chirality of the sem-(*n,m*) SWNTs using a series of systematically designed fluorene-based copolymers[26-28]. Moreover, I revealed that the PFO copolymers with a bulky optically active moiety could separate the right- and left-handed semiconducting-SWNTs[29]. However, there are several serious problems when using PFOs; that is, difficulty in the removal of the wrapped PFOs from the SWNTs/PFO composites[30, 31] as well as their low extraction efficiency from the as-produced SWNTs[25].

The use of coordination bond formation is a facile and effective way to synthesize one-dimensional coordination polymers with well-regulated geometries around metal ions by a simple bottom-up self-assembly method[32, 33]. One of the most important features of such coordination polymers is reversible bond formation (polymerization) and depolymerization to the monomer components by an outer stimulus, such as the addition of an acid, change in pH or temperature, photo irradiation, etc[34, 35].

Here I describe the separation of the sem- and met-SWNTs based on a supramolecular approach. As the goal, I designed molecules (solubilizers) that efficiently recognize/solubilize semiconducting-SWNTs based on the difference in the solubility product between the sem- and met-SWNTs followed by detachment of the solubilizers from the SWNT surfaces. The chemical structures of these molecules are coordination polymers (**CPs**) composed of fluorene moieties and metal complexes, shown in Fig. 1 as **PhenFO** and **CP-M**, in which **PhenFO**, **CP** and **M** denote the phenanthroline (ligand for metal)-fluorene moiety, coordination polymer and metal ions, respectively. The fluorene backbone acts as the semiconducting-SWNT recognition

moiety and the phenanthroline–based metal complexes form polymers via coordination bonding. I report in this study: i) the synthesis of **PhenFO** and **CP-M** (M= is Co(II), Ni(II), Cu(II) and Zn(II) ions), ii) efficient solubilization of SWNTs, iii) separation of sem- and met-SWNTs from their mixture based on selective met-SWNT sedimentation and iv) removal of **CP-M** to provide highly pure semiconducting-SWNTs together with met-enriched SWNTs (see Fig. 4-1). Mayer et al.[36] and Chan-Park et al.[37] reported the use of degradable PFO-alternating copolymers, with a photo-cleavable or acid-sensitive moiety, to irreversibly cleave the wrapping polymers in order to remove them from the composites. Though they could obtain the semiconducting-SWNTs as bundles, the purity of the semiconducting-SWNTs was rather low and complete removal of the wrapping polymer was not discussed. Other groups have reported the solubilization of SWNTs based on the formation/deformation of supramolecules on the sidewall of SWNTs[38, 39], but their target was not selective sem- and met-SWNT separation.

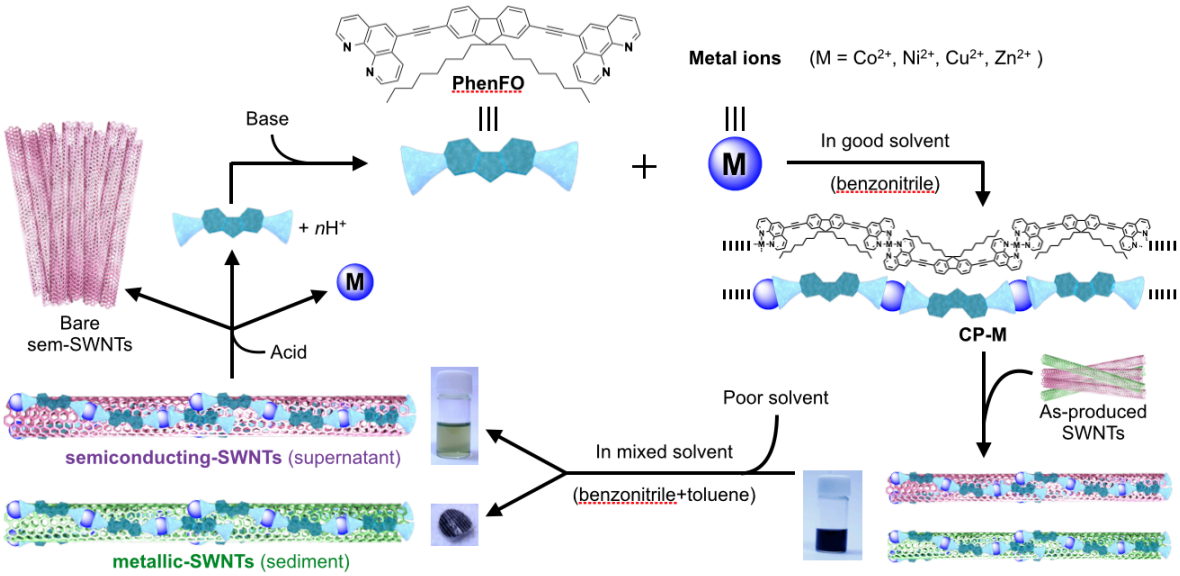

Figure 4-1. A method for highly pure (~99%) sem-SWNT sorting. Adapted from ref. 49 with kind permission. Copyright 2014 Springer Nature.

4-2. Experimental

4-2-1. Materials. All chemicals and solvents used in the syntheses were of reagent grade and used without further purification. 5-Bromo2,7-phenanthroline and 2,7-bisethynyl-9,9-dioctylfluorene were synthesized according to the literature[47, 48]. The SWNTs (HiPco) were purchased from Unydim Co., Ltd. (Lot No. P0261) and used as received.

4-2-2. Synthesis of PhenFO. **PhenFO** was synthesized via the Sonogashira coupling (Fig. 2): 5-bromo2,7-phenanthroline (170 mg, 0.656 μmol), 2,7-bisethynyl-9,9-dioctylfluorene (141 mg, 0.322 μmol), tetrakis(triphenylphosphine)palladium (70 mg, 0.061 μmol), copper(I) iodide (19 mg, 0.010 μmol) and triethylamine (50 ml) were placed in a 100-ml-two-necked flask and stirred at 70°C for 6 h under flowing nitrogen, then cooled to room temperature and filtered. The filtrate was concentrated and purified using silica gel column chromatography eluted by dichloromethane. The first fraction was collected and recrystallized from hexane to provide **PhenFO** as yellow needle-like crystals. Yield: 86%. ^{1}H NMR (300 MHz, $CDCl_3$): 9.28 (d, *J*=4.3, 2H), 9.22 (d, *J*=4.3 2H), 8.92 (d, *J*=8.3 2H), 8.26 (d, *J*=8.2 2H), 8.17 (s, 2H), 7.80 (m, 4H), 7.70 (m, 4H), 7.66 (s, 2H), 2.09 (m, 4H), 1.26−1.06 (m, 20H), 0.80−0.66 (m, 10H). High-resolution mass spectroscopy (ESI, *m/z*): [M+H$^+$] calcd. for C57H55N4, 795.0870; found, 795.0872.

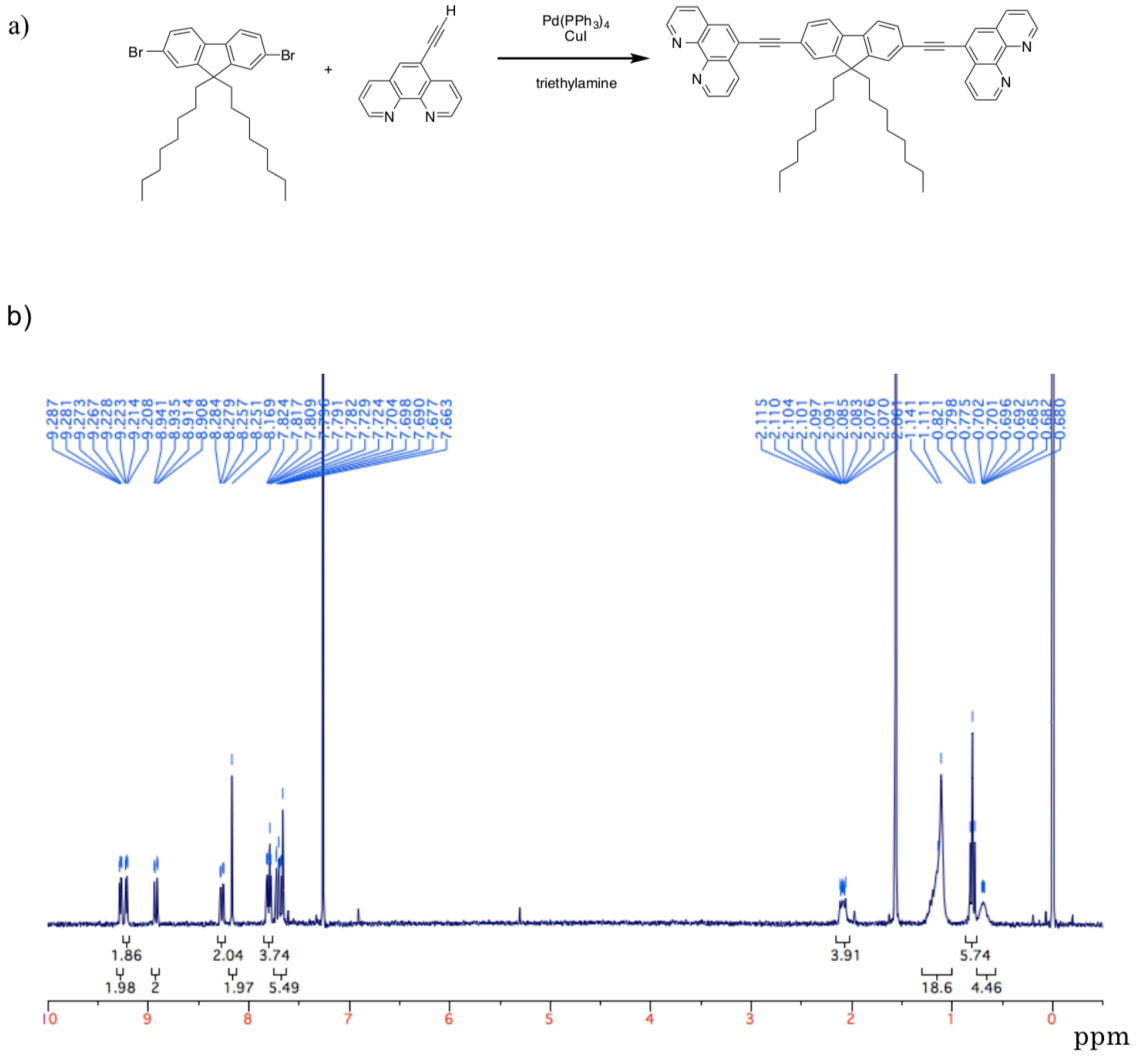

Figure 4-2. a) Synthetic route, b) ^{1}H NMR (300 MHz, $CDCl_3$), c) ^{13}C NMR spectrum (75 MHz, $CDCl_3$) of **PhenFO**. Adapted from ref. 49 with kind permission. Copyright 2014 Springer Nature.

4-2-3. Method for the preparation of CP-M. A 3.0 ml portion of **PhenFO** (0.1 mM in benzonitrile) was added to an equimolar solution of the perchlorate salt of Co(II), Ni(II), Cu(II), or Zn(II) ion to immediately produce **CP-M**. A concentration dependent titration of each metal ion in the **PhenFO** solution revealed that the **PhenFO** and each metal ion formed complexes with the molar ratios =1:1, indicating the formation of linear coordination polymers (●Fig. S1). The molecular masses of the **CP-M** were measured by an ESI-TOF-Mass spectrometer (Bruker Co., Ltd., micrOTOF-QIII) and oligomers of up to 10-mer ($[\mathbf{PhenFO}_{10}\mathbf{M}_9(ClO_4)_9]^{9+}$) were found in the benzonitrile solution (Fig. 4-3).

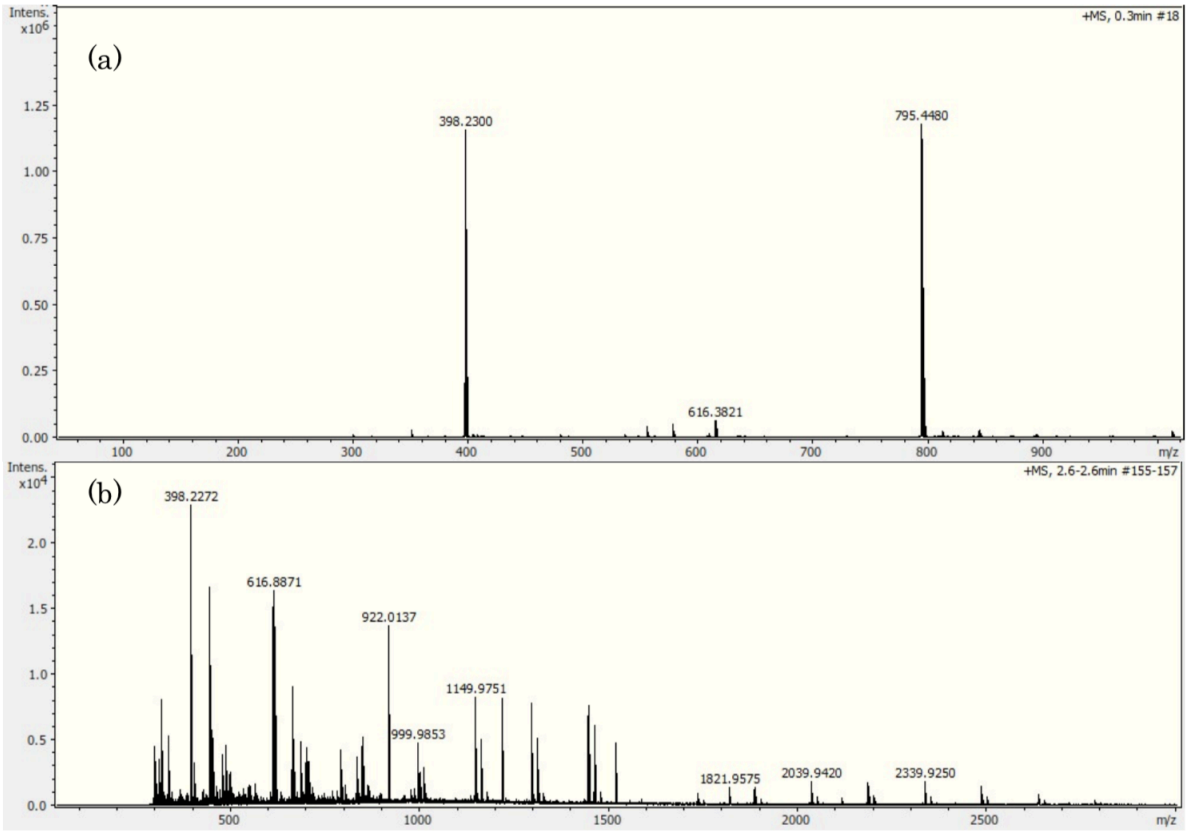

Figure 4-3. ESI-TOF-Mass spectra of (a) **PhenFO** and (b) **CP-Zn**. Adapted from ref. 49 with kind permission. Copyright 2014 Springer Nature.

4-2-4. General method for the solubilization of SWNTs. A typical procedure for the SWNT dissolution using **CP-M** (M=Co, Ni, Cu, or Zn) is as follows: Crude SWNTs (1 mg) were dispersed in a 0.1 mM (for the **PhenFO**) benzonitrile solution of **CP-M** (3 ml) using a bath-type sonicator (Emerson Japan, Ltd., Bransonic) for 1 h, followed by centrifugation at 10 000 *g* for 1 h, then the upper-80% of the supernatant collected. The vis-NIR absorption spectra were measured using a spectrophotometer (JASCO, Co., Ltd., type V-670). The PL spectra were measured by a spectrofluorometer (Horiba-Jobin Yvon, SPEX Fluorolog-3-NIR) equipped with a liquid-nitrogen-cooled InGaAs near-IR detector. The excitation and emission wavelengths were in the range of 500-900 nm and 900-1300 nm, respectively. The Raman spectra at 532 nm, 633 nm and 785 nm were recorded by a Raman spectrometer (Nanophoton Co., Ltd., Raman Touch). Atomic force microscopy (AFM) images were taken using a scanning probe microscope (Agilent Technologies, type 5500). Mica was used as the substrate.

4-2-5. Selective separation of sem- and met-SWNTs. The obtained supernatants (2 mL each) were added to toluene (2ml) followed by gentle swirling (caution: gentle swirling is important because vigorous stirring caused precipitation of all the SWNTs in the supernatant), then kept overnight at room temperature. The obtained solution was centrifuged at 10 000 *g* for 1 h, then the upper-80% of the supernatant collected. After removing the lower 20% of the supernatant, the sediments were collected and then redispersed in benzonitrile to obtain a homogenized solution.

4-2-6. Removal of CP-M from the solubilized SWNTs. The obtained top-80% of the supernatant and the redispersed solutions of the sediments were filtered using PTFE filters (AVANTEC, 0.1 μm pore size). Each collected solid was dispersed in 3 ml of benzonitrile to which a 0.5 ml-portion of trifluoroacetic acid (15 wt%, 4.4 mmol) was added to immediately

generate a black suspension, which was filtered through a PTFE filter (AVANTEC, 0.1 μm pore size) and washed with 10 ml of benzonitrile followed by washing with methanol until the absorption of **CP-M** disappeared in the UV-vis absorption spectrum of filtered liquid. Each obtained SWNT solid was redispersed in 3 ml of a 5 wt% SDS aqueous solution to measure their vis-NIR absorption, Raman and PL spectra.

4-2-7. Molecular mechanics calculation. The molecular mechanics simulations were carried out using MacroModel (Schrodinger, version 9.4) with the OPLS-2005 force field. The dielectric constant of toluene (2.3) was used in the calculation. Minimization of the calculation was carried out using the Polak-Ribiere conjugate gradient with a convergence threshold on the gradient of 0.05 kJ/mol. Default values were used for all the other parameters.

4-3. Results and discussion

4-3-1. Synthesis of CP-M.

The phenanthroline moiety is known to accept various metal ions[40]. I examined the coordination of **PhenFO** with the perchlorate salts of Co(II), Ni(II), Cu(II) and Zn(II) ions using the titration spectral change upon the addition of the metal ion into the solutions of **PhenFO** in benzonitrile. Based on the Job plots of each absorption maximum at 379 nm, 387 nm and 410 nm as a function of the ratios of **PhenFO** and Cu(II) ion (Fig. 4-4), I found that a linear polymer was formed at metal:ligand=1:1 via coordination bonding[24]. Similar behavior was observed when using Co(II), Ni(II) and Zn(II) in place of Cu(II) (Fig. 4-5).

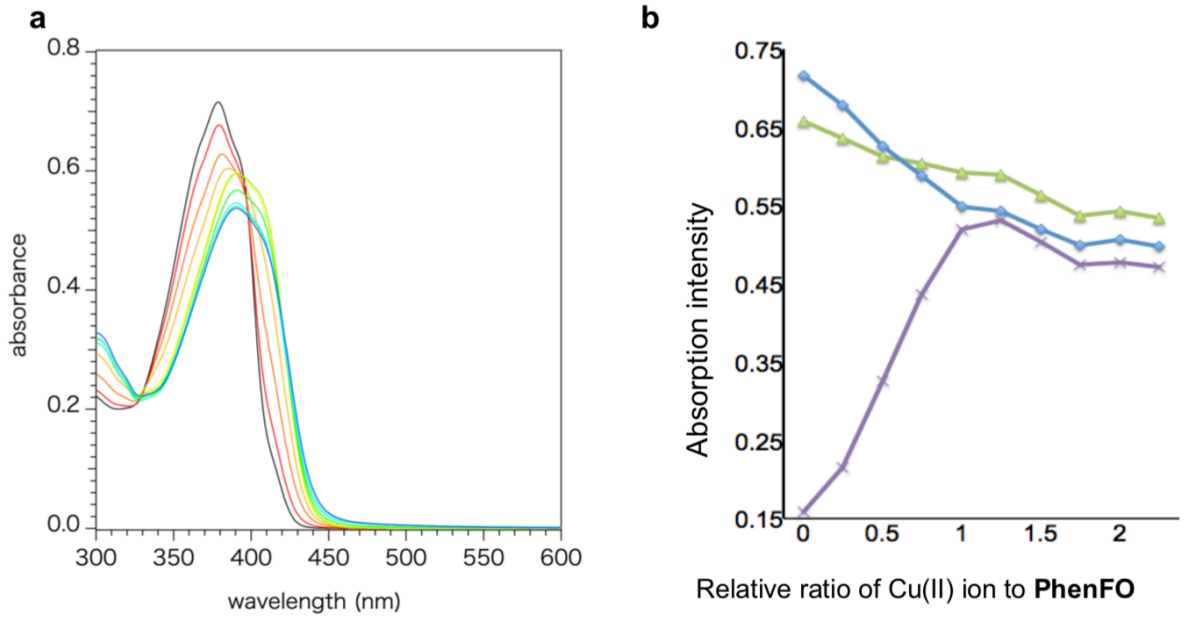

Figure 4-4. a, Vis-near-IR absorption titration spectra of **PhenFO** upon adding $Cu(ClO_4)_2$. **b**, Job plot of the change in absorption intensity at 379 nm (blue), 387 nm (green) and 410 nm (blue) as a function of molar ratios between **PhenFO** and Cu(II) ion on the titration. Adapted from ref. 49 with kind permission. Copyright 2014 Springer Nature.

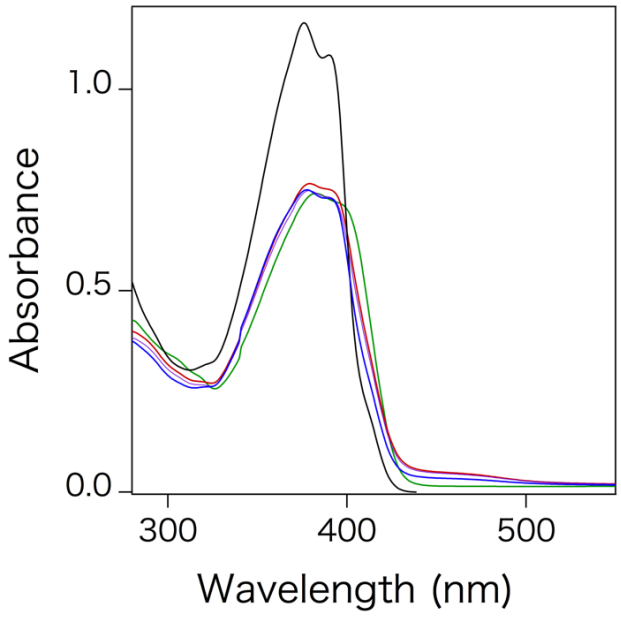

Figure 4-5. Absorption spectra of **PhenFO** in benzonitrile (0.01 mM, black) and spectra after adding 0.01M of **CP-M** (M=cobalt(II) (red), nickel(II) (purple), copper (II) (blue), and zinc(II) (green) ions). Adapted from ref. 49 with kind permission. Copyright 2014 Springer Nature.

4-3-2. Solubilization of SWNTs by CP-M.

I first used benzonitrile as the solvent since this is a good solvent for **CP-M**. In this solvent, **CP-M** was found to dissolve the SWNTs but it dissolved both the sem- and met-SWNTs. It is known that PFOs exhibit selective semiconducting-SWNT sorting only when aromatic solvents, such as toluene and xylene, are used[41]. However, the use of such solvents was difficult due to the poor solubility of the **CP-M** in such solvents. I thus tested mixed solvents of toluene/benzonitrile with the volume ratios of 1/3, 1/1 and 3/1, however, such mixed solvents did not dissolve **CP-M**. In order to obtain homogeneously dispersed SWNT solutions, I added a benzonitrile solution of **PhenFO** to equimolar metal ion solutions to prepare the **CP-M** in benzonitrile, to which the SWNTs were subsequently added and sonicated for 1 h, then centrifuged at 10,000 *g* for 1 h, followed by collection of the upper-80% of each supernatant.

As shown in Fig. 4-6a, absorbance (optical path length=1 mm) of the **CP-M**-solubilized SWNTs in the range of the first (S_{11}) and second (S_{22}) semiconducting exciton bands reached 0.4 (M=Co), 0.3 (M=Fe), 0.2 (M=Cu) and 0.2 (M=Zn), which are ~20-40 times greater than that achieved when using conventional polyfluorenes, such as, poly(9,9-di-n-octylfluorenyl-2,7-diyl) in benzonitrile (absorbance of SWNTs in the same regions were lower than 0.01 (optical length= 1 mm) (Fig. 4-7)).

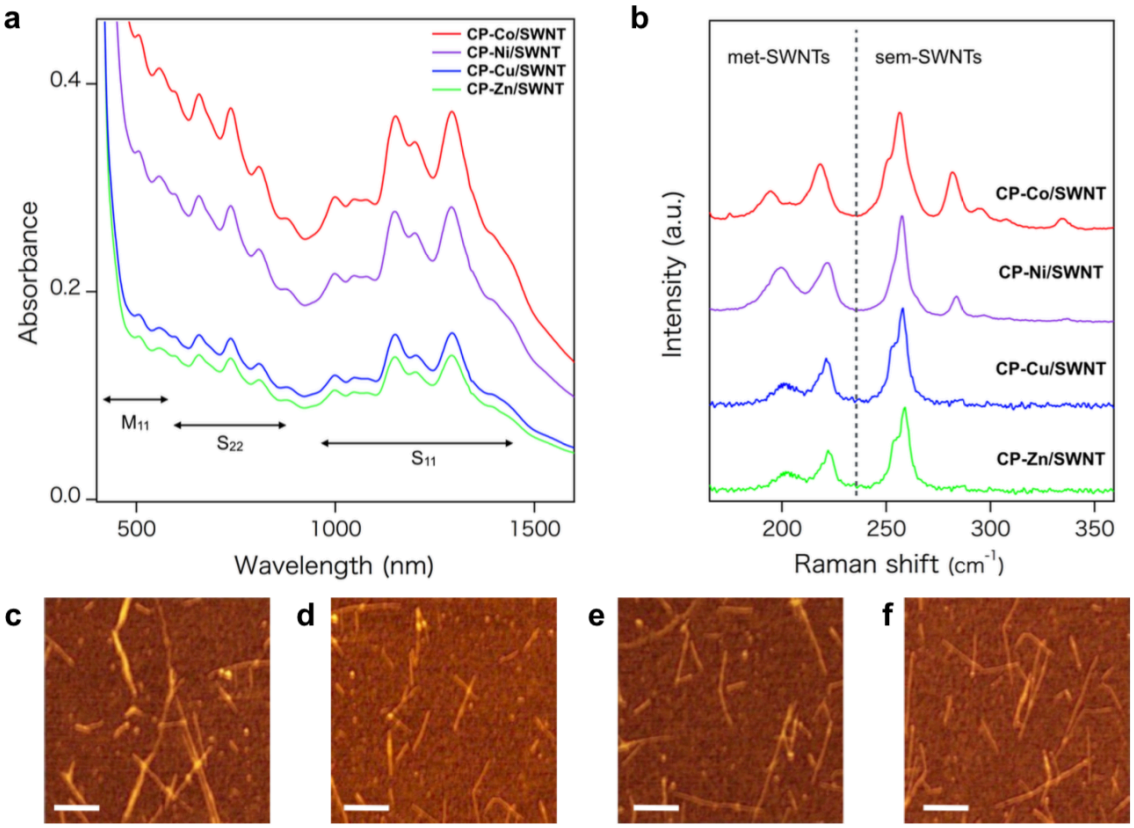

Figure 4-6. Characterization of individualized SWNTs by the aid of CP-M in benzonitrile. Vis-near IR absorption spectra (optical cell length, 1 mm) (**a**) and the Raman spectra in the RBM region of SWNTs (excitation wavelength: 633 nm) (**b**) of the solubilized SWNTs using CP-M (M=cobalt(II) (red), nickel(II) (purple). zinc(II) (blue), and copper(II) (green) ions). **c-f**. AFM images of the individually dispersed SWNTs wrapped with (**c**) CP-Co, (**d**) CP-Ni, (**e**) CP-Cu and (**f**) CP-Zn. Used substrates were mica. Scale bars, 200 nm. Adapted from ref. 49 with kind permission. Copyright 2014 Springer Nature.

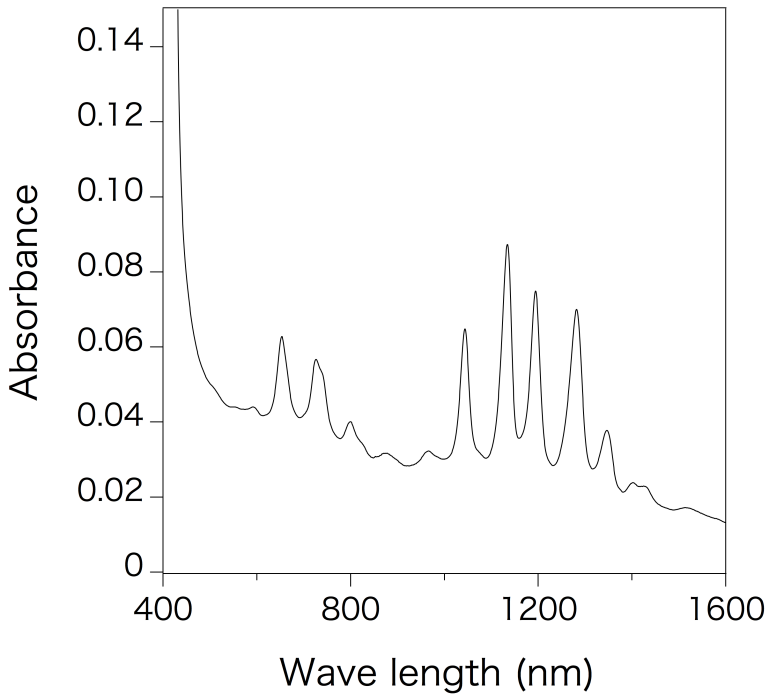

Figure4-7. Vis-NIR absorption spectrum of the SWNTs solubilized by poly(9,9-di-n-octylfluorenyl-2,7-diyl in benzonitrile (optical cell length: 1 cm). Adapted from ref. 49 with kind permission. Copyright 2014 Springer Nature.

The absorption intensities of the solubilized SWNTs were found to increase in ascending order of atomic number of the used metal ions on the **CP-M** (Fig. 4-6a). According to coordination chemistry, cobalt(II) and nickel(II) ions are expected to form a square-planar structure on **CP-M**, while copper(II) and zinc(II) ions form a tetrahedral structure[42]. The difference in such coordination geometry may explain the difference in the amounts of the dissolved SWNTs. However, as shown in Fig. 4-6b, the Raman spectra of the solubilized SWNTs were shown to contain both, sem- and met-SWNTs, and therefore the separation was unsuccessful at this stage.

To obtain the structure of the solubilizezd SWNTs, I carried out AFM measurements of

SWNT/**CP-M** composites (for M= Co, Ni, Cu and Zn) (Figs. 4-6c~f) and the results for their height-distribution are shown in Fig. 4-8, in which I observe SWNTs with heights (average for each 100 points) of 1.21±0.03 nm for M=,Co, Ni, Cu and Zn, suggesting individual dissolution of the SWNTs in all samples. Such height values agree with those of the optimized structures that I discuss in the molecular mechanics calculation section.

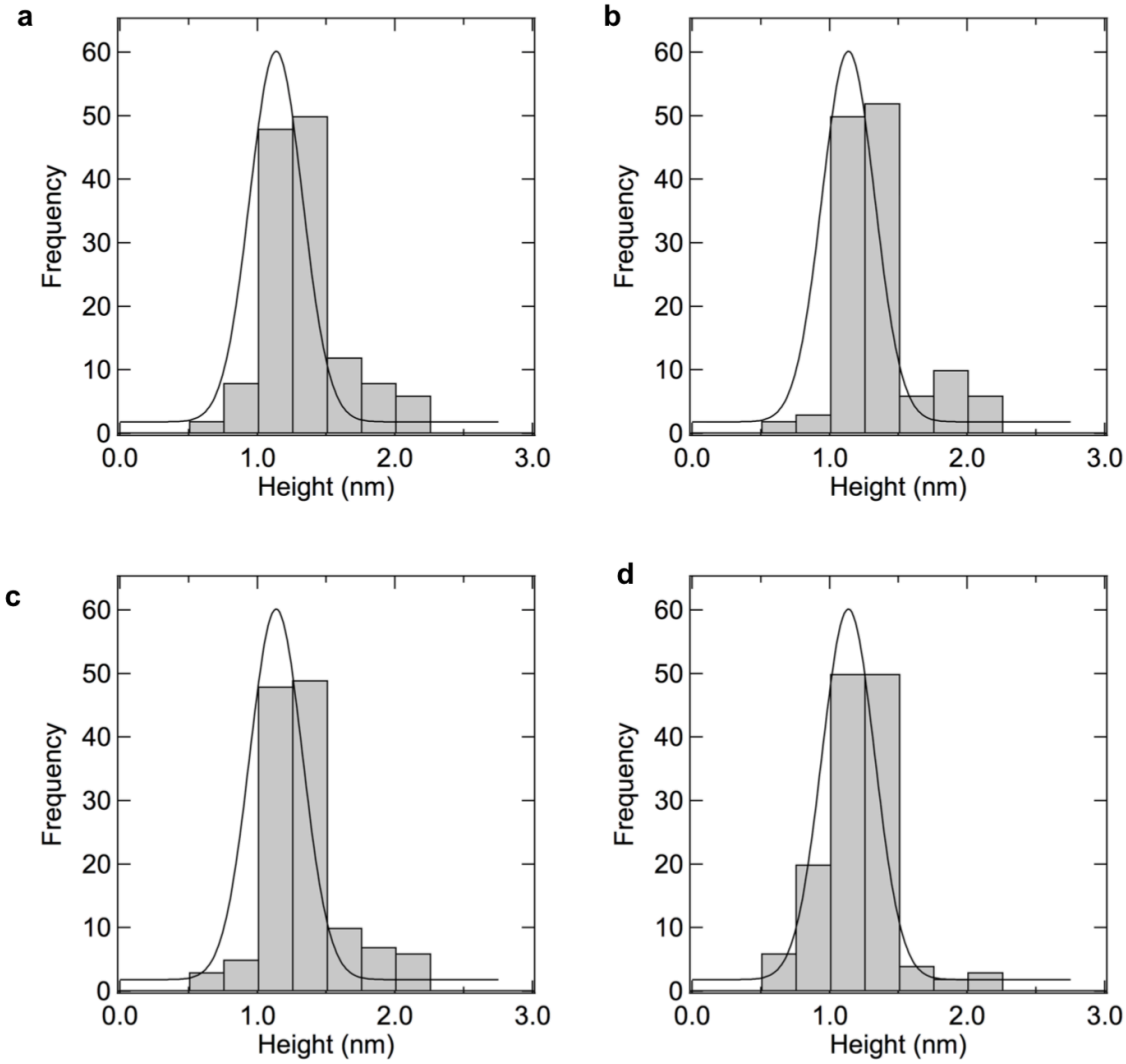

Figure 4-8. Height distribution diagrams calculated from AFM images of individually dispersed SWNTs. Used **CP-M** polymers are (**a**) **CP-Co**, (**b**) **CP-Ni**, (**c**) **CP-Cu** and (**d**) **CP-Zn**. Adapted from ref. 49 with kind permission. Copyright 2014 Springer Nature.

4-3-3. Separation of semiconducting-SWNTs and met-SWNTs.

I now describe how to separate the sem- and met-SWNTs from their mixtures. I discovered that the "solubility product" was different for the **CP-M**-wrapped semiconducting-SWNTs and met-SWNTs such that the addition of toluene (50 vol%) to the benzonitrile solutions of the SWNT-**CP-M** (M= Co, Ni, Cu or Zn) caused precipitates. Under ambient conditions, the concentrations of the SWNTs in the supernatant solutions reached equilibrium in 12 h. Interestingly, I found that only the semiconducting-SWNTs remained in the supernatants and the met-SWNTs were enriched in the sediments. I call this technique a "solubility product" method for the separation of sem- or met-SWNTs. The four different supernatants including the SWNT-**CP-M** (M= Co, Ni, Cu, or Zn) were filtered to remove the excess **CP-M** and the obtained residues were used for Raman spectral measurements. I also measured the vis-near IR (NIR) spectra of the residues that were completely redissolved in benzonitrile. The results are shown in Fig. 4-9 and Fig 4-10 (for the Raman spectra in the range of 500-2000 cm^{-1}, see Fig. 4-11).

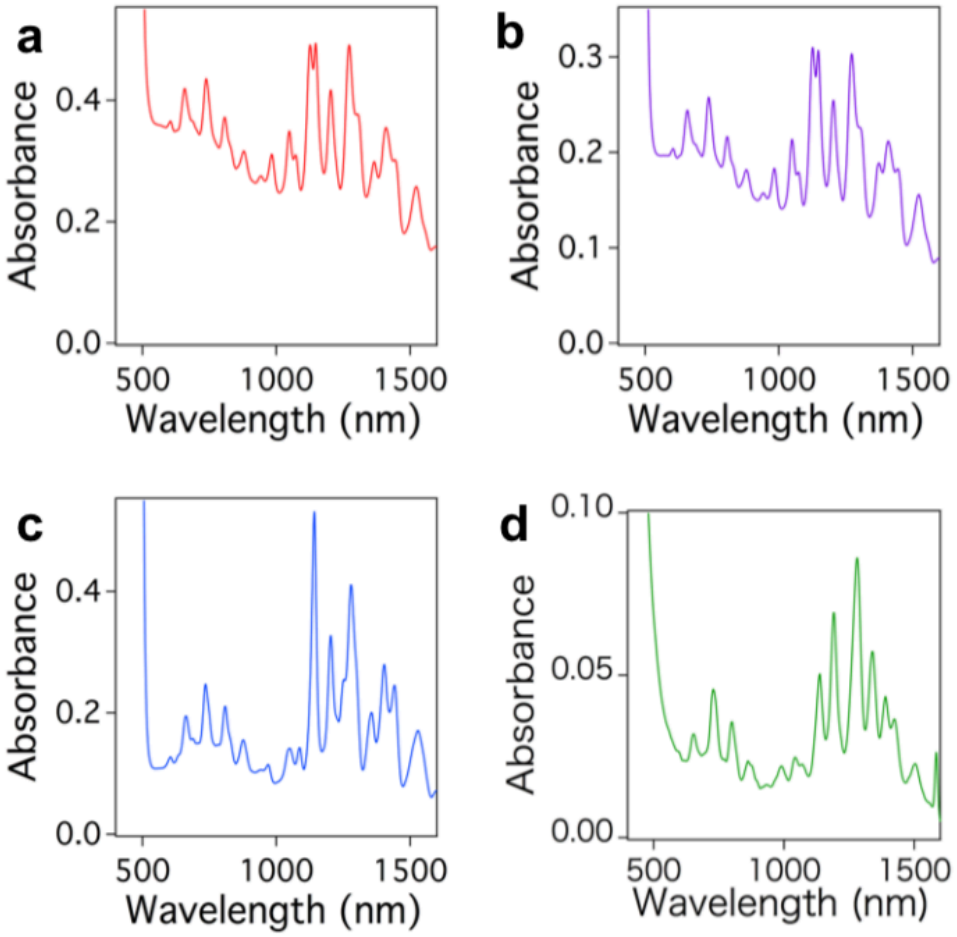

Figure 4-9. Vis-NIR absorption spectra of the supernatant solutions obtained after adding toluene (50wt%) to CP-M-solbilized SWNTs in benzonitrile. a-d, vis-NIR absorption spectra of sorted sem-SWNTs using **CP-Co** (**a**), **CP-Ni** (**b**), **CP-Cu** (**c**) and **CP-Zn** (**d**) (Optical cell length: 2 mm). Adapted from ref. 49 with kind permission. Copyright 2014 Springer Nature.

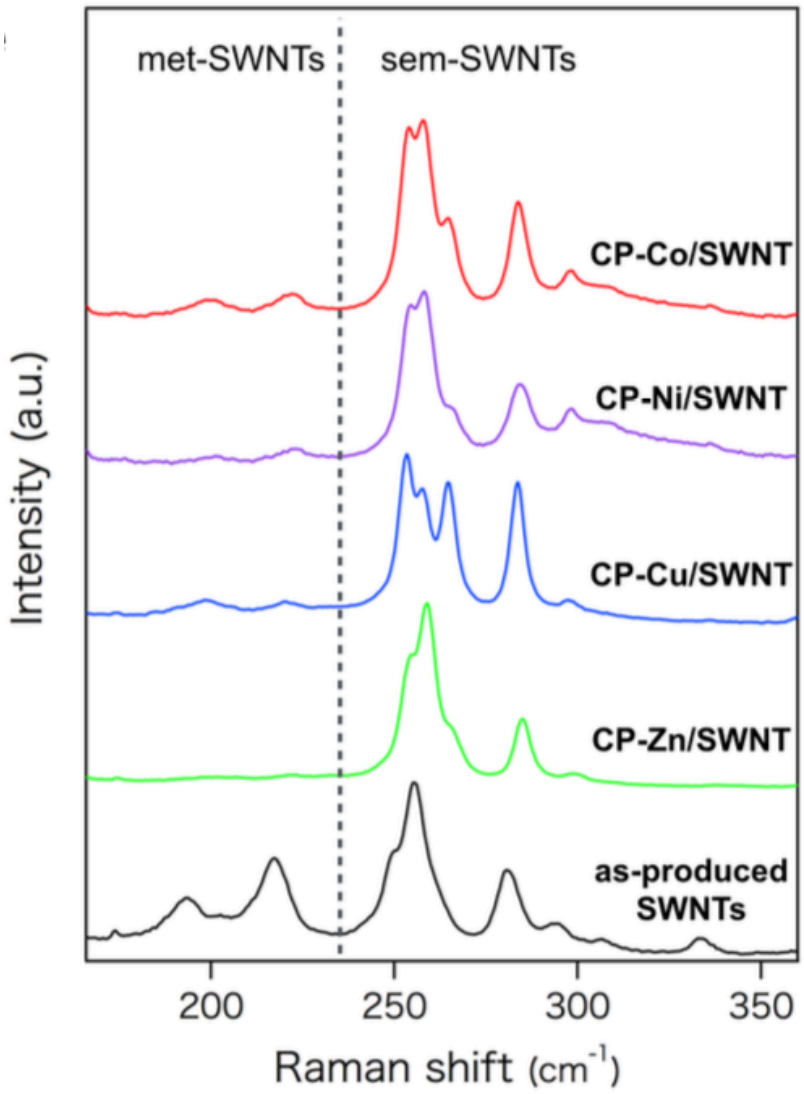

Figure 4-10. Raman spectra (excitation wavelength: 633 nm) of the solids obtained by filtration of the supernatant solutions. Raman spectrum of the pristine HiPco-SWNTs is also shown for comparison (black line). Adapted from ref. 49 with kind permission. Copyright 2014 Springer Nature.

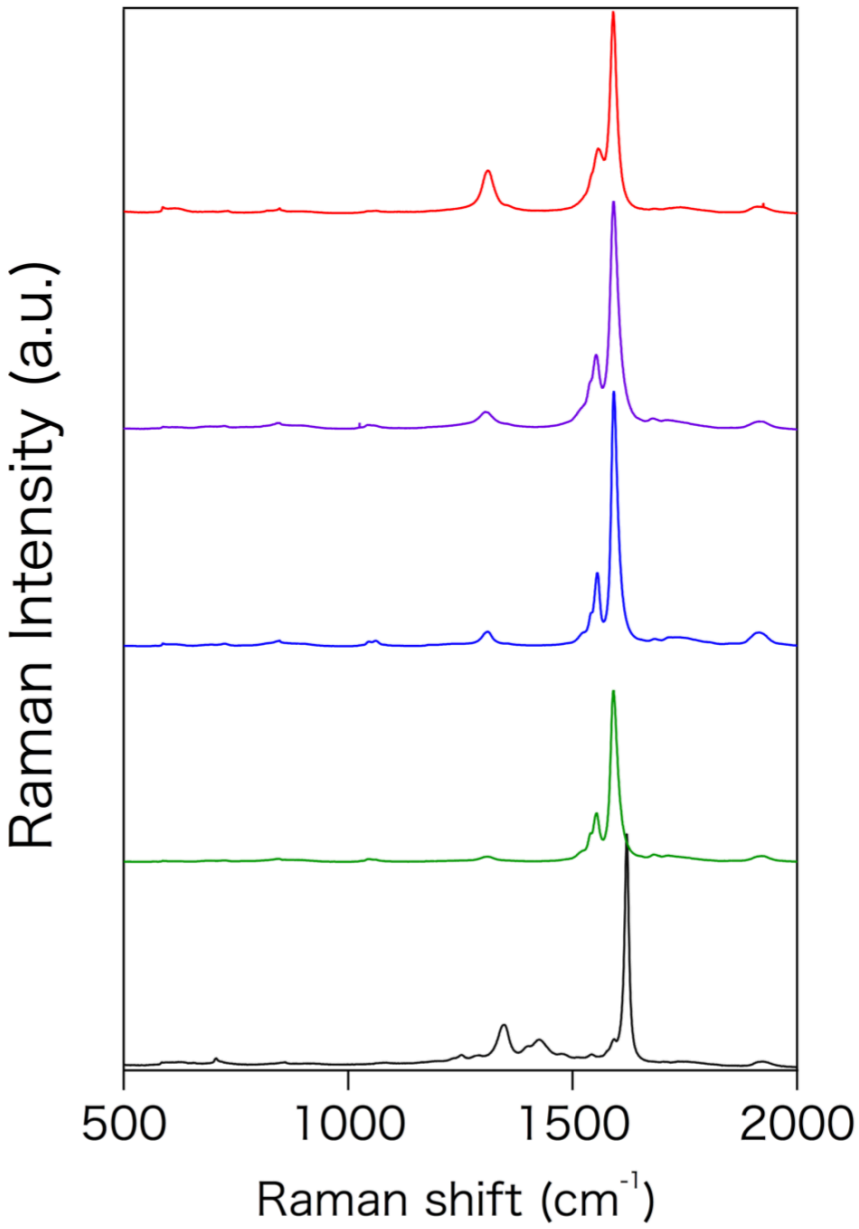

Figure 4-11. Raman spectra (excitation wavelength: 633 nm) of the solids generated by adding toluene to the supernatant solutions: **CP-M** (M=cobalt(II) (red), nickel(II) (purple), copper (II) (blue), and zinc(II) (green) ions). For comparison, the Raman spectrum of the pristine HiPco-SWNTs is shown in black line. Adapted from ref. 49 with kind permission. Copyright 2014 Springer Nature.

Notably, by comparison to the absorption spectra shown in Fig. 2a, I recognized the disappearance of the met-SWNT bands around 450-600 nm (Fig. 4-9a-d). The Raman spectra provided proof of the separation of the met- and semiconducting-SWNTs[43]. Compared to the spectrum of the as-produced SWNTs (black line in Fig. 4-10), the metallic band around 180-240 cm^{-1} greatly decreased in the spectra of the **CP-M**-SWNTs obtained after the "solubility product" procedure (Fig. 4-10). Notably, when using **CP-M** (M=Zn or Cu), the purity of the semiconducting-SWNTs reached ~99% (for M=Zn) and ~90% (for M=Cu). To the best of our knowledge, this extraction produced the highest reported purity of semiconducting-SWNTs and is a major advantage of our method.

When using the **CP-M** (M= Co and Ni) the extracted sem-purity was ~81%. As shown in Fig. 4-6a, the amounts of SWNTs dissolved by **CP-M** (M=Co and Ni) were much greater than those using the **CP-M** (M=Cu and Zn). The degree of the semiconducting-SWNT selectivity and the amounts of the extracted SWNTs might be related[41]. Such behavior is understandable since it is expected that greater amounts of solubilized SWNTs may undergo a loss of the high sem-/met-SWNT sorting selectivity.

The sediments generated by the solubility product procedure were also analyzed. They were fully dissolved in benzonitrile by sonication for 30 min. Based on their absorption and Raman spectra (Figs. 4-12 and 4-13), the met-SWNTs were greatly enriched in the solutions compared to the as-produced SWNTs; namely, the determined met-SWNT/semiconducting-SWNT ratios were 3/1, 2/1, 1/1 and 1/1 for **CP-Co**, **CP-Ni**, **CP-Cu** and **CP-Zn**, respectively, which were greater than that of the as-produced SWNT (met-SWNTs/semiconducting-SWNTs = 3/7). The observed metal dependency on the met-SWNT enrichment is related to the initial amounts of the solubilized SWNTs.

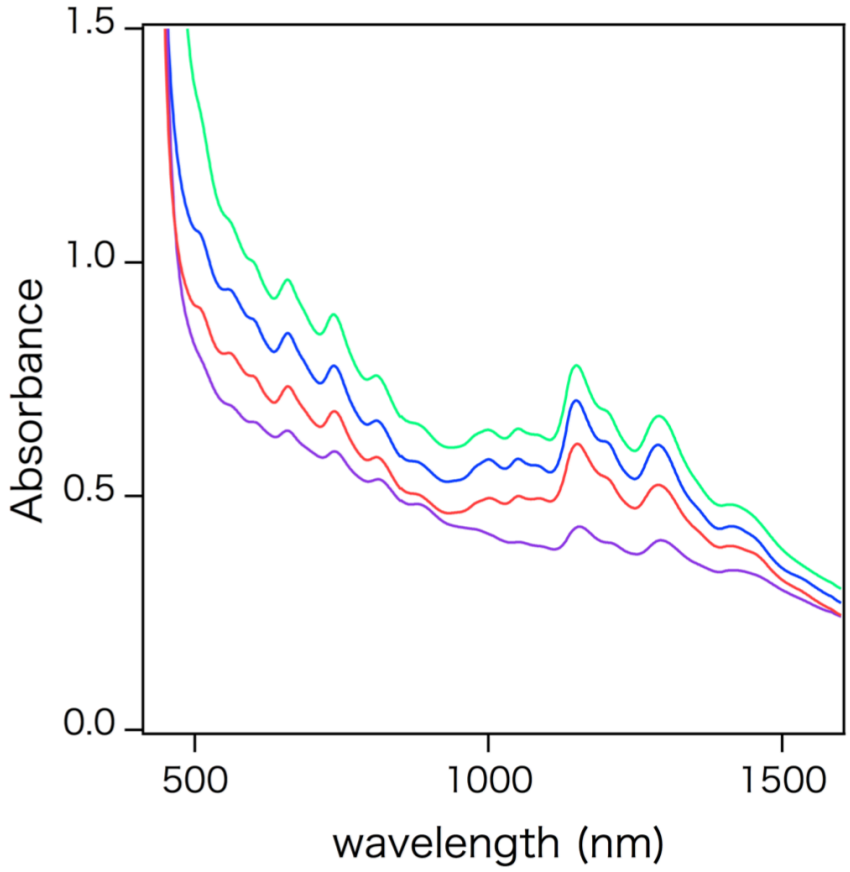

Figure 4-12. Absorption spectra of the redispersed solutions of the sediments obtained by "solubility product" procedures. CP-M (M=cobalt(II) (red), nickel(II) (purple), copper (II) (blue), and zinc(II) (green) ions). Adapted from ref. 49 with kind permission. Copyright 2014 Springer Nature.

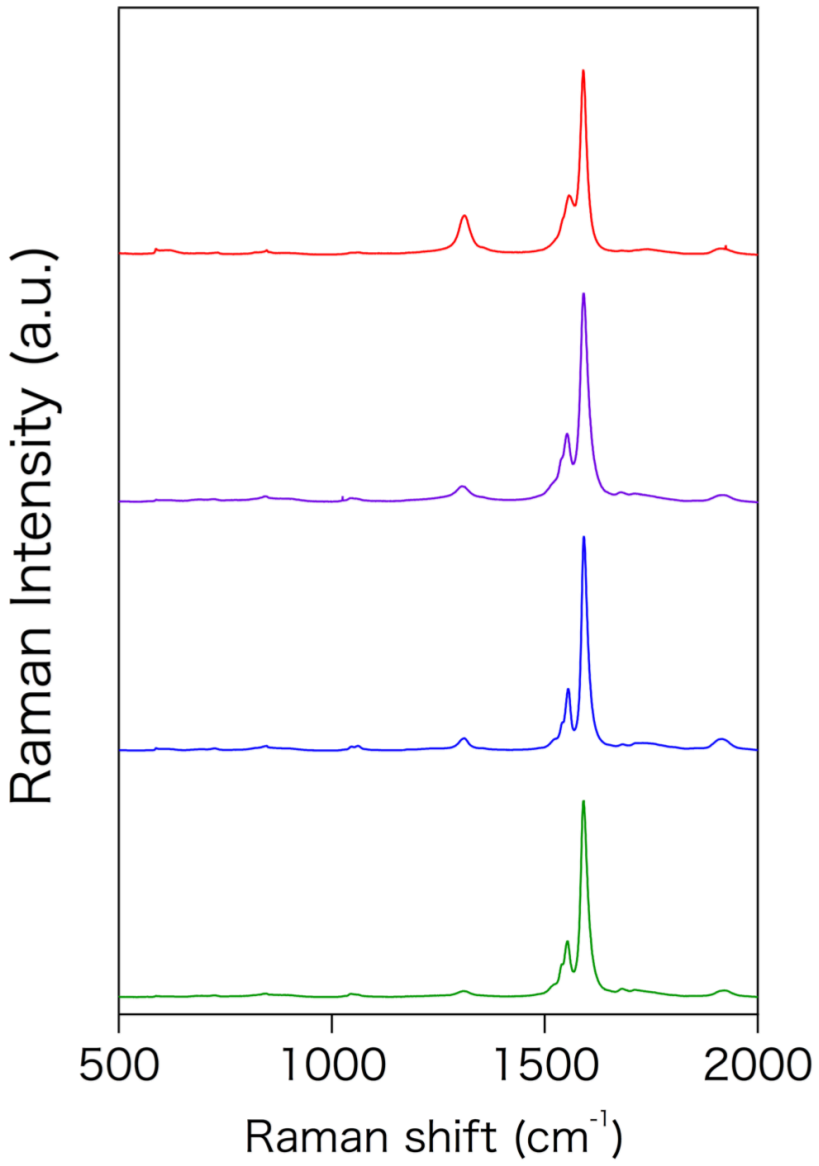

Figure 4-13. Raman spectra (excitation wavelength: 633 nm) of the solid (sediments on the filter papers) obtained by the "solubility product" procedures. CP-M (M=cobalt(II) (red), nickel(II) (purple), copper (II) (blue), and zinc(II) (green) ions) are used. Adapted from ref. 49 with kind permission. Copyright 2014 Springer Nature.

4-3-4. Removal of the CP-M.

As mentioned above, removal of the SWNT adsorbents (solubilizers) is essential for the efficient use of sem- and met-SWNTs in many applications. I now focus on how to produce pure semiconducting-SWNTs by the removal of **CP-M** from the CP-M/semiconducting-SWNT composites. When using conventional PFOs and their copolymers, their removal from the SWNT composites is quite difficult due to the strong interactions between the PFOs and SWNTs. The removal of adsorbents in our samples, on the other hand, was quite simple because the adsorbents are not covalent polymers but coordination polymers, which are readily depolymerized to the corresponding monomer units by the addition of an acid[34]. Eventually, the addition of a large excess trifluoroacetic acid to the supernatants generated precipitates, which were filtered, rinsed with benzonitrile and then methanol followed by air-drying. The obtained solids were analyzed by XPS and the result is shown in Fig. 4-14b, in which no peak of the metal ions and nitrogen appeared, indicating complete removal of the **CP-M**.

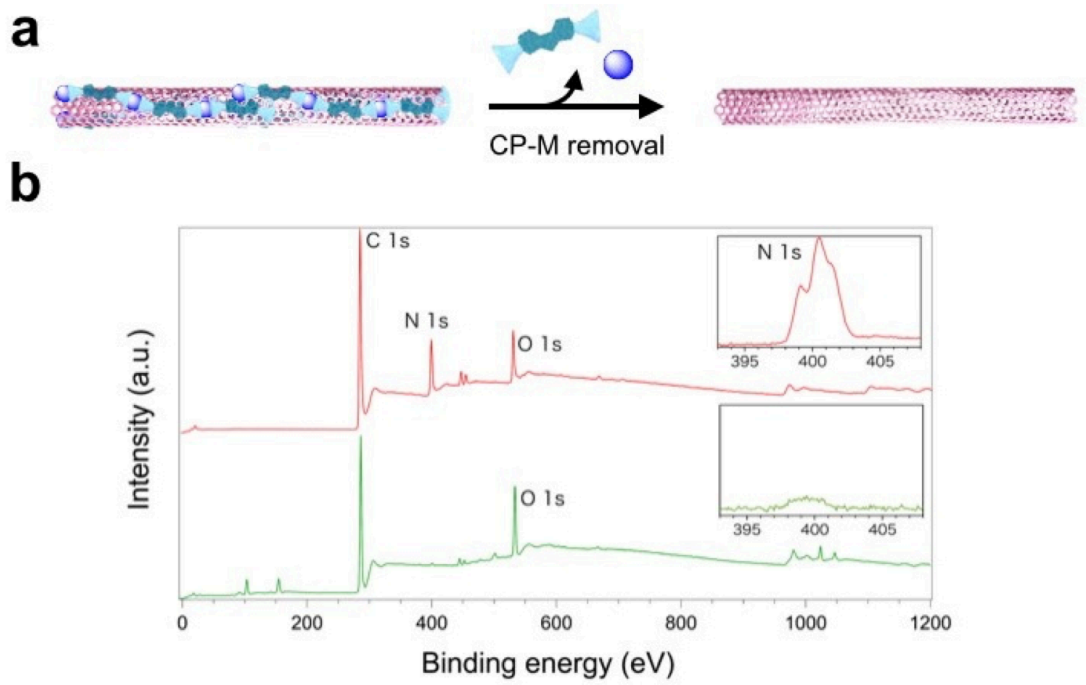

Figure 4-14. Validation of CP-M removal from SWNT surfaces. a, Schematic illustration of the removal of **CP-M** from the sem-SWNT surfaces via depolymerization of the **CP-M**. **b**, XPS spectra of the SWNTs before (red line) and after (green line) the depolymerization procedure. Adapted from ref. 49 with kind permission. Copyright 2014 Springer Nature.

The four different obtained solids after the removal of **CP-M** (M=Co, Ni, Cu and Zn) were each dispersed in 5 wt% sodium dodecylsulfate (SDS) aqueous micelle solutions in order to confirm the removal of the **CP-M** together with the determination of the (n,m) chiralities based on the analysis of their two dimensional photoluminescence (2D-PL) mappings. As shown in Fig. 4-15, **CP-M** completely quenched the PL of the SWNTs before acid treatment, due to the well-known heavy atom effect. Following acid treatment however, I observed evident PL signals for the SDS-redispersed samples, which are direct evidence that the **CP-M** (M=Zn) was removed from the **CP-M** (M=Zn)/SWNT composite (Fig. 4-16). The same behavior was observed when **CP-M** (M=Co, Ni and Cu) was used in place of **CP-Zn** (Fig. 4-17).

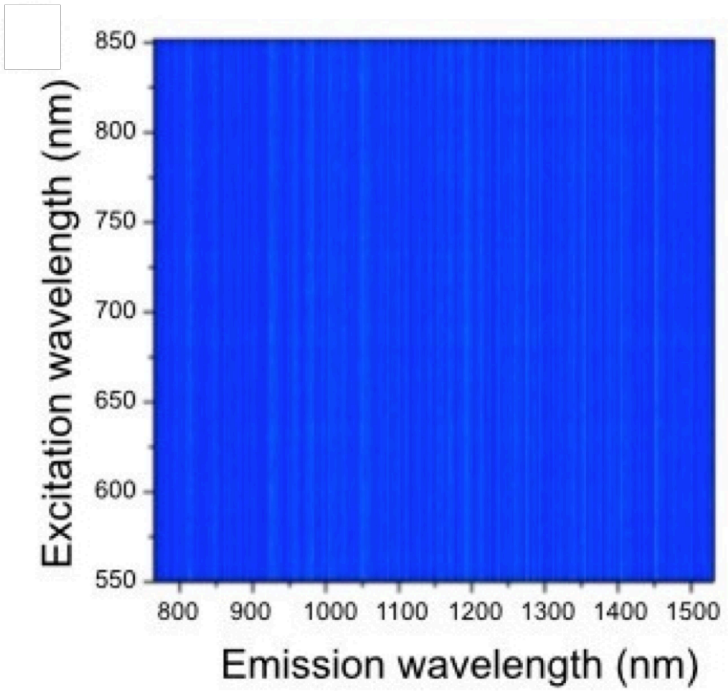

Figure 4-15. 2D-PL mappings of the SDS-solubilized SWNTs before the removal of **CP-Zn**. Adapted from ref. 49 with kind permission. Copyright 2014 Springer Nature.

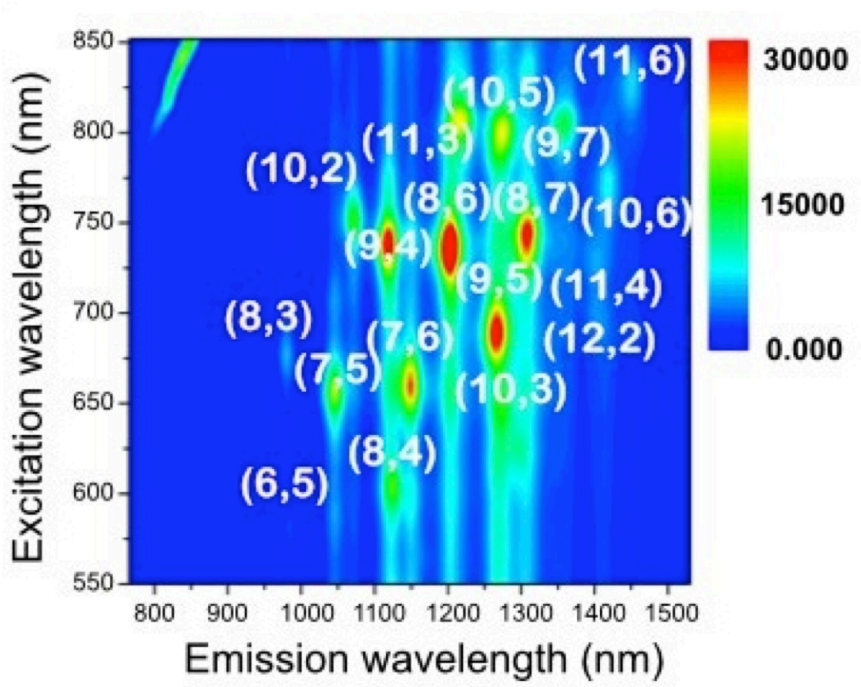

Figure 4-16. 2D-PL mappings of the SDS-solubilized SWNTs after the removal of **CP-Zn**. Adapted from ref. 49 with kind permission. Copyright 2014 Springer Nature.

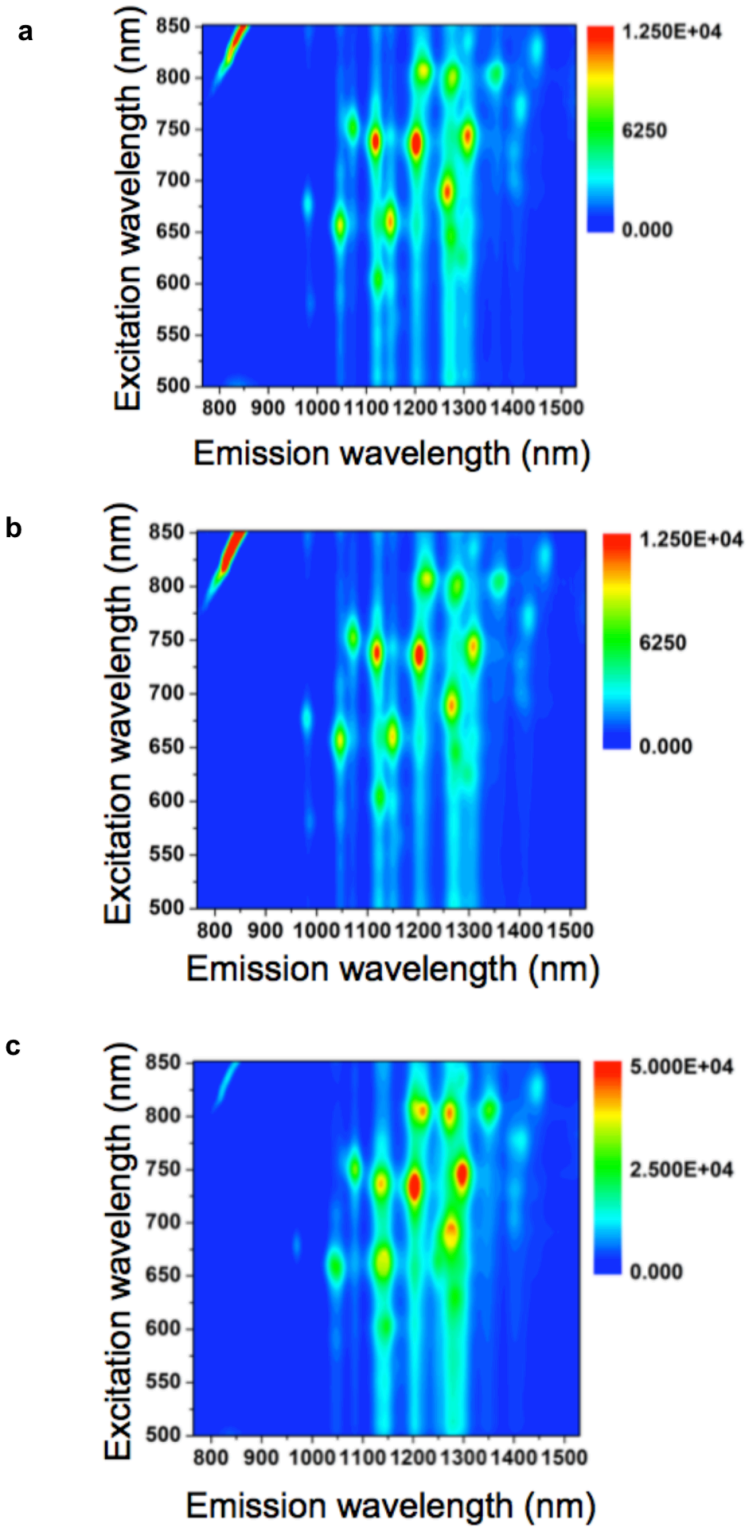

Figure 4-17. 2D-PL mapping of the SWNTs obtained after the removal of CP-M from the CP-M/SWNT composites. Used CP-M polymers are: (**a**) CP-Co, (**b**) CP-Ni and (**c**) CP-Cu. For the PL measurements, the SWNTs were dissolved in aqueous SDS micelle solutions. Adapted from ref. 49 with kind permission. Copyright 2014 Springer Nature.

I can now readily determine the (n,m) SWNT chiralities from the PL-mapping. As shown in Fig. 4-16, semiconducting-SWNTs with (n,m) = (6,5), (7,5), (7,6), (8,3), (8,4), (8,6), (8,7), (9,4), (9,5), (9,7), (10,2), (10,3), (10,5), (10,6), (11,3), (11,4), (11,6) and (12,2) were found to exist in the solution. The calibrated contents of the SWNT species deduced from the PL mapping are shown in Table S1, in which SWNTs with (n,m)=(7,6), (8,6), (9,4) and (10,2) were enriched. I also calculated the calibrated contents for the three samples (Tables 4-1 ~ 4-4).

Table 4-1. Calibrated content of the SWNT species deduced from the PL mapping of the samples obtained after removal of CP-M (M=Zn) from extracted sem-SWNTs. Adapted from ref. 49 with kind permission. Copyright 2014 Springer Nature.

(n,m)	PL peak intensity	Calculated PL intensity	Calibrated PL peak intensity	Calibrated content
(6,5)	166.99	0.67	111.88	0.43
(7,5)	2250.41	0.71	1597.79	6.16
(7,6)	5580.05	0.47	2622.62	10.12
(8,3)	651.09	2.13	1386.81	5.35
(8,4)	3498.19	0.46	1609.17	6.21
(8,6)	8690.48	0.49	4258.34	16.43
(8,7)	5334.99	0.30	1600.50	6.17
(9,4)	4070.12	0.70	2849.09	10.99
(9,5)	5462.74	0.28	1529.57	5.90
(9,7)	1724.12	0.27	465.51	1.80
(10,2)	1748.09	2.38	4160.46	16.05
(10,3)	2527.86	0.28	707.80	2.73
(10,5)	1986.03	0.47	933.43	3.60
(10,6)	867.17	0.21	182.11	0.70
(11,3)	2505.95	0.59	1478.51	5.70
(11,4)	717.76	0.20	143.55	0.55
(11,6)	675.05	0.26	175.51	0.68
(12,2)	551.06	0.20	110.21	0.43

Table 4-2. Calibrated content of the SWNT species deduced from the PL mapping of the samples obtained after removal of CP-M (M=Co) from extracted sem-SWNTs. Adapted from ref. 49 with kind permission. Copyright 2014 Springer Nature.

(n,m)	PL peak intensity	Calculated PL intensity	Calibrated PL peak intensity	Calibrated content
(6,5)	2020.32	0.67	1353.61	0.68
(7,5)	21450.69	0.71	15229.99	7.66
(7,6)	29839.71	0.47	14024.66	7.05
(8,3)	5522.27	2.13	11762.44	5.92
(8,4)	18453.28	0.46	8488.51	4.27
(8,6)	47862.51	0.49	23452.63	11.8
(8,7)	32748.61	0.3	9824.58	4.94
(9,4)	35665.24	0.7	24965.67	12.56
(9,5)	35245.35	0.28	9868.7	4.96
(9,7)	13439.19	0.27	3628.58	1.83
(10,2)	17441.22	2.38	41510.1	20.88
(10,3)	16291.99	0.28	4561.76	2.29
(10,5)	23304.23	0.47	10952.99	5.51
(10,6)	7828.46	0.21	1643.98	0.83
(11,3)	23453.45	0.59	13837.54	6.96
(11,4)	5242.35	0.2	1048.47	0.53
(11,6)	6707.11	0.26	1743.85	0.88
(12,2)	4607.08	0.2	921.42	0.46

Table 4-3. Calibrated content of the SWNT species deduced from the PL mapping of the samples obtained after removal of CP-M (M=Ni) from extracted sem-SWNTs. Adapted from ref. 49 with kind permission. Copyright 2014 Springer Nature.

(n,m)	PL peak intensity	Calculated PL intensity	Calibrated PL peak intensity	Calibrated content
(6,5)	202.90	0.67	135.94	0.59
(7,5)	1865.35	0.71	1324.40	5.73
(7,6)	2570.83	0.47	1208.29	5.23
(8,3)	513.12	2.13	1092.94	4.73
(8,4)	1601.25	0.46	736.57	3.19
(8,6)	5570.56	0.49	2729.57	11.82
(8,7)	4435.24	0.30	1330.57	5.76
(9,4)	4067.12	0.70	2846.98	12.33
(9,5)	4106.18	0.28	1149.73	4.98
(9,7)	2458.14	0.27	663.70	2.87
(10,2)	1823.94	2.38	4340.97	18.80
(10,3)	2212.90	0.28	619.61	2.68
(10,5)	3804.86	0.47	1788.29	7.74
(10,6)	1354.41	0.21	284.43	1.23
(11,3)	3677.90	0.59	2169.96	9.40
(11,4)	946.03	0.20	189.21	0.82
(11,6)	1179.45	0.26	306.66	1.33
(12,2)	888.25	0.20	177.65	0.77

Table 4-4.| Calibrated content of the SWNT species deduced from the PL mapping of the samples obtained after removal of CP-M (M=Cu) from extracted sem-SWNTs. Adapted from ref. 49 with kind permission. Copyright 2014 Springer Nature.

(n,m)	PL peak intensity	Calculated PL intensity	Calibrated PL peak intensity	Calibrated content
6,5)	166.99	0.67	111.88	0.43
(7,5)	2250.41	0.71	1597.79	6.16
(7,6)	5580.05	0.47	2622.62	10.12
(8,3)	651.09	2.13	1386.81	5.35
(8,4)	3498.19	0.46	1609.17	6.21
(8,6)	8690.48	0.49	4258.34	16.43
(8,7)	5334.99	0.30	1600.50	6.17
(9,4)	4070.12	0.70	2849.09	10.99
(9,5)	5462.74	0.28	1529.57	5.90
(9,7)	1724.12	0.27	465.51	1.80
(10,2)	1748.09	2.38	4160.46	16.05
(10,3)	2527.86	0.28	707.80	2.73
(10,5)	1986.03	0.47	933.43	3.60
(10,6)	867.17	0.21	182.11	0.70
(11,3)	2505.95	0.59	1478.51	5.70
(11,4)	717.76	0.20	143.55	0.55
(11,6)	675.05	0.26	175.51	0.68
(12,2)	551.06	0.20	110.21	0.43

The removed **PhenFO** molecules in the acid treatment were quantitatively deprotonated under basic conditions, indicating that reuse of the recovered **CP-M** for a further SWNT solubilization experiment is possible, which is another significant advantage of our method.

Finally, I discuss the extraction/separation efficiency of our solubility product method. Based on the decrease in the absorbance intensity between the sample solutions before and after the solubility product method, the semiconducting-SWNT sorting efficiencies were 66%, 57%, 91% and 32% for **CP-Co**, **CP-Ni, CP-Cu** and **CP-Zn**, respectively. By repeating the solubility product method for the precipitates, such efficiency is expected to be enhanced. I emphasize that the present method is simple and efficient for the separation of the sem- and met-SWNTs. It is also expected that by changing the metal ions, counter anions, solvents and ligands, a more efficient selective collection of the semiconducting-SWNTs with a specific chirality might be possible.

4-3-5. Molecular mechanics simulations.

As described above, **CP-Zn** sorted the semiconducting-SWNTs (especially, sem-(8,6)SWNTs) with a very high efficiency, while **CP-Co** did not. In an effort to understand these recognition differences, a computer simulation technique was used to model the sem-(8,6)- and met-(7,7) SWNTs as the typical sem- and met-SWNTs, respectively, since their diameters are close (0.952 nm and 0.949 nm, for (8,6)- and (7,7)SWNTs, respectively). I carried out an all-atomic molecular mechanical calculation using the OPLS2005 force field[44]. The used initial structure of the **CP-M** strip was a 6-mer (oligomer), which was found in the ESI-TOF-Mass spectrum (Fig. 4-3).

The length of each SWNT used in this calculation was 30 nm, which is efficient for the contact of the **CP-M** with the center 1/3 of the SWNT. Considering the surface areas of the SWNTs, four different **CP-M** strips were placed to cover the SWNTs and used as the initial structures. This model was equilibrated in toluene by simulation using a low-mode sampling and the structures were minimized using the OPLS2005 force field. I calculated the optimized structures for the combination of **CP-Zn** with sem-(8,6)SWNT (Fig. 4-18a), or met-(7,7)SWNT (Fig. 4-18b), as well as those of **CP-Co** with sem-(8,6)SWNT (Fig. 4-18c) or met-(7,7)SWNT (Fig. 4-18d). To predict the binding strengths between the **CP-M** and the (8,6)- and (7,7)SWNTs, the binding energies ($E_{stabilizing}$) of each SWNT with the **CP-M** complex was calculated as:

$$E_{stabilizing} = E_{\text{complex}} - (E_{\text{SWNT}} + 4 \text{ x } E_{\textbf{CP-M}}) \qquad (1)$$

where E_{complex}, E_{SWNT} and $E_{\textbf{CP-M}}$ are the energies of the SWNT/**CP-M** complexes, SWNT and **CP-M**, respectively[45, 46]. The results are summarized in Table 1 for the calculated potential and stabilizing energy of the **CP-Co** and **CP-Zn** systems, respectively. The stabilizing energy for the interaction between the **CP-Zn** and the sem-(8,6)SWNT was 3,254 kcal/mol, which is much higher than that between the **CP-Zn** and met-(7,7)SWNT (1,880 kcal/mol). In contrast, the stabilizing energies between the **CP-Co** with the (8,6)- and (7,7)SWNTs were comparable (1,435 kcal/mol and 1,401 kcal/mol, respectively). In the optimized simulated structure of **CP-Zn**/SWNT, the fluorene moieties semi-helically aligned on both the sem-(8,6) and met-(7,7)-SWNTs when the complexes take a tetrahedral configuration (Figs. 4-18a and 4-18b, respectively). On the other hand, the square-planar complex of **CP-Co** preferred to take a

straight configuration on the met-SWNT (Figs. 4-18c, 4-18d). This different recognition behavior together with the obtained binding energies indicates that **CP-Zn** with a tetrahedral coordination structure favors sem-(8,6)SWNT rather than met-(7,7)SWNT in toluene, which is consistent with the experimental results.

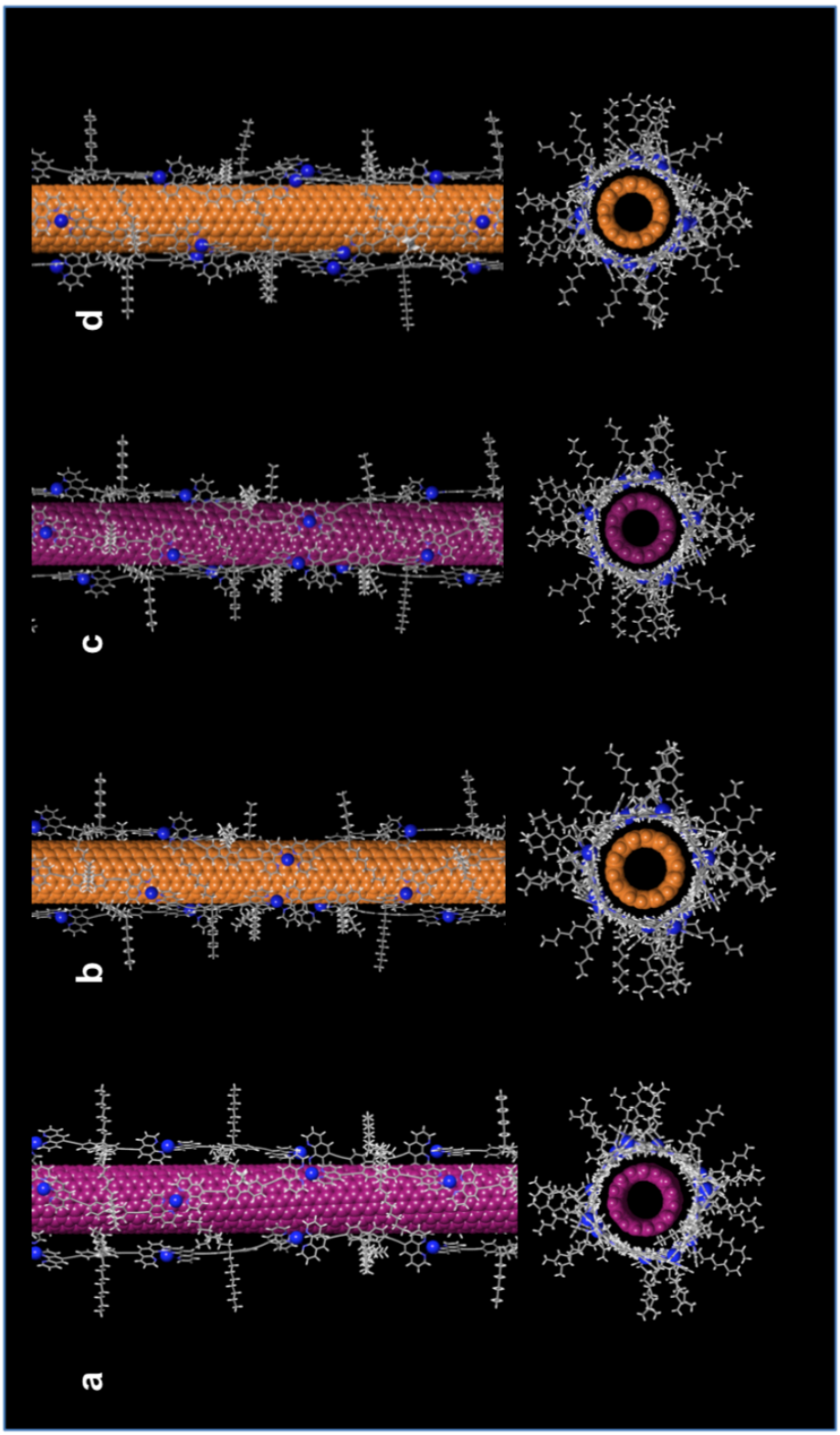

Figure 4-18. Optimized structures of the simulated composites using four CP-M strips on the SWNTs. a-d, Top views (top row) and side views (bottom row) of CP-Zn/sem-(8,6)-SWNT (**a**), CP-Zn/met-(7,7)-SWNT (**b**), CP-Co/sem-(8,6)-SWNT (**c**) and CP-Co/met-(7,7)-SWNT(**d**). Blue-highlighted spheres represent metal ions. Adapted from ref. 49 with kind permission. Copyright 2014 Springer Nature.

Table 4-5. Calculated potential and stabilizing energies between the (n,m)SWNTs with the CP-M (M=Zn or Co). All energies are in kcal/mol. Adapted from ref. 49 with kind permission. Copyright 2014 Springer Nature.

Chirality (n,m)	**CP-M**	potential energy of SWNT E_{SWNT}	potential energy of **CP-M** $E_{CP\text{-}M}$	Total potential energy (E_{SWNT} + 4x $E_{CP\text{-}M}$)	Potential energy of complex $E_{complex}$	stabilizing energy $E_{stabilizing} = E_{complex} -$ (E_{SWNT} +4 x $E_{CP\text{-}M}$)
(8,6)	**CP-Zn**	38722.4	3357.8	42080.3	38826.2	-3254.6
(7,7)	**CP-Zn**	39753.1	3357.8	43110.9	41230.9	-1880.9
(8,6)	**CP-Co**	38722.4	3293.6	42016.0	40580.8	1435.2
(7,7)	**CP-Co**	39753.1	3293.6	43047.0	41645.4	1401.6

4-4. Conclusion

In conclusion, a novel strategy for the efficient extraction of highly pure semiconducting-SWNTs based on supramolecular coordination chemistry is presented. The most interesting features are summarized as follows: i) I designed and synthesized coordination polymers **CP-M** (M= Co, Ni, Cu and Zn) that exhibited an excellent SWNT solubilizing ability in benzonitrile, ii) based on our "solubility product" procedure, I isolated the sem-SWMTs with a 99% purity, iii) I have succeeded in the complete removal of the wrapping **CP-M** by a simple acid treatment and iv) the selectivity of the met- and semiconducting-SWNTs was explained by molecular mechanics simulations. Such an efficient and easy extraction of the semiconducting-SWNTs with very a high purity is a great advance in the chirality separation science of SWNTs and opens a new field for use of such materials in many applications. For the further development of such supramolecular removable solubilizers, other weak bond based supramolecular system will be applicable. It is important to use more mild conditions to break wrapping polymers other than acid or base to prevent the doping effect of the purified SWCNTs. Further investigation is undergoing to develop more clean supramolecular system with mild external stimuli.

References

1 Dresselhaus, M. S., Dresselhaus, G. & Avouris, P. Carbon Nanotubes Synthesis, Structure, Properties and Applications (Springer, 2001).

2. D'Souza, F., Kadish, K. M., Eds. Handbook of Carbon Nano Materials. (World Scientific, 2011).

3. R. Krupke, F. Hennrich, in *Chemistry of Carbon Nanotubes* (ed. V. A. Basiuk, E. V. Basiuk) Chap. 7 (American Scientific Publisher, 2008).

4. Ajayan, P. M. Nanotubes from carbon. *Chem. Rev.* **99**, 1787-1799 (1999).

5. Tanaka, Y. *et al*. Experimentally determined redox potentials of individual (n,m) single-walled carbon nanotubes. *Angew. Chem. Int. Ed.* **48,** 7655–7659 (2009).

6. Hirana, Y., Tanaka, Y., Niidome, Y. & Nakashima, N. Strong micro-dielectric environment effect on the band gaps of (n,m)single-walled carbon nanotubes. *J. Am. Chem. Soc.* **132,** 13072–13077 (2010).

7. Park, J. S. *et al*. Observation of Negative and Positive Trions in the Electrochemically Carrier-Doped Single-Walled Carbon Nanotubes. *J. Am. Chem. Soc.* **134**, 14461–14466 (2012).

8. Jorio, A. *et al*. Structural (n, m) determination of isolated single-wall carbon nanotubes by resonant Raman scattering. *Phys. Rev. Lett.* **86**, 1118-1121 (2001).

9. Bachilo, S. M. et al. Structure-assigned optical spectra of single-walled carbon nanotubes. *Science* **298**, 2361-2366 (2002).

10. Hirana, Y. *et al*. Empirical Prediction of Electronic Potentials of Single-Walled Carbon Nanotubes With a Specific Chirality (n,m). *Sci. Rep.* **3,** 2959 (2013).

11. Cao, Q. & Rogers, J. A. Ultrathin Films of Single-Walled Carbon Nanotubes for Electronics and Sensors: A Review of Fundamental and Applied Aspects. *Adv. Mat.* **21,** 29–53 (2009).

12. Hasan, T. *et al*. Nanotube–Polymer Composites for Ultrafast Photonics. *Adv. Mat.* **21,** 3874–3899 (2009).

13. Zhang, J. et al. Robust digital VLSI using carbon nanotubes. *IEEE Trans. CAD* **31**, 453–471 (2012).

14. Blackburn, J. L. *et al*. Transparent Conductive Single-Walled Carbon Nanotube Networks with Precisely Tunable Ratios of Semiconducting and Metallic Nanotubes. *ACS Nano* **2,** 1266–1274 (2008).

15. Krupke, R., Hennrich, F., Löhneysen, H. v. & Kappes, M. M. Separation of Metallic from Semiconducting Single-Walled Carbon Nanotubes. *Science* **301 ,** 344–347 (2003).

16. Tu, X., Manohar, S., Jagota, A. & Zheng, M. DNA sequence motifs for structure-specific recognition and separation of carbon nanotubes. *Nature* **460,** 250–253 (2009).

17. Kato, Y., Inoue, A., Niidome, Y. & Nakashima, N. Thermodynamics on Soluble Carbon Nanotubes: How Do DNA Molecules Replace Surfactants on Carbon Nanotubes? *Sci. Rep.* **2,** 733 (2012).

18. Chen, J. *et al*. Noncovalent engineering of carbon nanotube surfaces by rigid, functional conjugated polymers. *J. Am. Chem. Soc.* **124**, 9034–9035 (2002).

19. Arnold, M. S., Green, A. a, Hulvat, J. F., Stupp, S. I. & Hersam, M. C. Sorting carbon nanotubes by electronic structure using density differentiation. *Nature Nanotech.* **1**, 60–65 (2006).

20. Ghosh, S., Bachilo, S. M. & Weisman, R. B. Advanced sorting of single-walled carbon nanotubes by nonlinear density-gradient ultracentrifugation. *Nature Nanotech.* **5**, 443–450 (2010).

21. Tanaka, T., Hehua, J., Miyata, Y. & Kataura, H. High-yield separation of metallic and semiconducting single-wall carbon nanotubes by agarose gel electrophoresis. *App. Phys. Exp.* **1,** 1–3 (2008).

22. Liu, H., Nishide, D., Tanaka, T. & Kataura, H. Large-scale single-chirality separation of single-wall carbon nanotubes by simple gel chromatography. *Nature Commun.* **2**, 309 (2011).

23. Hirano, A., Tanaka, T. & Kataura, H. Thermodynamic Determination of the Metal/Semiconductor Separation of Carbon Nanotubes Using Hydrogels. *ACS Nano* **11**, 10195–10205 (2012).

24. Chen, F., Wang, B., Chen, Y. & Li, L.-J. Toward the extraction of single species of single-walled carbon nanotubes using fluorene-based polymers. *Nano Lett.* **7,** 3013–3017 (2007).

25. Nish, A., Hwang, J., Doig, J. & Nicholas, R. Highly selective dispersion of single-walled carbon nanotubes using aromatic polymers. *Nature Nanotech.* **2,** 640-646 (2007).

26. Ozawa, H. *et al*. Rational concept to recognize/extract single-walled carbon nanotubes with a specific chirality. *J. Am. Chem. Soc.* **133,** 2651–2657 (2011).

27. Ozawa, H., Fujigaya, T., Song, S., Suh, H. & Nakashima, N. Different Chiral Selective Recognition/Extraction of (n,m)Single-walled Carbon Nanotubes Using Copolymers Carrying a Carbazole or Fluorene Moiety. *Chem. Lett.* **40,** 470–472 (2011).

28. Ozawa, H., Ide, N., Fujigaya, T., Niidome, Y. & Nakashima, N. One-pot Separation of Highly Enriched (6,5)-Single-walled Carbon Nanotubes Using a Fluorene-based Copolymer. *Chem. Lett.* **40,** 239–241 (2011).

29. Akazaki, K., Toshimitsu, F., Ozawa, H., Fujigaya, T. & Nakashima, N. Recognition and one-pot extraction of right- and left-handed semiconducting single-walled carbon nanotube enantiomers using fluorene-binaphthol chiral copolymers. *J. Am. Chem. Soc.* **134,** 12700–12707 (2012).

30. Izard, N. *et al*. Semiconductor-enriched single wall carbon nanotube networks applied to field effect transistors. *App. Phys. Lett.* **92,** 243112 (2008).

31. Jakubka, F. *et al*. Effect of Polymer Molecular Weight and Solution Parameters on Selective Dispersion of Single-Walled Carbon Nanotubes. *ACS Macro Lett.* **1,** 815–819 (2012).

32. Steed, J. W., Atwood, J. L., Supramolecular Chemistry (Wiley, 2009)

33. Kurth, D. G. & Higuchi, M. Transition metal ions: weak links for strong polymers. *Soft Matt.* **2**, 915–927 (2006).

34. Paulusse, J. M. J. & Sijbesma, R. P. Reversible Mechanochemistry of a Pd^{II} Coordination Polymer. *Angew. Chem. Int. Ed.* **116**, 4560–4562 (2004).

35. Wang, Y., Xu, H. & Zhang, X. Tuning the Amphiphilicity of Building Blocks: Controlled Self-Assembly and Disassembly for Functional Supramolecular Materials. *Adv. Mat.* **21,** 2849–2864 (2009).

36. Lemasson, F. *et al*. Debundling, selection and release of SWNTs using fluorene-based photocleavable polymers. *Chem. Comm*. **47**, 7428–7430 (2011).

37. Wang, W. Z. *et al*. Degradable Conjugated Polymers: Synthesis and Applications in Enrichment of Semiconducting Single-Walled Carbon Nanotubes. *Adv. Func. Mat*. **21**, 1643–1651 (2011).

38. Chichak, K. S., Star, A., Altoé, M. V. P. & Stoddart, J. F. Single-walled carbon nanotubes under the influence of dynamic coordination and supramolecular chemistry. *Small* **1**, 452–461 (2005).

39. Llanes-Pallas, A. *et al*. Modular engineering of H-bonded supramolecular polymers for reversible functionalization of carbon nanotubes. *J. Am. Chem. Soc*. **133**, 15412–15424 (2011).

40. Schmittel, M., Kalsani, V., Kishore, R. S. K., Cölfen, H. & Bats, J. W. Dynamic and Fluorescent Nanoscale Phenanthroline/Terpyridine Zinc(II) Ladders. Self-Recognition in Unlike Ligand/Like Metal Coordination Scenarios. *J. Am. Chem. Soc*. **127**, 11544–11545 (2005).

41. Hwang, J.-Y. *et al*. Polymer structure and solvent effects on the selective dispersion of single-walled carbon nanotubes. *J. Am. Chem. Soc*. **130**, 3543–3553 (2008).

42. Moulton, B. & Zaworotko, M. J. From Molecules to Crystal Engineering: Supramolecular Isomerism and Polymorphism in Network Solids. *Chem. Rev*. **101**, 1629–1658 (2001).

43. Dresselhaus, M., Dresselhaus, G., Saito, R. & Jorio, A. Raman spectroscopy of carbon nanotubes. *Phys. Rep*. **409,** 47–99 (2005).

44. Mohamadi, F. *et al*. Macromodel—an integrated software system for modeling organic and bioorganic molecules using molecular mechanics. *J. Comp. Chem*. **11,** 440–467 (1990).

45. Ozawa, H., Fujigaya, T., Niidome, Y. & Nakashima, N. Effect of Backbone Chemical Structure of Polymers on Selective (n,m)Single-Walled Carbon Nanotube Recognition/Extraction Behavior. *Chem. Asian J*. **6,** 3281–3285 (2011).

46. Ozawa, H. *et al*. Supramolecular hybrid of gold nanoparticles and semiconducting single-walled carbon nanotubes wrapped by a porphyrin-fluorene copolymer. *J. Am. Chem. Soc*. **133,** 14771–14777 (2011).

47. Girardot, C. *et al*. Novel ruthenium(II) and zinc(II) complexes for two-photon absorption related applications. *Dalton Trans*. **3**, 3421–3426 (2007).

48. Khan, M. S. *et al*. Synthesis, characterisation and optical spectroscopy of diynes and polyynes containing derivatised fluorenes in the backbone. *Dalton Trans*. **1**, 74–84 (2003).

49. Toshimitsu, F. & Nakashima, N., *Nat. Commun.* **5,** 5041 (2014).

Chapter 5

Removable hydrogen-bonding polymer based on fluorene units for the selective sorting of long and pure semiconducting SWCNTs

5-1. Introduction

SWCNTs have attracted special interests as materials with remarkable electronic, mechanical, thermal and photophysical properties due to their unique one-dimensional structures.[1-4] Their characteristic quantum-confined structures due to their chiral indices (n,m) provide unique opto-nanoelectronic behaviors.[5-9] Therefore, the separation/purification of the semiconducting-SWCNTs based on their chiralities is one of the most important issues in the science and applications of carbon nanotubes[10,11]. However, to achieve chiral- and chemical-purifications at the same time is still challenging because most of the commercially supplied as-produced SWCNTs contains both semiconducting-SWCNTs and metallic-SWCNTs as well as metal catalysts and other carbon forms. A typical purification requires solution-phase processes using surfactants[12], which also chemically contaminate the semiconducting-SWCNTs by changing the surrounding environments that alter the intrinsic properties of the semiconducting-SWCNTs.[13-15]

Many attempts toward the goal of selective semiconducting-SWCNT sorting have been reported and the typical methods include polymer-wrapping,[16-24] density gradient ultracentrifugation[25,26] and gel chromatography.[27-29] However, for almost all of them, the

procedures are not very simple, but rather complex. In addition, such methods involve a serious drawback, that is, complete removal of the used adsorbents from the sorted SWCNT surfaces is difficult. [30-32] Even after the suitable adsorbent removal procedure, some adsorbent molecules still remain on the sorted SWCNTs.[33-36] I previously reported an efficient SWCNT sorting using a supramolecular coordination polymers (**CP**s)[37] followed by complete removal of the **CP**s based on dynamic supramolecular coordination chemistry[38], which was the first report to utilize a supramolecular system for the selective sorting of the semiconducting-SWCNTs not containing the used adsorbent. In contrast, other reported polymers for the chemical purification of SWCNTs usually lack a chirality sorting ability and/or adsorbent-removal process.[30-34,38,39] Furthermore, in order to maintain the original semiconducting-SWCNT properties after the sorting processes, structural identities of the semiconducting-SWCNTs, such as the length and crystallinity of the graphitic surface structure, must be preserved,[40] which is very difficult under conventional solubilizing/sorting experimental conditions using strong sonication,[25,41-43] which is a destructive process for the SWCNTs. This issue is especially important for the semiconducting-SWCNTs with smaller diameters, such as chemical vapor deposition-produced HiPco- and CoMoCAT-SWCNTs having much larger band gaps than those of the SWCNTs with large diameters synthesized by the arc-discharged or laser-ablation method. [44] Such small diameter SWCNTs are promising materials for use in optoelectronic device applications, such as thin film transistors, transistors, sensors, etc.

Here, I report a mild and highly chirality-selective extracting method for the chemically pure smaller diameter semiconducting-SWCNT sorting using newly-designed and synthesized supramolecular hydrogen-bond polymers (**HBP**s) as shown in Fig. 5-1 together with the concept of this study. The semiconducting-SWCNT selectivity is programmed in the **HBP**s by introducing fluorene moieties, which features molecular recognition of the semiconducting-SWCNTs[16-18, 20-22, 30,35-37], and the formation of a linear polymer conformation achieved by the

combination of a carboxylic acid and 4-aminopyridine on both ends of the fluorene is designed for the selective sorting of smaller diameter SWCNTs. As a **HBP**, I designed and synthesized two building blocks, 2,7-bis-4-aminopyridyl-9,9'-dioctylfluorene (**1**) and 2,7-dicarboxyl-9,9'-dioctylfluorene (**2**). Furthermore, the simplicity of the **HBP** conformations aided in determining the mechanism of the chiral-selectivity of the **HBP** by considering the molecular surface area and the molecular weight of the composite with semiconducting-SWCNTs, which is the first trial to evaluate the selectivity extracting specific chiral semiconducting-SWCNTs based on the dynamic supramolecular chemistry.

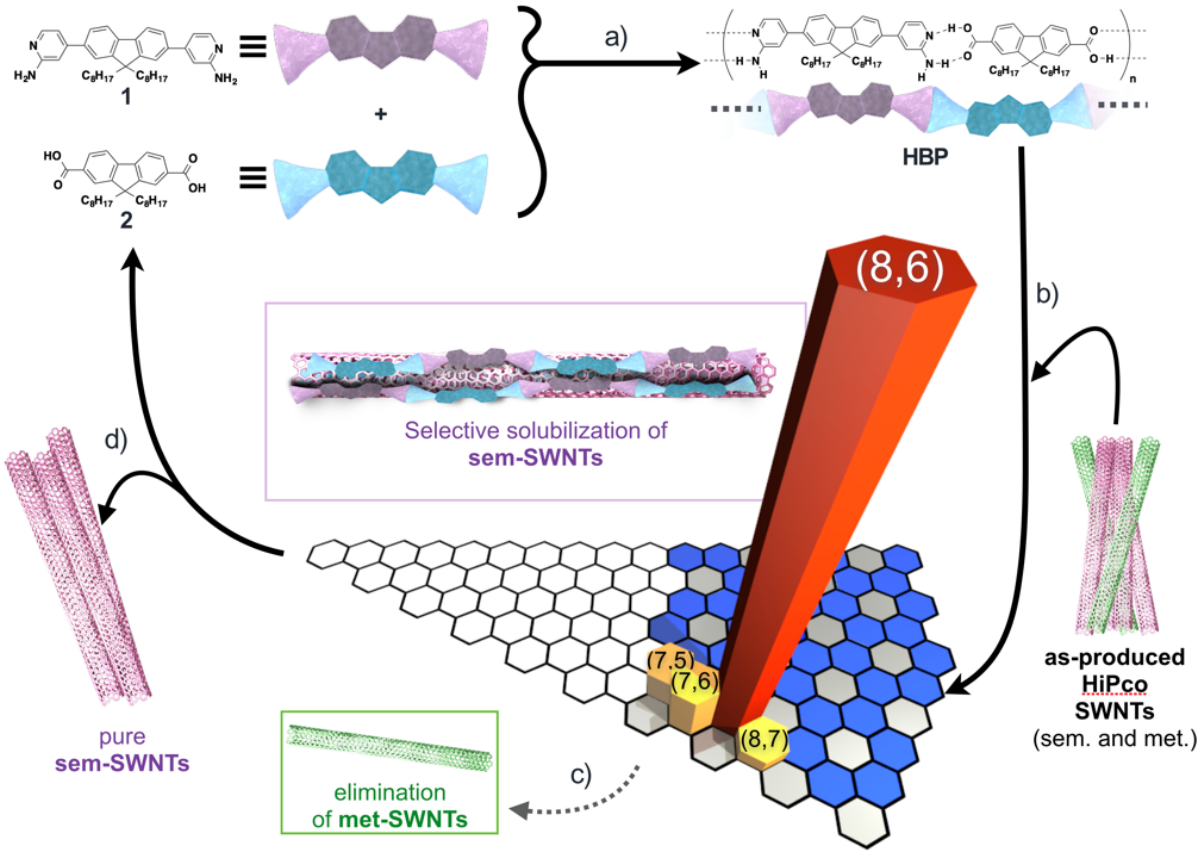

Figure 5-1. Schematic illustration of the purification cycle of sem-SWNTs using HBP made of 1 and 2. (a) Chemical structures of **1**, **2** and **HBP** formed by **1** and **2**. (b) Solubilization/sorting of the sem-SWNTs using the **HBP** takes place with (c) the elimination of met-SWNTs in toluene-acetone mixed solvent. (d) The reversible formation and deformation of **HBP** enabled regeneration of fresh **1** and **2** after the separation of chemically-pure sem-SWNTs. Adapted from ref. 49 with kind permission. Copyright 2015 Springer Nature.

In this study, our goal is to extract long semiconducting-SWCNTs with smaller tube diameters while retaining their structural properties. During this study, using a concept that is similar to our previous report based on dynamic supramolecular chemistry[37], Pochorovski et al. [44] focused on the extraction of large-diameter SWCNTs and reported the extraction of arc-discharge-produced SWCNTs with diameters in the range of 1.28-1.39 nm using an **HBP** with a wide zigzag polymer structure as well as the removal of the used polymer adsorbent. The dispersion of such larger-diameter tubes using the reported **HBP** with sheet- or ribbon-structures needed sonication by a tip-sonicator with a higher-power.[39,44] The SWCNTs with small tube diameters have highly tensioned graphitic surfaces, and for the dispersion of such tubes, sheet-shaped solubilizers and high power sonication are not suitable. Instead, our designed and synthesized linear **HBP** dispersed the SWCNTs with small diameters under mild condition, which is one of advantages of this study.

5-2. Experimental

5-2-1. Materials. Compounds **1** were synthesized by the Suzuki-Miyaura coupling between 2,7-dibromo-9,9'-dioctylfluorene and 2-amino-4-iodopyridine (● Fig. 6) and **2** were prepared according to the literature.[48] HiPco-SWCNTs were purchased from Unydim (lot# P0261) and used as received. Toluene and acetone were purchased from Tokyo Chemical Industry Co., Ltd. Japan (spectra analysis grade).

5-2-2. Solubilization of SWCNTs using HBP. Into a 13.5 mL vial, 1.72 mg (3.00 mmol) of **1** and 1.44 mg (3.00 mmol) of **2** were solubilized using 1.5 mL of acetone and 1.5 mL of toluene, then 1.0 mg of the as-produced HiPco-SWCNT were added. A brief 10-min sonication using a

bath-type sonicator (5510J-MTH, Emerson Japan, Ltd., Bransonic) was applied to roughly debundle the SWCNTs followed by shaking (ASONE Corporation, Neo Shaker, 700 rpm) for ~1w. After a 1h centrifugation, the resulting supernatant was corrected and analyzed.

5-2-3. Molecular mechanics simulations. The molecular-mechanics simulations were carried out using the MacroModel program (Schrödinger, version 9.8) with the OPLS-2005 force field. The dielectric constant of toluene (2.3) was used in the calculations. Minimization of the calculations was carried out by using the Polak-Ribiere conjugate gradient (PRCG) with a convergence threshold on the gradient of 0.05 kJ/mol. Default values have been used for all the other parameters. The molecular surface was calculated for the optimized structures of the composite between the semiconducting-SWCNTs and HBP with probe diameter of 0.1 nm and van-der-Waals radius scale was 1.0.

5-2-4. Removal of HBP from sorted semiconducting-SWCNT surface. The semiconducting-SWCNT solutions with **HBP** were filtered using PTFE filters (AVANTEC, 0.1 μm pore size). The collected black solids were dispersed in 50 ml of acetone and sonicated for 10 min. to immediately generate a black suspension, which was filtered through a PTFE filter (AVANTEC, 0.1 μm pore size) followed by three washings with 10 ml of acetone and confirming no absorption of **1** and **2** observed in the UV-vis absorption spectrum of the filtrates. The obtained SWCNT solid was dried in vacuo and used for the XPS analysis.

5-3. Results and Discussion

5-3-1. Formation of an HBP from compounds 1 and 2.

It has been reported that the selective extraction of the semiconducting-SWCNTs using fluorene-based copolymers is only possible in toluene and related aromatic solvents[16,20,22] ; however, the synthesized compound **2** was insoluble in such solvents, but very soluble in polar solvents such as acetone. Since the complementary hydrogen-bonding of a carboxylic acid and 2-aminopyridine is a competitive reaction over self-dimerization by themselves,[45,46] I carefully chose the solvent combination. In this study, I used a mixed solvent of toluene and acetone. The complementary **HBP** formation in this mixed solvent was confirmed based on the ^{1}H NMR titration, in which I recognized a shift in the aromatic region of both building blocks, **1** and **2**, and an indicative shift of the amino-proton of **1** from 5.0 to 5.2 ppm as shown by the arrows in Fig. 5-2 (for the entire NMR spectra, see Fig. 5-3). Furthermore, no end-capping molecule was observed, indicating that the **HBP** has a high molecular weight.[39,44]

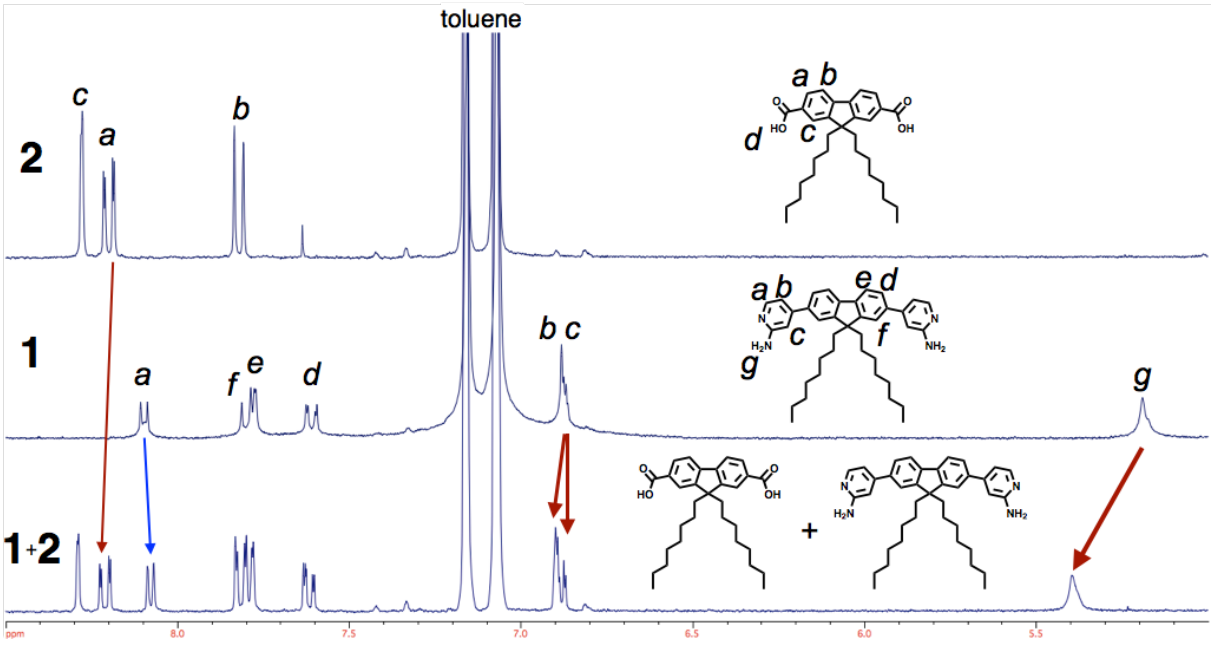

Figure 5-2. **^{1}H NMR spectra** (300 MHz, toluene-d_8: acetone-d_6=1:1, selected region) of compounds **1**, **2** and an equimolar mixture of **1** and **2**. The red arrows indicate the shift in the corresponding peaks. The concentration of each molecule in the mixed solution is 2.0 mM. Adapted from ref. 49 with kind permission. Copyright 2015 Springer Nature.

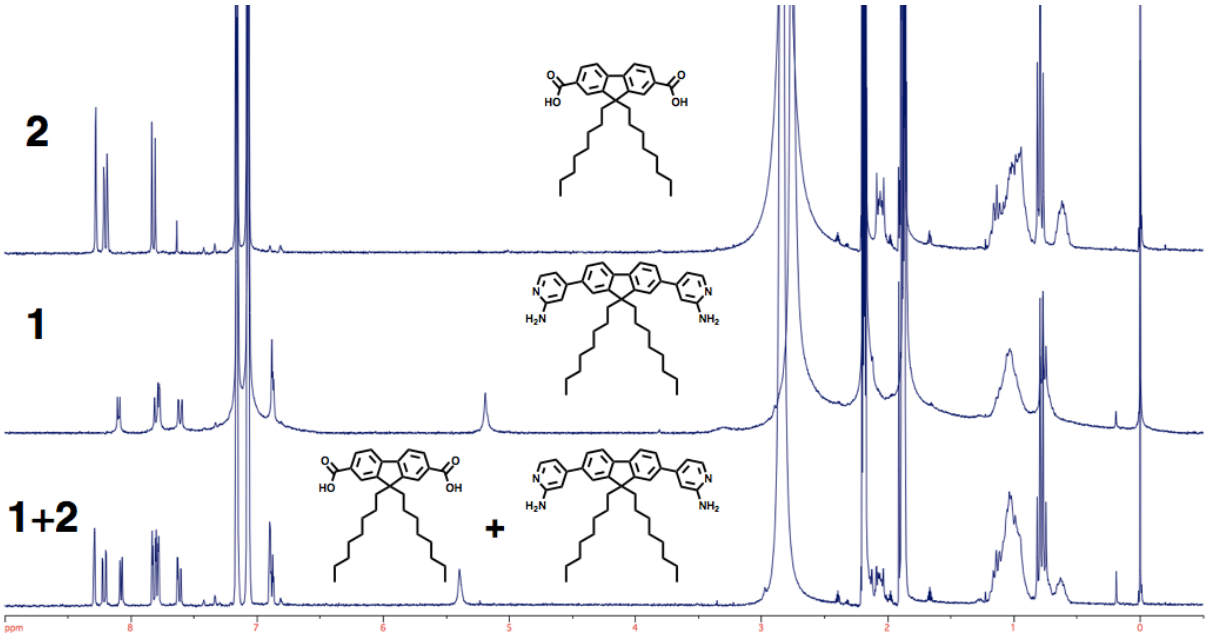

Figure 5-3. **^{1}H NMR spectra** (300 MHz, toluene-d_8: acetone-d_6=1:1) of compounds **1**, **2** and an equimolar mixture of **1** and **2** (2.0 mM). Adapted from ref. 49 with kind permission. Copyright 2015 Springer Nature.

5-3-2. Solubilization of HiPco-SWCNTs using the HBP.

I first confirmed that both **HBP**-building blocks, **1** and **2,** have no ability to dissolve the SWCNTs by themselves (Fig. 5-4). The method for the solubilization of the smaller-diameter SWCNTs using the **HBP** formed by the hydrogen binding of **1** and **2** is quite different from conventional techniques,[20-25, 32, 34-38] in which 1 h or longer sonication time is required. Under such severe experimental conditions, the **HBP** was found to be unable to retain their hydrogen bonding structure and did not solubilize the SWCNTs at all (Fig. 5-5). Hence, in this study, instead of heavy-duty sonication, an ~10-min mild sonication with a bath-type sonicator followed by an ~1-week shaking using a shaker were done to solubilize the as-produced HiPco-SWCNTs. Fig. 5-6 shows the Vis-NIR absorption spectra of the solubilized SWCNTs collected by centrifugation at 10,000x*g*, in which sharp bands corresponding to the Es^{11} (1000-1600 nm) and the Es^{22} (600-800 nm) of the semiconducting-SWCNTs are clearly observed, while no such absorption peak was detected in the metallic-SWCNT region (400-600 nm). This behavior indicates that the **HBP** formed by **1** and **2** exclusively solubilized and extracted the semiconducting-SWCNTs, which is similar to the results using the other fluorene (co)polymers.[20-22, 30, 35-37] Furthermore, only four major absorption peaks were observed in both the Es^{11} and Es^{22} regions, that are ascribable to the chiralities of the semiconducting-SWCNTs with (n,m)=(7,5), (7,6), (8,6) and (8,7). Compared to the other fluorene-based polymers, **HBP** in this study has a high chiral selectivity.

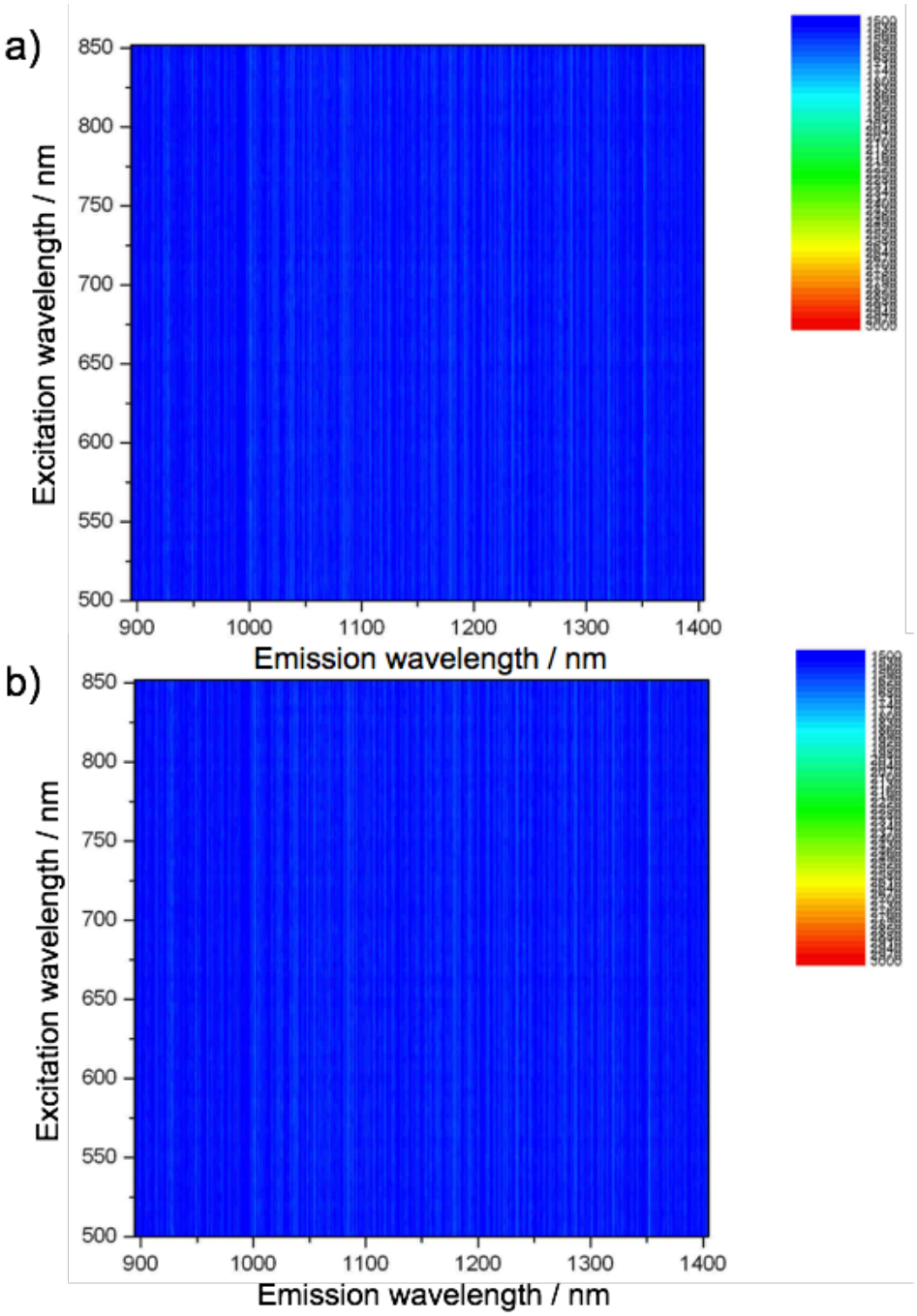

Figure 5-4. **PLE mappings for the SWNT region** of a solution obtained by a shaking-based solubilization procedure using (a) **1** or (b) **2** in a mixed solvent of toluene and acetone (1/1 vol%). No peak in the SWNT absorption area was observed. Adapted from ref. 49 with kind permission. Copyright 2015 Springer Nature.

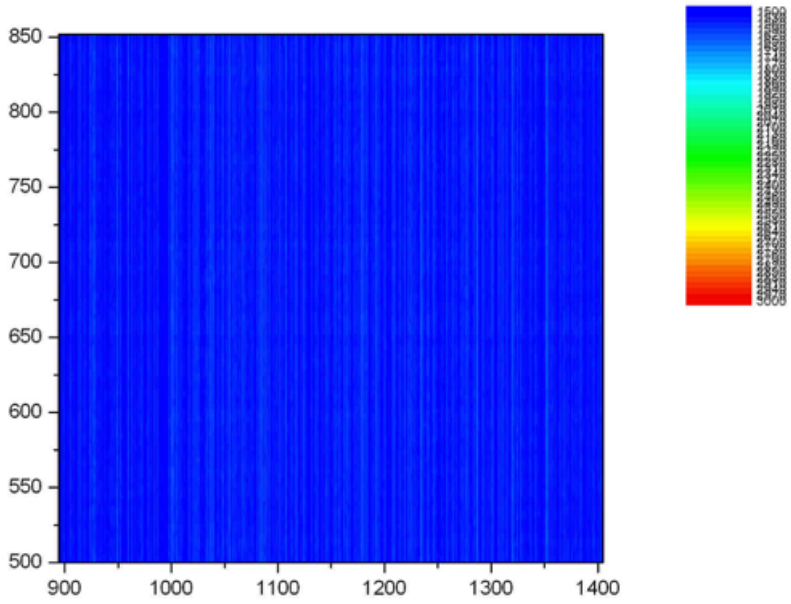

Figure 5-5. **PLE mapping of a solution** obtained by a sonication-based solubilization procedure for the as-produced SWNTs using **1** and **2** in a mixed solvent of toluene and acetone (1/1 vol%). No peak in the SWNT absorption area was observed. Adapted from ref. 49 with kind permission. Copyright 2015 Springer Nature.

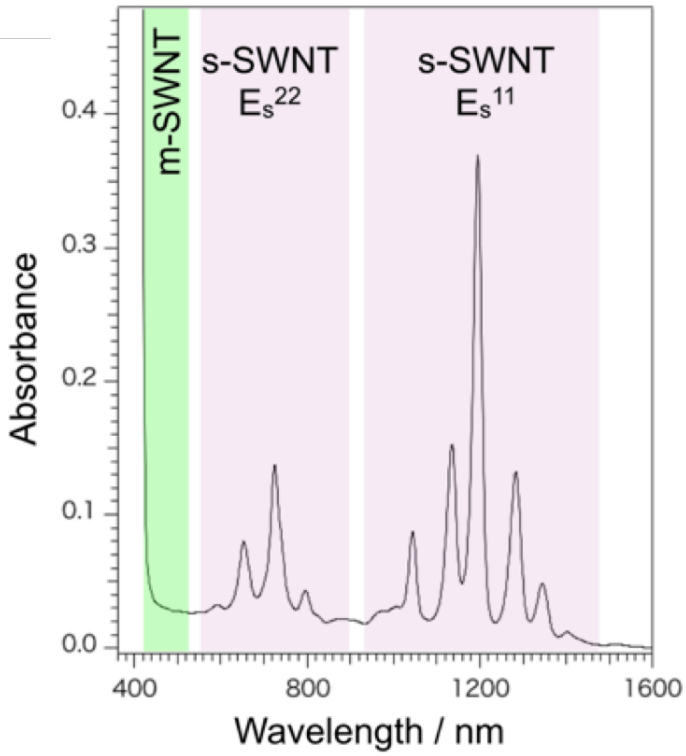

Figure 5-6. Vis-NIR Absorption, spectra of sorted sem-SWNTs using a mixture of compounds **1** (1.0 mM) and **2** (1.0 mM) in toluene/acetone. (optical path length = 1.0 cm). Adapted from ref. 49 with kind permission. Copyright 2015 Springer Nature.

In order to determine the abundance according to the chirality of the sorted semiconducting-SWCNTs, photoluminescense vs. excitation (PLE) mapping[6] was measured (Fig. 5-7); the result is summarized in Table 5-1. The amount ratios of the extracted semiconducting-SWCNT chiralities of (7,5), (7,6), (8,6) and (8,7) were 7, 15, 71 and 7%, respectively. Compared to many conventional fluorene-based copolymers,[20-22, 30, 35,36] the **HBP** was found to be highly selective in sorting the (8,6)-semiconducting-SWCNTs from the as-prepared HiPco-SWCNTs. I will address this chirality recognition behavior based on molecular mechanics simulations later.

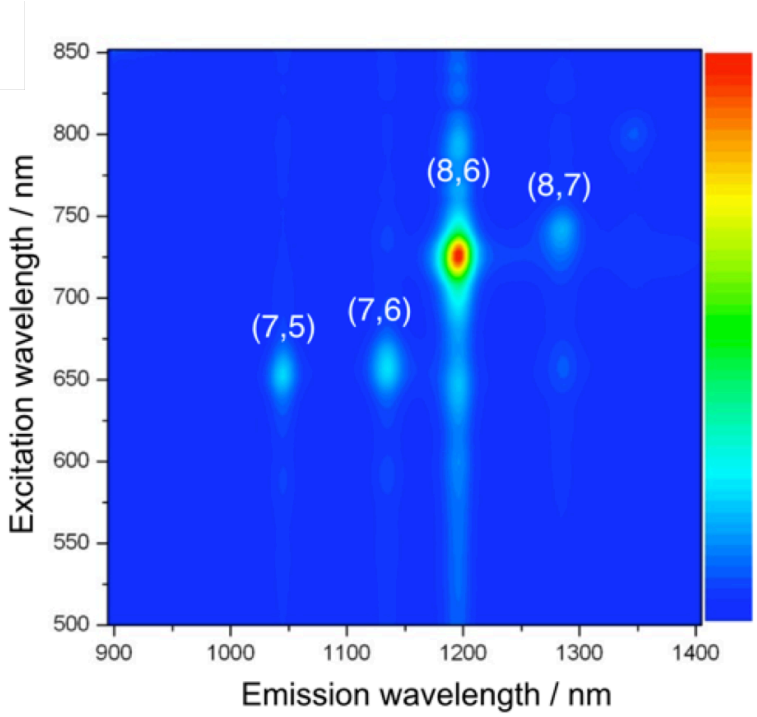

Figure 5-7. PLE spectra mapping of sorted sem-SWNTs using a mixture of compounds **1** (1.0 mM) and **2** (1.0 mM) in toluene/acetone. Adapted from ref. 49 with kind permission. Copyright 2015 Springer Nature.

Table 5-1. **Calibrated contents of the SWNT species** deduced from the PLE mapping of the extracted sem-SWNTs using the **HBP**. Adapted from ref. 49 with kind permission. Copyright 2015 Springer Nature.

(n,m)	Emission peak shift	PL peak intensity	Calculated PL intensity	Calibrated PL peak intensity	Calibrated content
(7,5)	1043	830.28	0.71	589.50	7.1
(7,6)	1139	2610.88	0.47	1227.11	14.9
(8,6)	1186	12046.17	0.49	5902.62	71.5
(8,7)	1279	1796.23	0.30	538.87	6.5

In order to evaluate the chiral-purity and the degree of the SWCNT crystalline structure of the extracted semiconducting-SWCNTs, the Raman spectra excited at 633-nm were measured, and the results shown in Fig. 5-8c, in which semiconducting-SWCNT peaks (240-300 cm^{-1}) in the radial breathing mode (RBM) region were observed, while no metallic peaks around 200-240 cm^{-1} were detected. Furthermore, as shown in Fig. 5-8d, the intensity of the defect band (D-band) of the sorted SWCNTs around 1310 cm^{-1} was much lower than that of the G-band; thus the D/G ratio was determined to be ~1/80, which is remarkably higher than those of the as-prepared SWCNTs since even in commercially available very high quality HiPco-SWCNTs, the D/G ratios are ~1/6. *Such a very high crystalline SWCNT sorting is one of the advantages of this study over previous studies*.

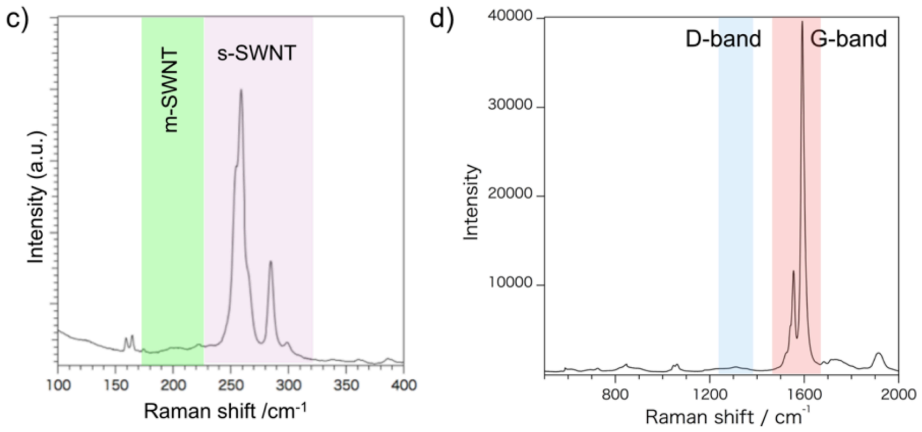

Figure 5-8. Raman spectra of sorted sem-SWNTs excitation with a 633-nm laser for (c) 100 ~ 400 cm^{-1} (RBM) and (d) 500 ~ 2000 cm^{-1} (D/G) regions. Adapted from ref. 49 with kind permission. Copyright 2015 Springer Nature.

Atomic force microscopy (AFM) measurements also revealed the advantage of this study using the mild-conditioned-extraction procedure. The observed average height from the AFM image (Fig. 5-9a, b) is 1.21 ± 0.04 nm, which well agrees with the value calculated from the simulated individualized structure of the **HBP**-wrapped (8,6) SWCNT (Fig. 5-9c). In the AFM image, I observed very long tubes (~10 μm) and the average length of one hundred of the individualized SWCNTs reaches ~3.5 μm (Fig. 5-9d), which is much longer than those of the SWCNTs based on the conventional sonication technique, in which the average diameter is usually less than 1.5 μm when using HiPco-SWCNTs as the material. *The obtained long tube sorting is due to the very weak dispersion method using a shaker, which is one more advantage of this study*.

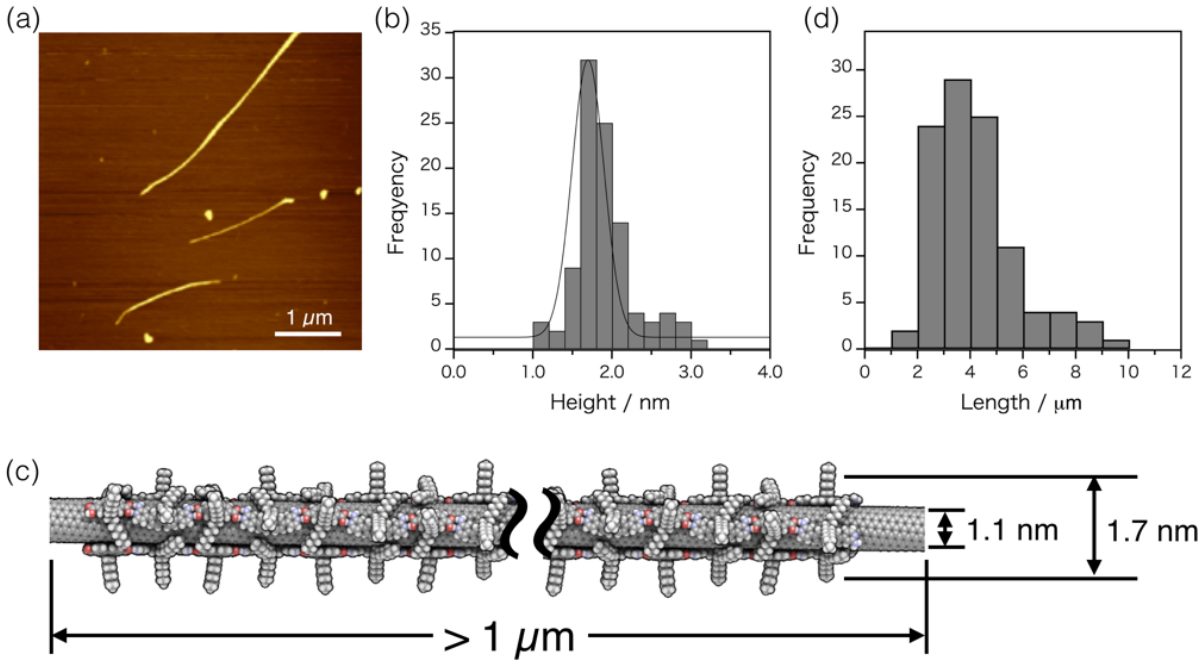

Figure 5-9. (a) A representative AFM image of isolated sem-SWNTs wrapped by **HBP** and (b) height distribution histogram. (c) A schematic illustration of the estimated dimensions for the structure-optimized composite structure of (8,6)sem-SWNT wrapped by **HBP**. (d) Length distribution histogram obtained from ten AFM images of sorted sem-SWNTs. Adapted from ref. 49 with kind permission. Copyright 2015 Springer Nature.

5-3-3. Molecular mechanics simulations on the composite of SWCNTs and HBPs.

As already described, the **HBP** showed a high chiral-selectivity for the semiconducting-SWCNTs compared to the other previously reported (co)polymers. For a deeper understanding of this behavior, especially for the interaction of the **HBP** and the sem-(8,6) SWCNTs, the optimized conformations of the **HBP**s on the tubes were modeled using molecular mechanics simulations (Fig. 5-10a-d). In order to rationally wrap the SWCNT surfaces with the **HBP**s, four strips of the **HBP** chains were placed on a 20-nm long semiconducting-SWCNT. After the structure optimization, all the included hydrogen-bonds between the molecules, **1** and **2**, maintained the rational distance of 1.98~2.12 Å in all the chiralities. The resulting conformations of the **HBP** were close to a linear structure, which reflected the programmed strict bond-angle and bond-length nature of the hydrogen bonds. Thus, the **HBP** wrapping is not very flexible compared to the helical wrapping manners presented by many other fluorene copolymers composed of a covalent- or coordination bonding,[20-22, 30, 35-37] which lead to a weak chirality selectivity.

In an effort to elucidate the specific chiral-selectivity of the **HBP** on the semiconducting-SWCNTs, I examined the relationship between the ratios of the experimentally-sorted SWCNT chiralities and the theoretically obtained structural information of the composites of the SWCNT and **HBP**. Gomulya et al.[47] estimated the interactions between several fluorene oligomers and two chiralities of SWCNT by the surface area and the binding energy using a molecular dynamics simulation. In our study, by contrast, I used only one kind of polymer (**HBP)** and it will not give a comparable binding energy difference. The relationship between the surface area and molecular weight of the composites was then discussed. Noteworthy is that the accurate determination of the molar density for such hollow and open-end SWCNTs with an encapsulation ability is very difficult, thus I regard the surface area and molecular weight as an indicator of the stabilization of the **HBP**-wrapped SWCNTs

in solvents. As shown in Table 5-2, the molecular surface area and molecular mass naturally increased with the increase in the number of atoms in the given composites, while the values of the molar mass divided by the surface area show a local maximum for the composite of (8,6)-SWCNT (Fig. 5-11). This behavior reflects the amount of the **HBP**'s molecular surface area and uncovered area of the SWCNT surfaces, which strongly influences the stability and the solubility of the composites. As a result, the composite of the sem-(8,6)SWCNT and **HBP**s showed the highest stability in the calculation analysis that strongly supports the specific recognition behavior of the **HBP**. Meanwhile, a conventional analysis using stabilizing energy did not provide a clear difference as shown in Table 5-3. Thus, our approach to theoretically estimate the chirality selectivity by means of the molecular surface area and the molecular weight is a good method to predict the interactions and stabilization of the SWCNT composites in the solution phase.

Table 5-2. The molecular surface area and the molecular mass calculated using the optimized structures of the composites of the sem-SWNTs with the **HBP**. Adapted from ref. 49 with kind permission. Copyright 2015 Springer Nature.

SWNT	Surface area of **HBP**-wrapped SWNT	Molecular mass of **HBP**-wrapped SWNT
(7,5)	16227.098	32599.36
(7,6)	16911.202	33955.36
(8,6)	17485.23	34795.36
(8,7)	17974.228	35959.36

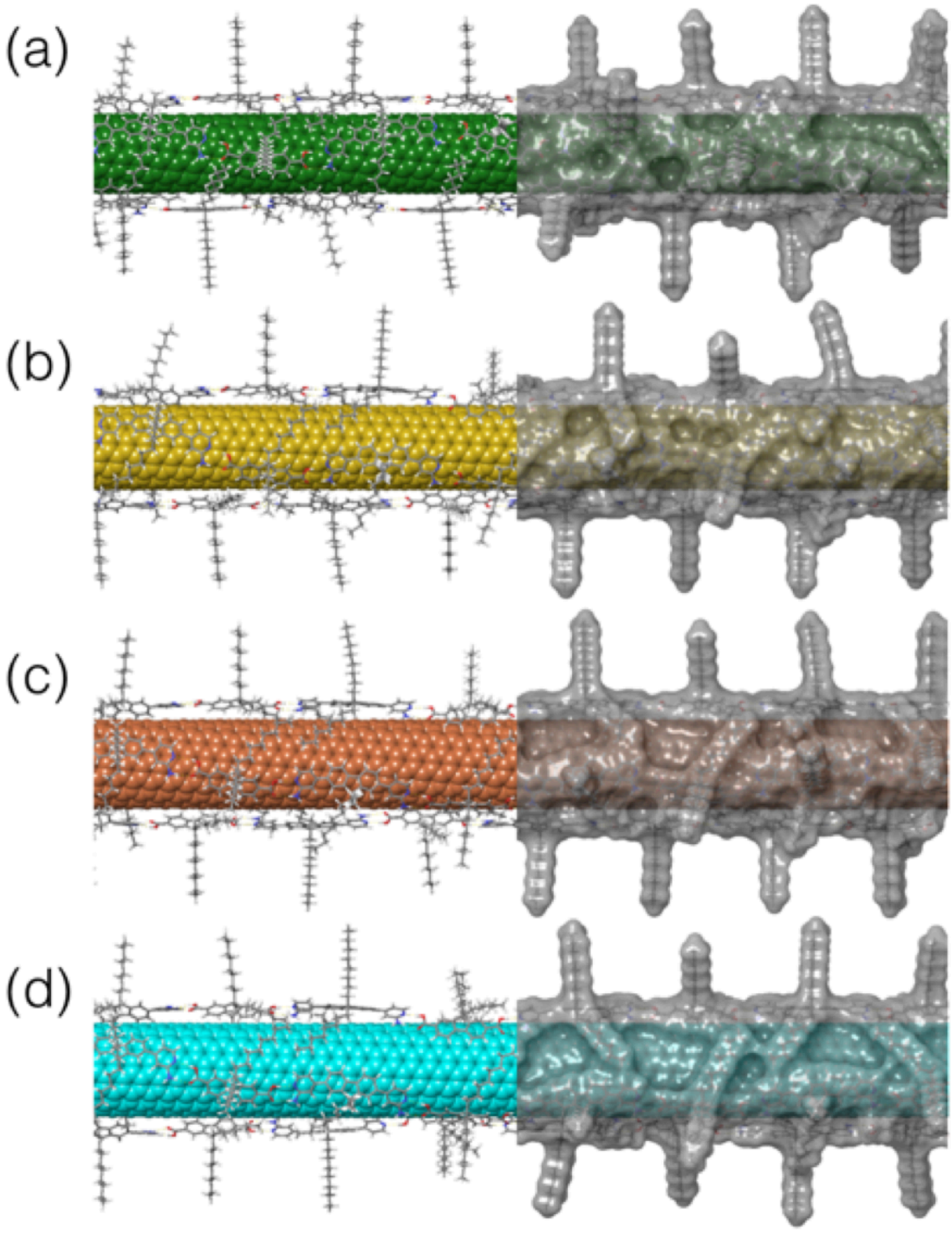

Figure 5-10. Optimized structures of HBP-wrapped sem-SWNTs. Molecular structures (left half) and molecular surfaces (right half) of **HBP**-wrapped (a) (7,5), (b) (7,6), (c) (8,6) and (d) (8,7) sem-SWNTs. Adapted from ref. 49 with kind permission. Copyright 2015 Springer Nature.

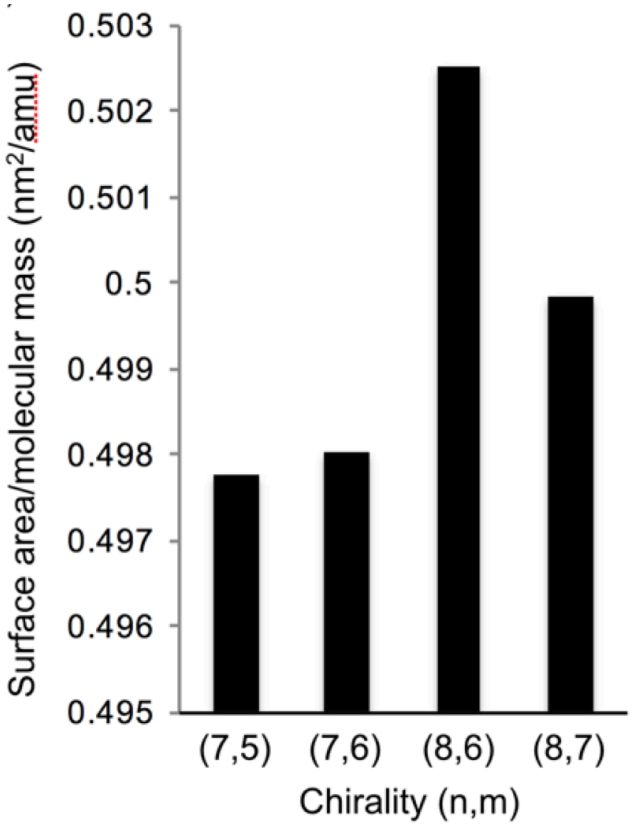

Figure 5-11. Molecular surface area and molecular mass for the **HBP**-wrapped four sem-SWNTs ((7,5), (7,6), (8,6) and (8,7), respectively). Quotient values of molar mass divided by the surface area of the **HBP**-wrapped four sem-SWNTs shown with the chirality of sem-SWNTs. Adapted from ref. 49 with kind permission. Copyright 2015 Springer Nature.

Table 5-3. Calculated potential and stabilizing energies between the (n,m)SWNTs with **HBP**. The energies are in kcal/mol. Adapted from ref. 49 with kind permission. Copyright 2015 Springer Nature.

SWNT	Potential energy of SWNT E_{SWNT}	Potential energy of **HBP** $E_{\mathbf{HBP}}$	Total potential energy of **HBP**-wrapped SWNT $E_{SWNT} + E_{\mathbf{HBP}}$	Structure-optimized potential energy of **HBP**-wrapped SWNT $E_{complex}$	Stabilizing energy $E_{stabization}$
(7,5)	97469.625	174.441	98167.389	93962.953	-4204.436
(7,6)	98891.578	174.441	99589.342	95283.492	-4305.85
(8,6)	101321.125	174.441	102018.889	97664.852	-4354.037
(8,7)	103584.281	174.441	104282.045	99885.383	-4396.662

5-3-4. Removing HBPs from semiconducting-SWCNT.

Removal of the **HBP** from the semiconducting-SWCNT surfaces is very important. As already described, compounds **1** and **2** were unable to form hydrogen bonding in many solvents except for the 1:1 toluene/acetone mix solvent. The removal of the **HBP** polymer was quite easy; namely, I completely removed the **HBP** by a very simple intense washing with a good solvent and obtained chemically pure semiconducting-SWCNTs. Typically, the **HBP**-wrapped semiconducting-SWCNTs solution (3 ml) was added to excess acetone (50 ml), then sonicated for 10 min to produce a black precipitate, which was filtered, then thoroughly washed with acetone to provide a black solid. The product was analyzed by the X-ray photoelectron spectroscopy (XPS)[37] and the result is shown in Fig. 5-12, in which I observed that the carbon peaks at around 284 eV became sharper after the removal-treatment, indicating the disappearance of the sp^3 alkyl carbon derived from the **1** and **2** monomers. A similar behavior was observed in the nitrogen and oxygen regions; namely, no nitrogen peak was detected after the removal-treatment. I observed a peak in the oxygen region after the removal, which is assigned not to the adsorbent, but the adsorbed water since a peak appeared at 533 eV. Noteworthy to recognize is that compounds **1** and **2** were not damaged during the removal process, hence they are readily reusable, indicating a highly efficient SWCNT sorting in this study. *This easy adsorbent removal is one more advantage of this study.*

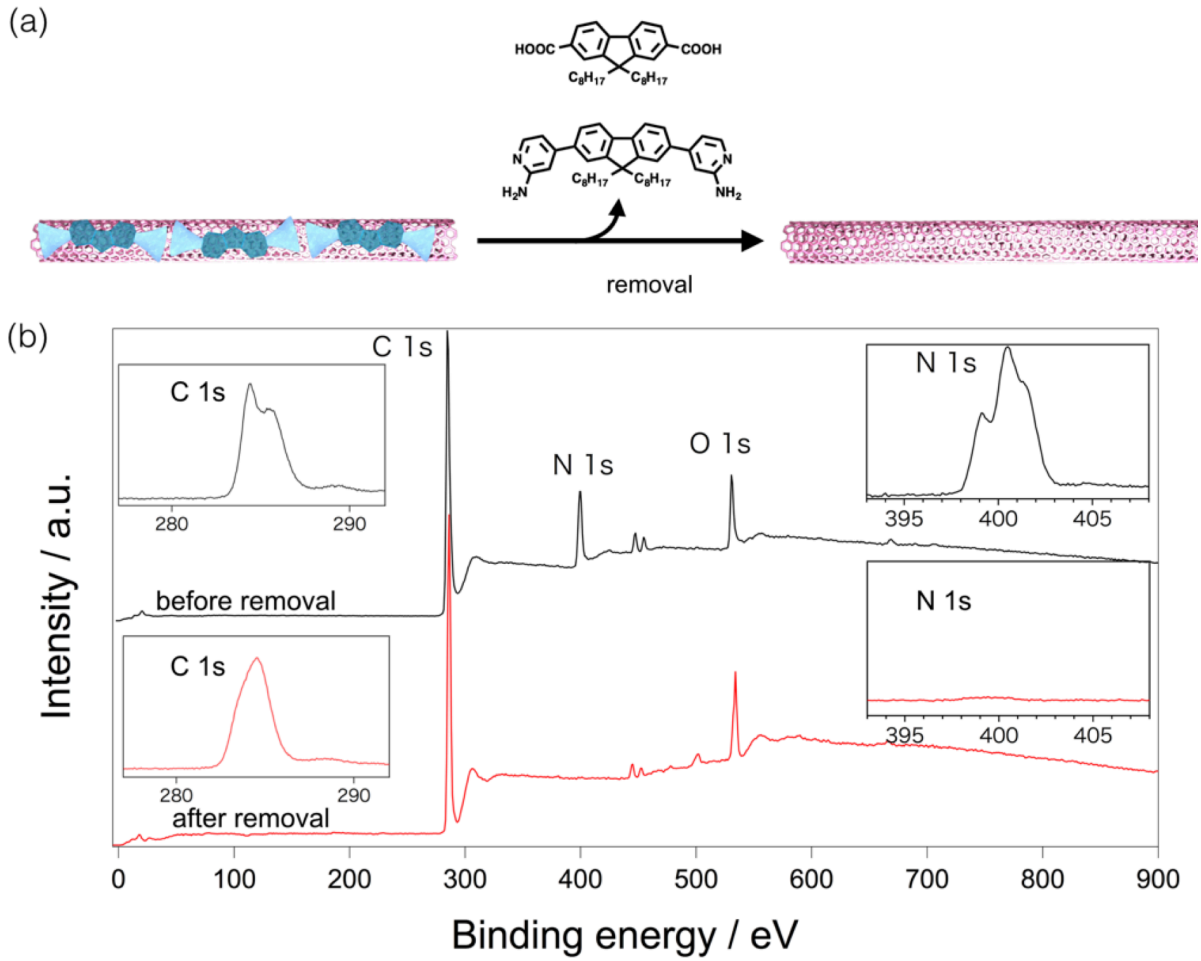

Figure 5-12. Adsorbent removal from sem-SWNTs. (a) Schematic drawing of the removal of **HBP** from the extracted sem-SWNT and (b) XPS spectra of the sem-SWNTs before (black line) and after (red line) the removal of **1** and **2** with the magnified C1s and N1s region (the insets). Adapted from ref. 49 with kind permission. Copyright 2015 Springer Nature.

5-4. Conclusions

In conclusion, a method for the efficient extraction of highly pure long-length semiconducting-SWCNTs with minute defects has been achieved using the hydrogen bonding polymer **HBP** along with a very mild conditioned-solubilizing/extracting procedure based on dynamic supramolecular chemistry. The amount ratios of the extracted semiconducting-SWCNTs with chiralities of (n,m) = (7,5), (7,6), (8,6) and (8,7) were 7, 15, 71 and 7%, respectively. A facile and highly selective one-pot sem-(8,6)SWCNT extraction is of interest, and the behavior was explained by molecular mechanics simulations.

The summarized advantages of this study using a very easy handling technique are: i) *very high crystalline semiconducting-SWCNT sorting*, ii) selective (8,6)SWCNT sorting, iii) long semiconducting-SWCNT sorting and iv) an easy and complete removal of the adsorbent from the sorted semiconducting-SWCNT surfaces. Such an efficient and easy extraction of the semiconducting-SWCNTs is a great advantage in the science of the chirality selective SWCNT separation, The study is highly important since the present sorted semiconducting-SWCNTs are highly pure (adsorbent free), chiral selective and sufficiently-long, which satisfy the strong demand in the use of such materials in many fundamental research studies and applications.

References

1 Dresselhaus, M. S., Dresselhaus, G. & Avouris, P. Carbon Nanotubes Synthesis, Structure, Properties and Applications (Springer, 2001).

2. D'Souza, F., Kadish, K. M., Eds. Handbook of Carbon Nano Materials. (World Scientific, 2011).

3. R. Krupke, F. Hennrich, in *Chemistry of Carbon Nanotubes* (ed. V. A. Basiuk, E. V. Basiuk) Chap. 7 (American Scientific Publisher, 2008).

4. Ajayan, P. M. Nanotubes from carbon. *Chem. Rev*. **99**, 1787-1799 (1999).

5**.** Jorio, A. *et al.* Structural (n, m) determination of isolated single-wall carbon nanotubes by resonant Raman scattering. *Phys. Rev. Lett.* **86**, 1118-1121 (2001).

6. Bachilo, S. M. et al. Structure-assigned optical spectra of single-walled carbon nanotubes. *Science* **298**, 2361-2366 (2002).

7. Hirana, Y. *et al.* Empirical Prediction of Electronic Potentials of Single-Walled Carbon Nanotubes With a Specific Chirality (n,m). *Sci. Rep.* **3**, 2959 (2013).

8. Cao, Q. & Rogers, J. A. Ultrathin Films of Single-Walled Carbon Nanotubes for Electronics and Sensors: A Review of Fundamental and Applied Aspects. *Adv. Mat.* **21**, 29–53 (2009).

9. Hasan, T. *et al.* Nanotube–Polymer Composites for Ultrafast Photonics. *Adv. Mat.* **21**, 3874–3899 (2009).

10. Krupke, R., Hennrich, F., Löhneysen, H. v. & Kappes, M. M. Separation of Metallic from Semiconducting Single-Walled Carbon Nanotubes. *Science* **301**, 344–347 (2003).

11. Blackburn, J. L. *et al.* Transparent Conductive Single-Walled Carbon Nanotube Networks with Precisely Tunable Ratios of Semiconducting and Metallic Nanotubes. *ACS Nano* **2**, 1266–1274 (2008).

12. O'Connell, M. J. *et al.* Band gap fluorescence from individual single-walled carbon nanotubes. *Science* **297,** 593–596 (2002).

13. Cheng, F., Imin, P., Maunders, C., Botton, G. & Adronov, A. Soluble , Discrete Supramolecular Complexes of Single-Walled Carbon Nanotubes with Fluorene-Based Conjugated Polymers. *Society* 2304–2308 (2008).

14. Lee, C. W. *et al.* Toward High-Performance Solution-Processed Carbon Nanotube Network Transistors by Removing Nanotube Bundles. *J. Phys. Chem. C* **112,** 12089–12091 (2008).

15. Izard, N. *et al*. Semiconductor-enriched single wall carbon nanotube networks applied to field effect transistors. *Appl. Phys. Lett*. **92,** 243112 (2008).

16. Nish, A., Hwang, J., Doig, J. & Nicholas, R. Highly selective dispersion of single-walled carbon nanotubes using aromatic polymers. *Nature Nanotech.* **2**, 640-646 (2007).

17. Chen, F., Wang, B., Chen, Y. & Li, L.-J. Toward the extraction of single species of single-walled carbon nanotubes using fluorene-based polymers. *Nano Lett.* **7**, 3013–3017 (2007).

18. Ozawa, H. *et al.* Rational concept to recognize/extract single-walled carbon nanotubes with a specific chirality. *J. Am. Chem. Soc.* **133**, 2651–2657 (2011).

19. Lee, H. W. *et al.* Selective dispersion of high purity semiconducting single-walled carbon nanotubes with regioregular poly(3-alkylthiophene)s. *Nat. Commun.* **2,** 541 (2011).

20. Ozawa, H., Ide, N., Fujigaya, T., Niidome, Y. & Nakashima, N. One-pot Separation of Highly Enriched (6,5)-Single-walled Carbon Nanotubes Using a Fluorene-based Copolymer. *Chem. Lett.* **40,** 239–241 (2011).
21. Akazaki, K., Toshimitsu, F., Ozawa, H., Fujigaya, T. & Nakashima, N. Recognition and one-pot extraction of right- and left-handed semiconducting single-walled carbon nanotube enantiomers using fluorene-binaphthol chiral copolymers. *J. Am. Chem. Soc.* **134**, 12700–12707 (2012).
22. Mistry, K. S., Larsen, B. A., Blackburn, J. L., Renewable, N. & States, U. High-Yield Dispersions of Single-Walled Carbon Nanotubes with Tunable Narrow Chirality Distributions. *ACS Nano,* **7**, 2231–2239 (2013).
23. Khripin, C. Y., Fagan, J. a & Zheng, M. Spontaneous partition of carbon nanotubes in polymer-modified aqueous phases. *J. Am. Chem. Soc.* **135,** 6822–5 (2013).
24. Tu, X., Manohar, S., Jagota, A. & Zheng, M. DNA sequence motifs for structure-specific recognition and separation of carbon nanotubes. *Nature* **460,** 250–3 (2009).
25. Arnold, M. S., Green, A. a, Hulvat, J. F., Stupp, S. I. & Hersam, M. C. Sorting carbon nanotubes by electronic structure using density differentiation. *Nature Nanotech.* **1**, 60–65 (2006).
26. Ghosh, S., Bachilo, S. M. & Weisman, R. B. Advanced sorting of single-walled carbon nanotubes by nonlinear density-gradient ultracentrifugation. *Nature Nanotech.* **5**, 443–450 (2010).
27. Liu, H., Nishide, D., Tanaka, T. & Kataura, H. Large-scale single-chirality separation of single-wall carbon nanotubes by simple gel chromatography. *Nature Commun.* **2**, 309 (2011).
28. Hirano, A., Tanaka, T. & Kataura, H. Thermodynamic Determination of the Metal/Semiconductor Separation of Carbon Nanotubes Using Hydrogels. *ACS Nano* **11**, 10195–10205 (2012).
29. Tulevski, G., Franklin, A. & Afzali, A. High Purity Isolation and Quantification of Semiconducting Carbon Nanotubes via Column Chromatography. *ACS Nano*, **7**, 2971–2976 (2013).
30. Cheng, F., Imin, P., Maunders, C., Botton, G. & Adronov, A. Soluble, Discrete Supramolecular Complexes of Single-Walled Carbon Nanotubes with Fluorene-Based Conjugated Polymers. *Society* 2304–2308 (2008).
31. Yi, W. *et al.* Wrapping of single-walled carbon nanotubes by a π-conjugated polymer: The role of polymer conformation-controlled size selectivity. *J. Phys. Chem. B* **112,** 12263–12269 (2008).
32. Imin, P., Imit, M. & Adronov, A. Supramolecular functionalization of single-walled carbon nanotubes (SWNTs) with dithieno[3,2-b:20,30-d]pyrrole (DTP) containing conjugated polymers. *Macromolecules* **44,** 9138–9145 (2011).
33. Umeyama, T. *et al.* Dispersion of carbon nanotubes by photo- and thermal-responsive polymers containing azobenzene unit in the backbone. *Chem. Commun.* **46,** 5969–5971 (2010).
34. Zhang, Z. *et al.* Reversible Dispersion and Release of Carbon Nanotubes Using Foldable Oligomers. *J. Am. Chem. Soc.* **132,** 14113–14117 (2010).
35. Lemasson, F. *et al.* Debundling, selection and release of SWNTs using fluorene-based photocleavable polymers. *Chem. Comm.* **47**, 7428–7430 (2011).

36. Wang, W. Z. *et al.* Degradable Conjugated Polymers: Synthesis and Applications in Enrichment of Semiconducting Single-Walled Carbon Nanotubes. *Adv. Func. Mat.* **21**, 1643–1651 (2011).
37. Toshimitsu, F. & Nakashima, N. Semiconducting single-walled carbon nanotubes sorting with a removable solubilizer based on dynamic supramolecular coordination chemistry. *Nat. Commun.* **5,** 5041 (2014).
38. Chichak, K. S., Star, A., Altoé, M. V. P. & Stoddart, J. F. Single-walled carbon nanotubes under the influence of dynamic coordination and supramolecular chemistry. *Small* **1,** 452–461 (2005).
39. Llanes-Pallas, A. et al. Modular engineering of H-bonded supramolecular polymers for reversible functionalization of carbon nanotubes. J. Am. Chem. Soc. 133, 15412–15424 (2011).
40. Sun, D. *et al.* Flexible high-performance carbon nanotube integrated circuits. *Nat. Nanotechnol.* **6,** 156–61 (2011).
41. Wu, Z. *et al.* Transparent, Conductive Carbon Nanotube Films. *Science* **305,** 1273–1276 (2004).
42. LeMieux, M. C. *et al.* Self-sorted, aligned nanotube networks for thin-film transistors. *Science* **321,** 101–4 (2008).
43. Liyanage, L. S. *et al.* Wafer-Scale Fabrication and Characterization of Thin-Film Transistors with Polythiophene-Sorted Semiconducting Carbon Nanotube Networks. *ACS Nano* **6,** 451–458 (2012).
44. Pochorovski, I. *et al.* H-Bonded Supramolecular Polymer for the Selective Dispersion and Subsequent Release of Large-Diameter Semiconducting Single-Walled Carbon Nanotubes. *J. Am. Chem. Soc.* **137,** 4328–4331 (2015).
45. Bensemann, I., Gdaniec, M., Łakomecka, K., Milewska, M. J. & Połoński, T. Creation of hydrogen bonded 1D networks by co-crystallization of N,N'-bis(2-pyridyl)aryldiamines with dicarboxylic acids. *Org. Biomol. Chem.* **1,** 1425–34 (2003).
46. Jebas, R. S., Periyasamy, B. K. & Balasubramanian, T. Hydrogen bonding patterns of 2-aminopyridinium nicotinic acetate. *J. Chem. Crystallogr.* **36,** 503–507 (2006).
47. Gomulya, W. *et al.* Semiconducting single-walled carbon nanotubes on demand by polymer wrapping. *Adv. Mater.* **25,** 2948–2956 (2013).
48. Ding, J., Day, M., Robertson, G. & Roovers, J. Synthesis and characterization of alternating copolymers of fluorene and oxadiazole. *Macromolecules* **35,** 3474–3483 (2002).
49. Toshimitsu, F. & Nakashima, N. Facile Isolation of Adsorbent-Free Long and Highly-Pure Chirality-Selected Semiconducting Single-Walled Carbon Nanotubes Using A Hydrogen-bonding Supramolecular Polymer. *Sci. Rep.* **5,** 18066 (2015).

Chapter 6

Gross Conclusion

The importance of purifying SWCNTs is reviewed in the chapter 1 from the point of view of semiconducting- or metallic-chirality. Various methods reported to date requires time and cost to achieve pure chirality-separation, but the removal of the solubilizeres from the sorted semiconducting-SWCNTs have been big issue.

In the present study of the Ph. D thesis, I have discovered facile and chirality-selective separation methods using fluorene-based synthetic copolymers. In chapter 2, I described the specific recognition and separation of right-handed and left-handed semiconducting-SWCNTs using copolymer containing binaphthyl moieties, which proved the contents of the fluorene-copolymers are possible to control not only the chirality-selectivity but also the selectivity based on the optical properties of SWCNTs.

In chapter 3, I examined the effect of bulky side chains carried along the main wrapping polymers by changing the contents of fullerene on the fluorene-copolymers. Fullerenes are consist of π-surfaces and it is reasonable that the fullerene amount in the copolymer increased the interactions between wrapping polymers and the SWCNTs. Furthermore, the fact that such bulky side chains do not disturb the chirality-selectivity for the semiconducting-SWCNT give general insights to design functional and high-yield semiconducting-SWCNT sorter for the next-generation nanocarbon devices.

The most advantageous finding in this study is that the supramolecular polymer-based SWCNT solubilizers, which are detachable, still exhibit smart chirality selectivity. In the

chapter 4, world first metal-ligand coordination polymers with chirality selectivity for the SWCNTs are described. Interestingly, the metal source affected the purity and yield of the sorted semiconducting-SWCNT, which suggest the further modifying is possible to control the chirality selectivity using supramolecular polymers. I describe in the chapter 5 the use of hydrogen-bond in the chirality selective semiconducting-SWCNT sorting. The removal process of the wrapping polymers is so mild with washing that the removed hydrogen-bond polymer components are not damaged and ready to reuse. This supramolecular method to purify specific chirality of SWCNTs open the door of a new molecular design for strategic supramolecular (n,m)-chiral selective recognition of SWNTs as well as specific functionality of the SWNTs via self-assembly of a designed molecule.

Now with the insight to design supramolecular solubilizers for the SWCNTs, application using such hybrids and purified SWCNT is ready. Using the enantiomers obtained in the chapter 2, investigation for the relationship between optical properties and the SWCNT chirality is undergoing. For the hybrids of SWCNTs with fullerene, photovoltaic or nanoelectronic circuit application is under estimation. The chemically purified semiconducting-SWCNTs using supramolecular polymers described in the chapter 4 and 5 are now applied in the nanoelectric circuit to evaluate transistor property. I wish I could contribute the next-generation nanocarbon-based science using supramolecular method for the purification of the SWCNTs.

List of publications

1. Yang, J., Toshimitsu, F., Yang, Z., Fujigaya, T. & Nakashima, N. Pristine carbon nanotube/iron phthalocyanine hybrids with a well-defined nanostructure show excellent efficiency and durability for the oxygen reduction reaction. *J. of Mat. Chem. A* **5**, 1184-1191 (2017)

2. Shiraki, T., Tsuzuki, A., Toshimitsu, F. & Nakashima, N. Thermodynamics for the Formation of Double-Stranded DNA-Single-Walled Carbon Nanotube Hybrids. *Chem. - A Eur. J.* **22,** 4774–4779 (2016).

3. Toshimitsu, F. & Nakashima, N. High efficiency separation of semiconducting carbon nanotubes: development of separating agent based on dynamic supramolecular coordination chemistry. *Kagaku (Kyoto, Japan)* **70,** 41–44 (2015).

4. Toshimitsu, F., Ozawa, H. & Nakashima, N. Hybrids of Copolymers of Fluorene and C60-Carrying-Carbazole with Semiconducting Single-Walled Carbon Nanotubes. *Chem. - A Eur. J.* **21,** 3359–3366 (2015).

5. Toshimitsu, F. & Nakashima, N. Facile Isolation of Adsorbent-Free Long and Highly-Pure Chirality-Selected Semiconducting Single-Walled Carbon Nanotubes Using A Hydrogen-bonding Supramolecular Polymer. *Sci. Rep.* **5,** 18066 (2015).

6. Shiraki, T., Shindome, S., Toshimitsu, F., Fujigaya, T. & Nakashima, N. Strong main-chain length-dependence for the β-phase formation of oligofluorenes. *Polym. Chem.* **6,** 5103–5109 (2015).

7. Kato, Y., Fukuzawa, M., Toshimitsu, F. & Nakashima, N. Separation of semiconducting single-walled carbon nanotubes using a flavin compound. *Chem. Lett.* **44,** 566–567 (2015).

8. Fukumaru, T., Toshimitsu, F., Fujigaya, T. & Nakashima, N. Effects of the chemical structure of polyfluorene on selective extraction of semiconducting single-walled carbon nanotubes. *Nanoscale* **6,** 5879–5886 (2014).

9. Toshimitsu, F. & Nakashima, N. Semiconducting single-walled carbon nanotubes sorting with a removable solubilizer based on dynamic supramolecular coordination chemistry. *Nat. Commun.* **5,** 5041 (2014).

10. Hong, L., Toshimitsu, F., Niidome, Y. & Nakashima, N. Microenvironment effect on the electronic potentials of individual (6,5)single-walled carbon nanotubes. *J. Mater. Chem. C Mater. Opt. Electron. Devices* **2,** 5223–5228 (2014).

11. Akazaki, K., Toshimitsu, F., Ozawa, H., Fujigaya, T. & Nakashima, N. Recognition and one-pot extraction of right- and left-handed semiconducting single-walled carbon nanotube enantiomers using fluorene-binaphthol chiral copolymers. *J. Am. Chem. Soc.* **134,** 12700–12707 (2012).

12. Dyes, P., Hayashi, M., Toshimitsu, F., Sakamoto, R. & Nishihara, H. Diethynylfumarate : Formation of Intensely Colored and Luminescent. *J. Am. Chem. Soc.* 14518–14521 (2011).

13. Maeda, H., Sakamoto, R., Nishimori, Y., Sendo, J., Toshimitsu, F., Yamanoi, Y.& Nishihara, H. Bottom-up fabrication of redox-active metal complex oligomer wires on an H-terminated Si(111) surface. *Chem. Commun. (Cambridge, United Kingdom)* **47,** 8644–8646 (2011).

14. Hayashi, M., Toshimitsu, F., Sakamoto, R. & Nishihara, H. Double Lactonization in Triarylamine-Conjugated Dimethyl Diethynylfumarate: Formation of Intensely Colored and Luminescent Quadrupolar Molecules Including a Missing Structural Isomer of Pechmann Dyes. *J. Am. Chem. Soc.* **133,** 14518–14521 (2011).

15. Rao, K.P., Kusamoto, T., Toshimitsu, F., Inayoshi, K., Kume, S., Sakamoto, R. & Nishihara, H. Double Protonation of 1,5-Bis(triarylaminoethynyl)anthraquinone To Form a Paramagnetic Pentacyclic Dipyrylium Salt. *J. Am. Chem. Soc.* **132,** 12472–12479 (2010).

16. Kurita, T., Nishimori, Y., Toshimitsu, F., Muratsugu, S., Kume, S. & Nishihara, H. Surface junction effects on the electron conduction of molecular wires. *J. Am. Chem. Soc.* **132,** 4524–5 (2010).

17. Nishimori, Y., Kanaizuka, K., Kurita, T., Nagatsu, T., Segawa, Y., Toshimitsu, F., Muratsugu, S., Utsuno, M., Kume, S., Murata, M. & Nishihara, H. Superior Electron-Transport Ability of π-Conjugated Redox Molecular Wires Prepared by the Stepwise Coordination Method on a Surface. *Chem. - An Asian J.* **4,** 1361–1367 (2009).

18. Utsuno, M., Toshimitsu, F., Kume, S. & Nishihara, H. Synthesis of an Anthraquinone-Bridged bis(terpyridine) Ligand and its Use in the Stepwise Fabrication of Complex Oligomer Wires on Gold. *Macromol. Symp.* **270,** 153–160 (2008).

Patents

1. Nishihara, H., Hayashi, M. & Toshimitsu, F. Preparation of condensed ring-containing triarylamine compounds useful for dyes and/or luminescent/photochromic materials. *Jpn. Kokai Tokkyo Koho* 18 pp. (2011).

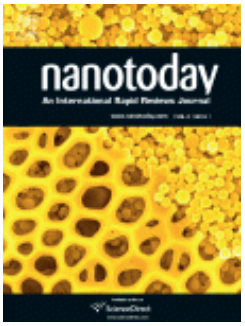

Title: Conjugated polymer sorting of semiconducting carbon nanotubes and their electronic applications

Author: Huiliang Wang,Zhenan Bao

Publication: Nano Today

Publisher: Elsevier

Date: December 2015

Order Completed

Thank you for your order.

This Agreement between Mr. Fumiyuki Toshimitsu ("You") and Elsevier ("Elsevier") consists of your license details and the terms and conditions provided by Elsevier and Copyright Clearance Center.

Your confirmation email will contain your order number for future reference.

printable details

License Number	4276230538223
License date	Jan 25, 2018
Licensed Content Publisher	Elsevier
Licensed Content Publication	Nano Today
Licensed Content Title	Conjugated polymer sorting of semiconducting carbon nanotubes and their electronic applications
Licensed Content Author	Huiliang Wang,Zhenan Bao
Licensed Content Date	Dec 1, 2015
Licensed Content Volume	10
Licensed Content Issue	6
Licensed Content Pages	22
Type of Use	reuse in a thesis/dissertation
Portion	figures/tables/illustrations
Number of figures/tables/illustrations	2
Format	both print and electronic
Are you the author of this Elsevier article?	No
Will you be translating?	No
Original figure numbers	1, 2
Title of your thesis/dissertation	Selective Sorting and Purification of Semiconducting-Single-Walled Carbon Nanotubes Based on Supramolecular Approach
Expected completion date	Mar 2018
Estimated size (number of pages)	130
Requestor Location	Mr. Fumiyuki Toshimitsu 744 Motooka Fukuoka, Fukuoka 819-0395 Japan Attn: Mr. Fumiyuki Toshimitsu
Publisher Tax ID	JP00022
Total	0.00 USD

ORDER MORE CLOSE WINDOW

Title:	Individual Dissolution of Single-Walled Carbon Nanotubes in Aqueous Solutions of Steroid or Sugar Compounds and Their Raman and Near-IR Spectral Properties
Author:	Ayumi Ishibashi,Naotoshi Nakashima
Publication:	Chemistry - A European Journal
Publisher:	John Wiley and Sons
Date:	Jul 6, 2006

Order Completed

Thank you for your order.

This Agreement between Mr. Fumiyuki Toshimitsu ("You") and John Wiley and Sons ("John Wiley and Sons") consists of your license details and the terms and conditions provided by John Wiley and Sons and Copyright Clearance Center.

Your confirmation email will contain your order number for future reference.

printable details

License Number	4276241034739
License date	Jan 25, 2018
Licensed Content Publisher	John Wiley and Sons
Licensed Content Publication	Chemistry - A European Journal
Licensed Content Title	Individual Dissolution of Single-Walled Carbon Nanotubes in Aqueous Solutions of Steroid or Sugar Compounds and Their Raman and Near-IR Spectral Properties
Licensed Content Author	Ayumi Ishibashi,Naotoshi Nakashima
Licensed Content Date	Jul 6, 2006
Licensed Content Pages	8
Type of use	Dissertation/Thesis
Requestor type	University/Academic
Format	Print and electronic
Portion	Figure/table
Number of figures/tables	1
Original Wiley figure/table number(s)	Figure 1
Will you be translating?	No
Title of your thesis / dissertation	Selective Sorting and Purification of Semiconducting-Single-Walled Carbon Nanotubes Based on Supramolecular Approach
Expected completion date	Mar 2018
Expected size (number of pages)	130

Requestor Location	Mr. Fumiyuki Toshimitsu 744 Motooka Fukuoka, Fukuoka 819-0395 Japan Attn: Mr. Fumiyuki Toshimitsu

SPRINGER NATURE LICENSE TERMS AND CONDITIONS

Jan 25, 2018

This Agreement between Mr. Fumiyuki Toshimitsu ("You") and Springer Nature ("Springer Nature") consists of your license details and the terms and conditions provided by Springer Nature and Copyright Clearance Center.

License Number	4276231175196
License date	Jan 25, 2018
Licensed Content Publisher	Springer Nature
Licensed Content Publication	Nature Communications
Licensed Content Title	Large-scale single-chirality separation of single-wall carbon nanotubes by simple gel chromatography
Licensed Content Author	Huaping Liu, Daisuke Nishide, Takeshi Tanaka, Hiromichi Kataura
Licensed Content Date	May 10, 2011
Licensed Content Volume	2
Type of Use	Thesis/Dissertation
Requestor type	non-commercial (non-profit)
Format	print and electronic
Portion	figures/tables/illustrations
Number of figures/tables/illustrations	1
High-res required	no
Will you be translating?	no
Circulation/distribution	<501
Author of this Springer Nature content	no
Title	Selective Sorting and Purification of Semiconducting-Single-Walled Carbon Nanotubes Based on Supramolecular Approach
Instructor name	n/a
Institution name	n/a
Expected presentation date	Mar 2018
Portions	Figure 1
Requestor Location	Mr. Fumiyuki Toshimitsu 744 Motooka Fukuoka, Fukuoka 819-0395 Japan Attn: Mr. Fumiyuki Toshimitsu
Billing Type	Invoice
Billing Address	Mr. Fumiyuki Toshimitsu 744 Motooka

JOHN WILEY AND SONS LICENSE TERMS AND CONDITIONS

Jan 25, 2018

This Agreement between Mr. Fumiyuki Toshimitsu ("You") and John Wiley and Sons ("John Wiley and Sons") consists of your license details and the terms and conditions provided by John Wiley and Sons and Copyright Clearance Center.

License Number	4276231379190
License date	Jan 25, 2018
Licensed Content Publisher	John Wiley and Sons
Licensed Content Publication	Small
Licensed Content Title	Single-Walled Carbon Nanotubes Under the Influence of Dynamic Coordination and Supramolecular Chemistry
Licensed Content Author	Kelly S. Chichak,Alexander Star,M. Virginia P. Altoé,J. Fraser Stoddart
Licensed Content Date	Feb 25, 2005
Licensed Content Pages	10
Type of use	Dissertation/Thesis
Requestor type	University/Academic
Format	Print and electronic
Portion	Figure/table
Number of figures/tables	1
Original Wiley figure/table number(s)	scheme 1
Will you be translating?	No
Title of your thesis / dissertation	Selective Sorting and Purification of Semiconducting-Single-Walled Carbon Nanotubes Based on Supramolecular Approach
Expected completion date	Mar 2018
Expected size (number of pages)	130
Requestor Location	Mr. Fumiyuki Toshimitsu 744 Motooka Fukuoka, Fukuoka 819-0395 Japan Attn: Mr. Fumiyuki Toshimitsu
Publisher Tax ID	EU826007151
Total	0.00 USD
Terms and Conditions	

TERMS AND CONDITIONS

This copyrighted material is owned by or exclusively licensed to John Wiley & Sons, Inc. or one of its group companies (each a"Wiley Company") or handled on behalf of a society with which a Wiley Company has exclusive publishing rights in relation to a particular work (collectively "WILEY"). By clicking "accept" in connection with completing this licensing transaction, you agree that the following terms and conditions apply to this transaction

Title: Modular Engineering of H-Bonded Supramolecular Polymers for Reversible Functionalization of Carbon Nanotubes

Author: Anna Llanes-Pallas, K. Yoosaf, Hassan Traboulsi, et al

Publication: Journal of the American Chemical Society

Publisher: American Chemical Society

Date: Oct 1, 2011

PERMISSION/LICENSE IS GRANTED FOR YOUR ORDER AT NO CHARGE

This type of permission/license, instead of the standard Terms & Conditions, is sent to you because no fee is being charged for your order. Please note the following:

- Permission is granted for your request in both print and electronic formats, and translations.
- If figures and/or tables were requested, they may be adapted or used in part.
- Please print this page for your records and send a copy of it to your publisher/graduate school.
- Appropriate credit for the requested material should be given as follows: "Reprinted (adapted) with permission from (COMPLETE REFERENCE CITATION). Copyright (YEAR) American Chemical Society." Insert appropriate information in place of the capitalized words.
- One-time permission is granted only for the use specified in your request. No additional uses are granted (such as derivative works or other editions). For any other uses, please submit a new request.

If credit is given to another source for the material you requested, permission must be obtained from that source.

Title: Recognition and One-Pot Extraction of Right- and Left-Handed Semiconducting Single-Walled Carbon Nanotube Enantiomers Using Fluorene-Binaphthol Chiral Copolymers

Author: Kojiro Akazaki, Fumiyuki Toshimitsu, Hiroaki Ozawa, et al

Publication: Journal of the American Chemical Society

Publisher: American Chemical Society

Date: Aug 1, 2012

PERMISSION/LICENSE IS GRANTED FOR YOUR ORDER AT NO CHARGE

This type of permission/license, instead of the standard Terms & Conditions, is sent to you because no fee is being charged for your order. Please note the following:

- Permission is granted for your request in both print and electronic formats, and translations.
- If figures and/or tables were requested, they may be adapted or used in part.
- Please print this page for your records and send a copy of it to your publisher/graduate school.
- Appropriate credit for the requested material should be given as follows: "Reprinted (adapted) with permission from (COMPLETE REFERENCE CITATION). Copyright (YEAR) American Chemical Society." Insert appropriate information in place of the capitalized words.
- One-time permission is granted only for the use specified in your request. No additional uses are granted (such as derivative works or other editions). For any other uses, please submit a new request.

BACK | CLOSE WINDOW

JOHN WILEY AND SONS LICENSE TERMS AND CONDITIONS

Jan 24, 2018

This Agreement between Mr. Fumiyuki Toshimitsu ("You") and John Wiley and Sons ("John Wiley and Sons") consists of your license details and the terms and conditions provided by John Wiley and Sons and Copyright Clearance Center.

License Number	4275270143812
License date	Jan 24, 2018
Licensed Content Publisher	John Wiley and Sons
Licensed Content Publication	Chemistry - A European Journal
Licensed Content Title	Hybrids of Copolymers of Fluorene and C60-Carrying-Carbazole with Semiconducting Single-Walled Carbon Nanotubes
Licensed Content Author	Fumiyuki Toshimitsu,Hiroaki Ozawa,Naotoshi Nakashima
Licensed Content Date	Jan 7, 2015
Licensed Content Pages	8
Type of use	Dissertation/Thesis
Requestor type	Author of this Wiley article
Format	Print and electronic
Portion	Full article
Will you be translating?	No
Title of your thesis / dissertation	Selective Sorting and Purification of Semiconducting-Single-Walled Carbon Nanotubes Based on Supramolecular Approach
Expected completion date	Mar 2018
Expected size (number of pages)	130
Requestor Location	Mr. Fumiyuki Toshimitsu 744 Motooka Fukuoka, Fukuoka 819-0395 Japan Attn: Mr. Fumiyuki Toshimitsu
Publisher Tax ID	EU826007151
Total	0 JPY
Terms and Conditions	

TERMS AND CONDITIONS

This copyrighted material is owned by or exclusively licensed to John Wiley & Sons, Inc. or one of its group companies (each a"Wiley Company") or handled on behalf of a society with which a Wiley Company has exclusive publishing rights in relation to a particular work (collectively "WILEY"). By clicking "accept" in connection with completing this licensing transaction, you agree that the following terms and conditions apply to this transaction (along with the billing and payment terms and conditions established by the Copyright Clearance Center Inc., ("CCC's Billing and Payment terms and conditions"), at the time that you opened your RightsLink account (these are available at any time at http://myaccount.copyright.com).

Title: Semiconducting single-walled carbon nanotubes sorting with a removable solubilizer based on dynamic supramolecular coordination chemistry

Author: Fumiyuki Toshimitsu, Naotoshi Nakashima

Publication: Nature Communications

Publisher: Springer Nature

Date: Oct 3, 2014

Author Use

Authors of Springer Nature content do not require permission to use content from their article in most cases as stated in the author's guidelines.

Authors wishing to use their article for commercial purposes must request permission in the normal way.

For journal content questions, please contact Springer Nature's permissions department at journalpermissions@springernature.com

For book content questions, please contact Springer Nature's permissions department at bookpermissions@springernature.com